

Thesis for the Master's Degree  
in Chemistry

**Rena Samantha Record**

**Monolithic pre-columns in  
miniaturized liquid  
chromatography**

60 study points

**DEPARTMENT OF  
CHEMISTRY**

Faculty of Mathematics and Natural  
Sciences

**UNIVERSITY OF OSLO 03/2015**



## Acknowledgements

I would like to use this opportunity to express my sincere gratitude to my supervisors Professor Elsa Lundanes, Associate professor Steven Ray Haakon Wilson, and Ph.D. student Tore Vehus for all their kindness and support during my master degree. Without their supports, my accomplishments would not be possible. I would also like to thank all my colleagues at the Bio analytical group for the pleasant learning environment and thank to those who have helped me on this journey.

My special thanks goes to my Professor Elsa Lundanes who accepted me into the group and patiently guiding me along the way. My supervisor Tore Vehus for giving me many good advices and undergoing mass spectrometric experiments after I became pregnant. I would also like to thank my husband Tharald Griff Bye for encouragement, kindness and support. The last few years of research have been exciting and prosperous for me and this opportunity is priceless.

Oslo, March, 2015

Rena Samantha Record

## Abbreviations

AIBN	2,2'-azobis(2-methylpropionitrile)
ABCN	1,1' azobis(cyclohexanecarbonitrile)
AMBN	2,2'-azobis(2-methylbutyronitrile)
BMA	Butyl methacrylate
BMA-EDMA	poly(butyl methacrylate-co-ethylene dimethacrylate)
cLOD	concentration limit of detection
DDT	DL-dithiothreitol
DMF	N,N-dimethylformamide
DPPH	2,2-diphenyl-1-picrylhydrazyl hydrate
EDMA	Ethylene dimethacrylate
ESI	Electrospray ionization
ESI-MS	Electrospray ionization-mass spectrometry
FA	Formic acid
$\gamma$ -MAPS	3-(trimethoxysilyl)propyl methacrylate
H	Plate height
ID	Inner diameter
LC	(High-performance) liquid chromatography
LC-MS	Liquid chromatography-mass spectrometry
LC-UV	Liquid chromatography-ultraviolet
LHRH	Luteinizing hormone releasing hormone
LMA	Lauryl methacrylate
LP	Lauryl peroxide
MM	Molar mass
MP	Mobile phase
$m/z$	Mass-to-charge ratio
N	Number of plate
PLOT	Porous layer open tubular
POSS	Polyhedral oligomeric silsesquioxane
PS-DVB	Poly(styrene co-divinylbenzene)
RP	Reversed phase
RSD	Relative standard deviation

SD	Standard deviation
SEM	Scanning electron microscope
SP	Stationary phase
SPE	Solid phase extraction
SPE-MS/MS	Solid phase extraction-tandem mass spectrometry
TFA	Trifluoroacetic acid
Tris-HCl	Tris hydrochloride
UV	Ultraviolet
WT%	Weight %
w <sub>0.5</sub>	Peak width at half height

## Abstract

Poly(styrene co-divinylbenzene) (PS-DVB) monolithic pre-columns of 50  $\mu\text{m}$  inner diameter (ID) were developed for peptides and small molecules enrichment intended for use in automated miniaturized liquid chromatography-mass spectrometry (LC-MS) column switching system as alternative to 50  $\mu\text{m}$  ID poly(butyl methacrylate-co-ethylene dimethacrylate) (BMA-EDMA) monoliths. Monomer/porogen ratio, percentage of good solvent, polymerization temperature, and polymerization time, and thermal initiator, were investigated in order to optimise the monolithic structure with a high surface area and good permeability. The efficiency was measured on 10 cm long column using a simple liquid chromatography ultraviolet (LC-UV) test system with toluene as the test analyte.

In general, increasing polymerization temperature lead to a monolith with a higher number of small pores and backpressure. A ratio of 40/60 between monomers and porogens was required for a full structure of monolith. The columns made with LP yielded a better efficiency compare to the commonly used 2,2'-azobis(2-methylpropionitrile (AIBN) for both PS-DVB and BMA-EDMA monoliths. Reaction time strongly affected column efficiency.

The best monolithic PS-DVB pre-columns were prepared, using a binary porogenic solvent of toluene (9%) and 1-decanol (51%), lauryl peroxide (LP) as initiator and polymerization temperature of 73°C for 2 hours (plate height,  $H = 90 \mu\text{m}$ ). PS-DVB monoliths which provided good efficiency for toluene with reasonably backpressure gave a narrow elution peak for luteinizing hormone releasing hormone (LHRH) without breakthrough using gradient elution (10 cm length). The developed PS-DVB monolith gave better peak shape, trapping ability and loadability for peptides than a BMA-EDMA monolith using the solid phase extraction tandem mass spectrometry (SPE-MS/MS) system. When combining a PS-DVB monolithic pre-column (50  $\mu\text{m} \times 4 \text{ cm}$ , 500 nl/min flow rate) with a porous layer open tubular (PLOT) PS-DVB analytical column ( $\sim 0.75 \mu\text{m}$  film thickness, 10  $\mu\text{m} \times \sim 5 \text{ m}$ , 40 nl/min flow rate), a longer retention time ( $t_R$ ) ( $\sim 48 \text{ min}$ ) than expected was obtained. Thus, further development of a suitable pre-column for this system is needed.

# Table of Contents

<b>Acknowledgements.....</b>	<b>2</b>
<b>Abbreviations .....</b>	<b>3</b>
<b>Abstract.....</b>	<b>5</b>
<b>1. Introduction.....</b>	<b>9</b>
<b>1.1 Proteomics.....</b>	<b>9</b>
<b>1.2 Liquid chromatography in proteomics .....</b>	<b>9</b>
<b>1.3 Miniaturization.....</b>	<b>10</b>
<b>1.4 Large volume injection column switching system .....</b>	<b>11</b>
<b>1.5 Column performance in LC.....</b>	<b>13</b>
<b>1.6 Types of columns in LC .....</b>	<b>15</b>
1.6.1 Particle packed columns .....	16
1.6.2 Monolithic columns .....	16
<b>1.7 Pre-column .....</b>	<b>20</b>
1.7.1 Packed and monolithic pre-columns in nano LC.....	20
<b>1.8 Parameters important for monolithic structure .....</b>	<b>20</b>
1.8.1 Monomer and crosslinker .....	20
1.8.2 Porogenic solvents .....	21
1.8.3 Polymerization temperature.....	22
1.8.4 Initiator.....	23
1.8.5 Polymerization time .....	25
<b>1.9 Analytical column.....</b>	<b>25</b>
1.9.1 PLOT columns.....	26
<b>1.10 Steps for preparation of analytical columns and pre-columns in the capillary format.....</b>	<b>27</b>
1.10.1 Pre-treatment .....	27
1.10.2 Silanization .....	27
1.10.3 Polymerization .....	28
<b>1.11 Aim of study .....</b>	<b>29</b>
<b>2. Experimental.....</b>	<b>30</b>
<b>2.1 Chemicals and solutions.....</b>	<b>30</b>
<b>2.2 Preparation of samples and mobile phases .....</b>	<b>30</b>

<b>2.3 Equipment and materials</b>	<b>31</b>
2.3.1 Monolithic and PLOT columns preparation	31
2.3.2 Materials used during sample preparation of peptide mixture	32
2.3.3 LC-UV test systems	32
2.3.4 SPE-MS/MS and SPE-PLOT-MS/MS test systems	33
<b>2.4 Monolithic pre-columns and PLOT columns preparation</b>	<b>34</b>
<b>2.5 Test systems</b>	<b>36</b>
<b>3. Results and discussion</b>	<b>40</b>
<b>3.1 Evaluation of pre-columns</b>	<b>40</b>
<b>3.2 Test system considerations</b>	<b>41</b>
<b>3.3 Effect of ACN concentration on k</b>	<b>42</b>
<b>3.4 Choice of column ID and SP</b>	<b>44</b>
3.4.1 Column ID	44
3.4.2 PS-DVB and acrylate-based monoliths	44
<b>3.5 Effect of polymerization parameters on PS-DVB monolithic structure</b>	<b>45</b>
3.5.1 Percentage of good solvent	45
3.5.2 Temperature	48
3.5.3 Thermal initiator	50
3.5.4 Initiator concentration	58
3.5.5 Monomer to porogen ratio	61
3.5.6 Reaction time	62
<b>3.6 BMA-EDMA monolith</b>	<b>70</b>
<b>3.7 PLOT analytical column</b>	<b>72</b>
<b>3.8 Trapping of peptides on monolithic column</b>	<b>73</b>
<b>3.9 Loadability on PS-DVB monolith</b>	<b>76</b>
<b>3.10 Comparison of loadability on BMA-EDMA and PS-DVB monoliths</b>	<b>76</b>
<b>3.11 Comparison of pre-columns</b>	<b>77</b>
<b>3.12 PS-DVB monolith trapping repeatability</b>	<b>80</b>
<b>3.13 Compatibility testing of pre-columns with the PLOT system</b>	<b>81</b>
<b>4. Conclusion</b>	<b>83</b>
<b>5. Bibliography</b>	<b>85</b>
<b>6. Appendix</b>	<b>90</b>
<b>6.1 Tryptic peptide mixture preparation</b>	<b>90</b>

<b>6.2 Column preparation steps .....</b>	<b>90</b>
<b>6.3 %ACN on k .....</b>	<b>91</b>
<b>6.4 Thermal initiator .....</b>	<b>92</b>
<b>6.5 Initiator amount .....</b>	<b>97</b>
<b>6.6 Reaction time .....</b>	<b>98</b>
<b>6.7 Column repeatability (PS-DVB monolith).....</b>	<b>100</b>
<b>6.8 BMA-EDMA monolith.....</b>	<b>100</b>
<b>6.9 Trapping repeatability of PS-DVB monoliths .....</b>	<b>102</b>
<b>6.10 Comparison of loadability calculations .....</b>	<b>102</b>
<b>6.11 Structures of amino acid side chains .....</b>	<b>103</b>



# 1. Introduction

## 1.1 Proteomics

Proteomics can be characterized as the science that examines protein expression (the proteome) at a given time in, for example, cells, tissues or organs [1]. Proteins define the organism and its biology from structure roles to energy metabolism [1]. This makes it responsible for many important biological roles. Structure and functions of proteins can provide crucial information for the understanding of how illnesses arise and how they can be prevented. Therefore, suitable methods that can analyse the proteome are of value to biological research.

## 1.2 Liquid chromatography in proteomics

High-performance liquid chromatography (LC) is one of the most used analytical techniques for separation of various molecules present in a sample [2]. Its popularity is gained through its reliability and versatility that enable adjustments of both mobile phase (MP) and SP to match the need for the separation of the analytes [2]. LC coupled with mass spectrometry (MS) offers high resolution and sensitivity and thus has become the method of choice for protein identification in proteomics [3]. A long LC analytical column offers high resolution separation while a narrow column increases sensitivity when coupled to a concentration sensitive detector such as the electrospray ionization (ESI) MS. In short, LC-MS is an essential tool for the separation, identification, and quantification of complex samples such as peptides in tryptic digests of protein samples.

Proteins themselves are large and have complex structures, and so a digestion into smaller peptide fragments facilitates protein identification by MS analysis. This is referred to as the bottom-up approach and is usually preferred as peptides are easier to separate, ionize and fragment than intact proteins [4]. Determination of proteins without a digestion step is referred to as the top-down approach. This approach gives a complete protein sequence with the cost of very complex spectra generated by multiply charged proteins. In this study the bottom-up approach and the use of narrow capillaries were employed.

## 1.3 Miniaturization

There has been increasing demands for development of a more sensitive separation technique with increased sample throughput. These driving factors lead to developments of smaller ID columns in LC, and new types of SPs which allow a higher flow rate of MP at a reasonable backpressure.

Miniaturization is essentially a reduction of a column diameter [5], and this is done for various reasons. A small column ID reduces reagent and sample consumption, and it offers a good coupling with ESI which generates best signal with nano-flow rates. A reduction of column ID increases concentration sensitivity as the sensitivity is increased proportionally with the reduction of the column ID described by equation 1 [6].

$$f = \frac{d_{\text{conv}}^2}{d_{\text{micro}}^2} \quad (1)$$

Where  $f$  is the downscaling factor,  $d_{\text{conv}}$  is the ID of the conventional column,  $d_{\text{micro}}$  is the ID of the micro column

By reducing a column diameter from 4 mm to 1 mm for example, the sensitivity can be increased 16 fold. However, a reduction of column size can increase column backpressure and lower sample loading capacity. **Table 1** shows typical column ID of each column designation. In this study nano LC was used.

**Table 1.** Column designations and their IDs. Adapted from [7].

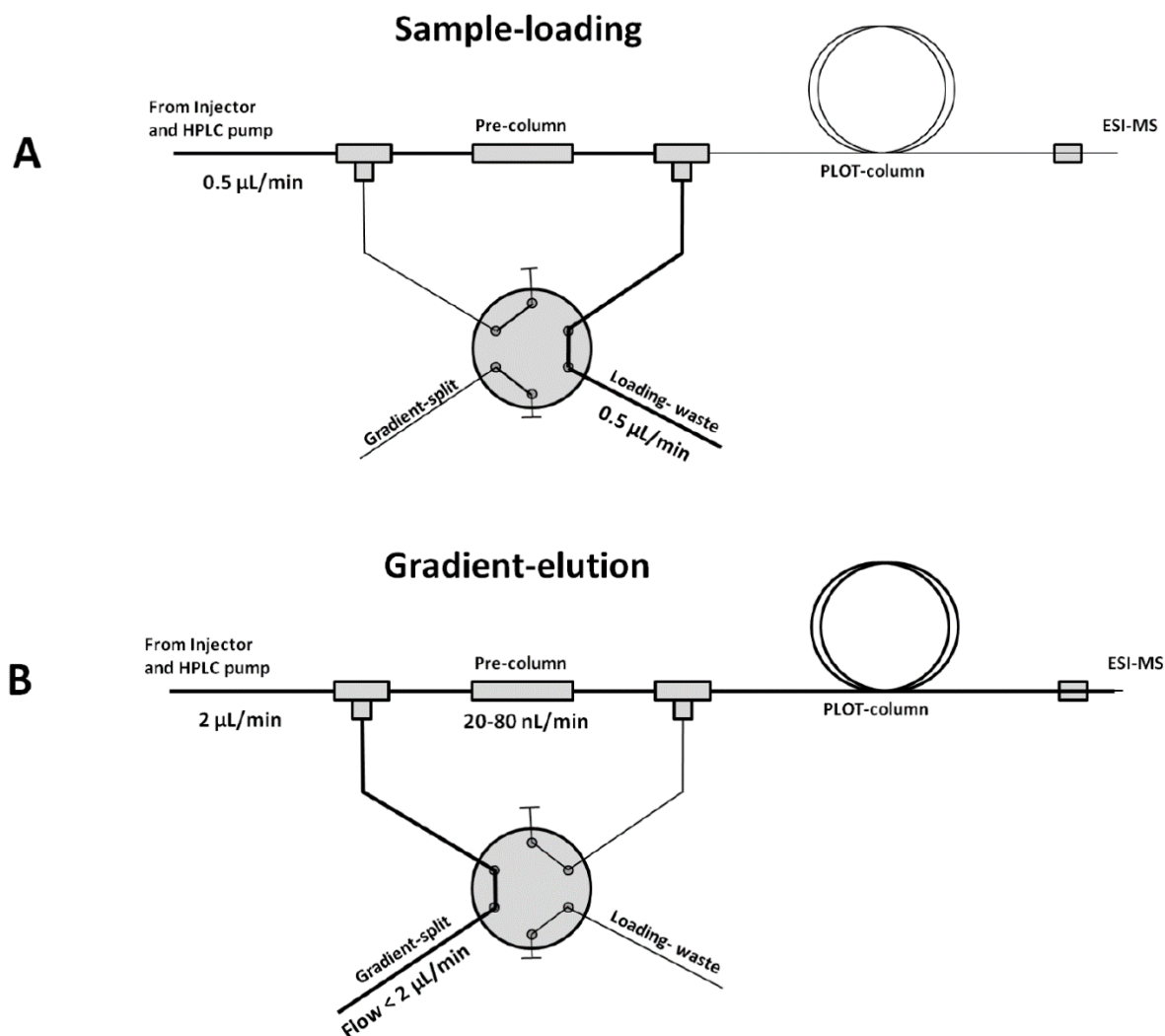
Column designation	Typical ID (mm)
Conventional HPLC	3 - 5
Narrow-bore HPLC	2
Micro LC	0.5 - 1
Capillary LC	0.1 - 0.5
Nano LC	0.01 – 0.1
Open tubular LC	0.005 – 0.05

In order to exploit more of the sample while maintaining low analysis time, a sample introduction on a pre-column in a large volume injection column switching system can be employed.

#### 1.4 Large volume injection column switching system

As a very low concentration of analyte is often the case in proteomics, the ability to detect a very small amount of analyte is essential. Although injections of a large sample volume can significantly improve the concentration limit of detection (cLOD), it can also cause sample overload in a miniaturized system and hence a loss of efficiency. Injection of a large sample volume also prolongs analysis time which is a disadvantage when a fast analysis is required. Therefore, a pre-column, also known as solid phase extraction (SPE) column, is used prior to separation on an analytical column. A large sample volume (micro-liters) is injected onto the pre-column for sample clean-up and enrichment using a relatively high flow rate (500 nl/min), thus, decreasing the analysis time.

The column switching system enables detection of a very low solute amount when coupling with a concentration sensitive detector such as ESI-MS. Many research groups have reported improvement of sample loading and sample clean-up with the use of pre-column in micro column LC [5]. **Figure 1** illustrates a column switching system used in a nano-flow LC.



**Figure 1.** A column switching system containing a pre-column and analytical column. The thick lines in both (A) and (B) indicate the flow paths. Figure by Magnus Røgeberg [8].

In sample loading, a non-eluting MP will allow solute focusing on the pre-column when an optimum flow rate is used. The compounds that are not retained will be transported to waste. In gradient elution, MP with elution strength will transfer the retained analytes onto the PLOT analytical column where they are separated.

When the system dimensions used are very small, a forward-flush is used to avoid extra-column band broadening. In larger dimensions, the back-flush is more common.

## 1.5 Column performance in LC

The efficiency of a column can be described as a plate number (N) or plate height (H), and they can be measured according to **Equation 2**. Large N corresponds to high column efficiency. H, on the other hand, is needed to be small as it corresponds to the length needed for one theoretical plate.

$$N = 5.54 \left( \frac{t_R}{W_{0.5}} \right)^2 \rightarrow H = \frac{L}{N} \quad (2)$$

Where  $t_R$  is retention time of the analyte,  $w_{0.5}$  is peak width at half peak height and L is column length.

For particle packed columns, the Van Deemter equation (**Equation 3**) describes what can be done in order to achieve large N or small H. For this type of column, fast chromatographic separations can be achieved by increasing the MP flow rate, decreasing column length or by reducing the column particle diameter [9]. However, a reduction in column length and/or increasing MP flow rate will decrease column efficiency [9]. To reduce analysis time and increase column efficiency, a reduction of particle size to less than 2  $\mu\text{m}$  can be made at the cost of increasing column's backpressure.

$$H = A + \frac{B}{u} + Cu = 2\lambda d_p + \frac{2\gamma D_M}{u} + \frac{f(k)d_p^2 u}{D_M} \quad (3)$$

Where u is the linear velocity. A, B and C are constants related to eddy diffusion, longitudinal diffusion and mass transfer in MP and SP, respectively.  $D_M$  is the analyte diffusion coefficient,  $\lambda$  is the structure factor of the packing material,  $\gamma$  is a constant termed tortuosity or obstruction factor,  $d_p$  is the particle diameter of column packing material and k is the retention factor of the analyte.

**Equation 3** is, however, not applicable for monolithic columns. For these columns, Gritti and Guiochon [10] proposed an alternative equation (**Equation 4**) to describe parameters which affect the system efficiency for polymer-based monolithic columns.

$$h = \frac{H}{d_{\text{skel}}} = \frac{B}{v} + A(v) + C_{\text{skel}}v + C_{\text{abs}}v \quad (4)$$

where  $h$  is the reduced plate height which is a dimensionless parameter to allow the direct comparison of the efficiency of columns with different particle size packing materials and structure.  $d_{\text{skel}}$  is the average size of the skeleton of the polymer-based monolith.  $v$  is the reduced MP velocity and it is defined as  $v = \frac{ud_{\text{skel}}}{D_M}$ . The skeleton-eluent mass transfer resistance due to the finite diffusivity is  $C_{\text{skel}}$  and the absorption release kinetics  $C_{\text{abs}}$  of the analyte in the polymer phase.

Both **Equations (3 and 4)** were derived from the general form of the Van Deemter equation (**Equation 5**). The terms  $A$ ,  $B$  and  $C$  present in both the equations suggest that the general form of Van Deemter equation may still be used to give an overview of what might affect the column performance of both packed and monolithic columns.  $C$ -term becomes significant for large molecules such as proteins since they have small diffusion coefficient [11].

$$H = A + \frac{B}{v} + Cv \quad (5)$$

Monolithic columns overcome several problems that are commonly found in particle packed columns. These include no packing of small particles involved and so no requirement for retaining frits, lower backpressure as the structure gives higher permeability and a low resistance to mass transfer. Although the diffusive pores of a packed column give access to a large surface area, analyte must diffuse in and out of the pores. The larger the solute, the slower the diffusion. Longer residence times in the column give rise to a larger  $C$ -term. A higher through-pore of a monolith results in a smaller  $C$ -term. This term remains almost horizontal in the Van Deemter curve even at higher flow rates [12]. Thus, a fast analysis while maintaining the system efficiency can be obtained by a monolithic column. According to Vaast et al. the efficiency of monolithic SP depends on the size of polymer microglobules and macropores similar to how particle size affects the efficiency in a packed column [13]. Therefore, by reducing the size of the globules, the plate height will decrease at the expense of column permeability [13]. Homogeneity of the SP is also crucial to minimise the  $A$ -term. Band broadening parameters ( $A$ ,  $B$  and  $C$  term) are typically determined based on isocratic measurement [13].

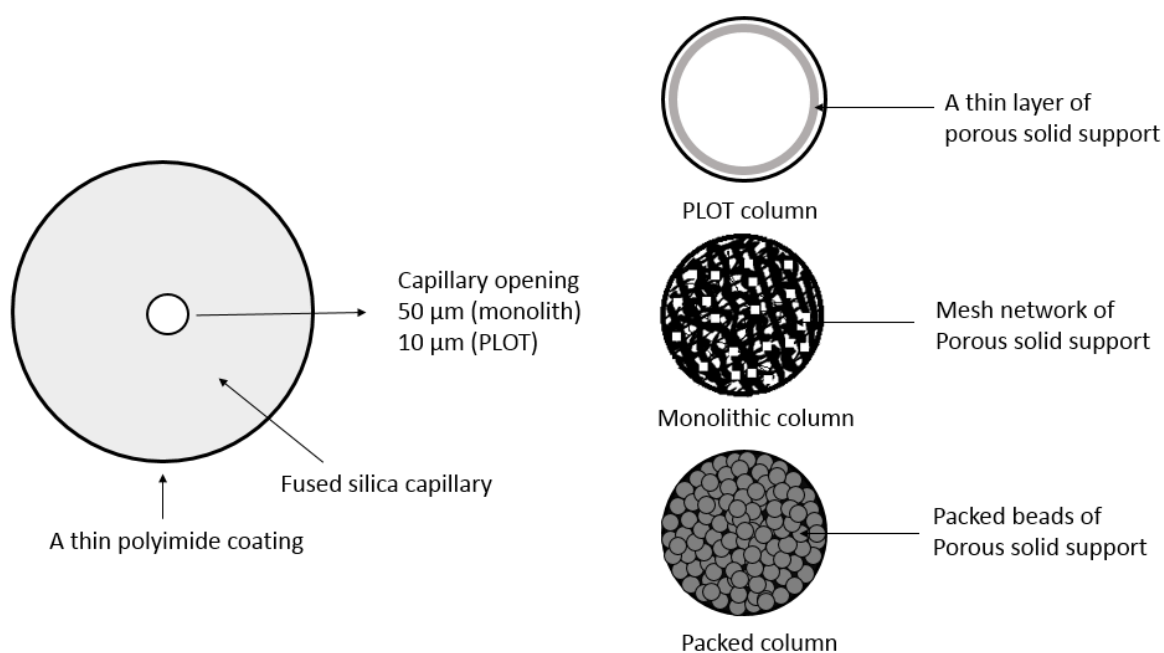
In order to allow retention on different columns to be compared, the unitless  $k$  is used.  $k$  is proportional to the total surface area of the absorbent [11]. Therefore, material with a high surface area is expected to interact strongly with the solutes, and thus a large  $k$  results. **Equation 6** describes how  $k$  can be measured.

$$k = \frac{t_R - t_m}{t_m} \quad (6)$$

Where  $t_R$  the elution is time of the analyte and  $t_m$  is the elution time of a non-retained compound.

## 1.6 Types of columns in LC

Capillary columns are often made in a thin fused-silica capillary of various IDs. The SPs are solid and come with various functionalities. **Figure 2** illustrates different types of capillary columns.



**Figure 2.** Different types of capillary columns.

### 1.6.1 Particle packed columns

Particle packed columns are currently the most common capillary columns [14]. Many functionalities and IDs are commercially available.

### 1.6.2 Monolithic columns

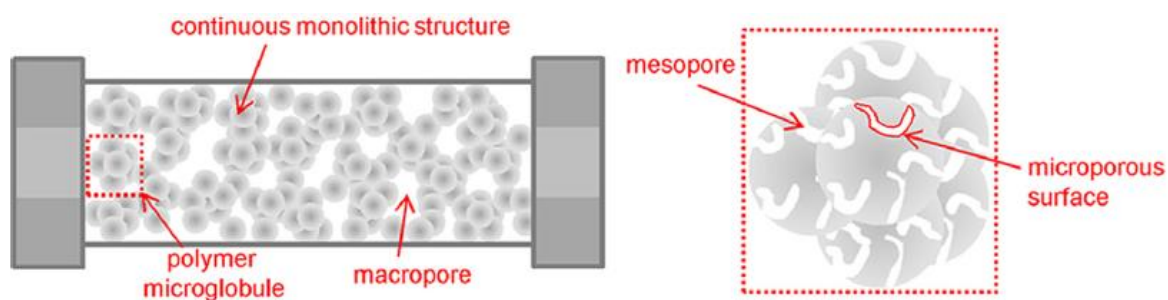
Monolithic polymers have been around since the 1990s, and their popularity has been increasing ever since [15]. Their rather rigid structure and high permeability have gained their popularity in the field of separation science. The ease of preparation allows monolithic columns to be prepared in a single step from a homogeneous polymerization mixture containing monomers, porogens and an initiator. The monolithic structure consists of a single porous material throughout the capillary. Monolithic columns can be used both as pre-columns for sample enrichment or as analytical columns for separations of molecules.

#### 1.6.2.1 Organic polymer-based and silica-based monoliths

There are two main types of monolithic columns: silica-based and polymer-based. Each one has its advantages and disadvantages. While the polymer-based offers a lower efficiency compared to the silica-based, they can be used in the entire pH range. Although polymer-based monoliths have poorer mechanical stability due to shrinking and swelling in organic solvents, they contain a higher number of macropores which gives rise to a lower backpressure and a faster analysis.

There are two main types of pores in organic polymer monolithic columns: mesopores and macropores. Mesopores (2 - 50 nm) are the pores filled with stagnant MP where the analyte accesses the active adsorption sites [16]. Macropores give larger flow-through of MP without significantly raising the backpressure. Micropores (< 2 nm) are absent in this type of monolith [17], and so polymeric monoliths have a lower surface area than silica-based monoliths. The micropores and mesopores contribute mainly to the surface area while macropores contribute mainly to the porosity [18]. Good monolithic columns consist of a large enough surface area and a high flow-through for retention and a low backpressure, respectively. **Figure 3** shows the porous structure of a monolithic column.





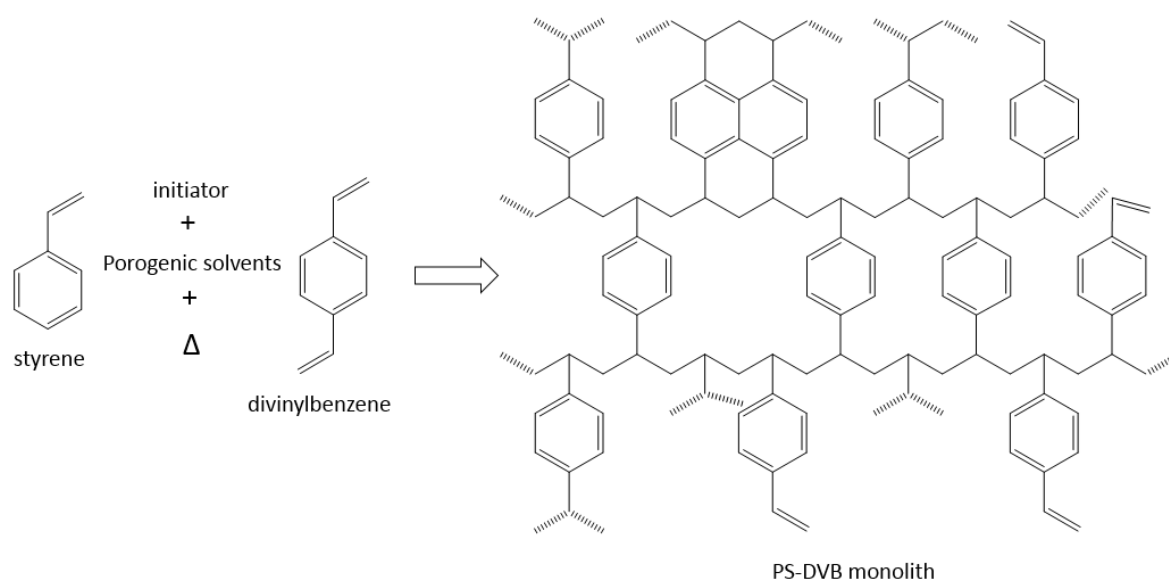
**Figure 3.** Porous structure of a monolithic column. Reprinted from [19].

#### 1.6.2.2 Types of polymer-based monoliths

There are several types of organic polymer monoliths. Both styrene and some methacrylate-based monoliths are commonly used in reversed phase (RP) LC for peptide and protein separations [12]. SP with RP functionality interacts with solute based on hydrophobicity.

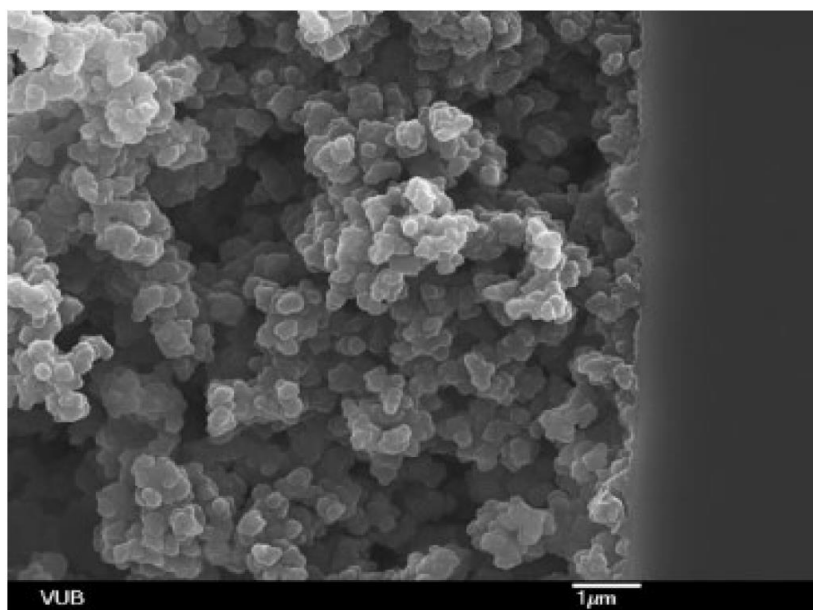
##### 1.6.2.2.1 Styrene-based monoliths

A mixture of styrene monomer, divinylbenzene (DVB) cross-linker, organic solvents and a thermal initiator such as AIBN is used for preparation of this type of monolith. The hydrophobicity of styrene-based monoliths is comparable with C<sub>4</sub> or C<sub>8</sub> RP packed beds column [20]. **Figure 4** shows the chemical structure of PS-DVB monolith.



**Figure 4.** Chemical structures of styrene, DVB and PS-DVB monolith. Adapted from [21].

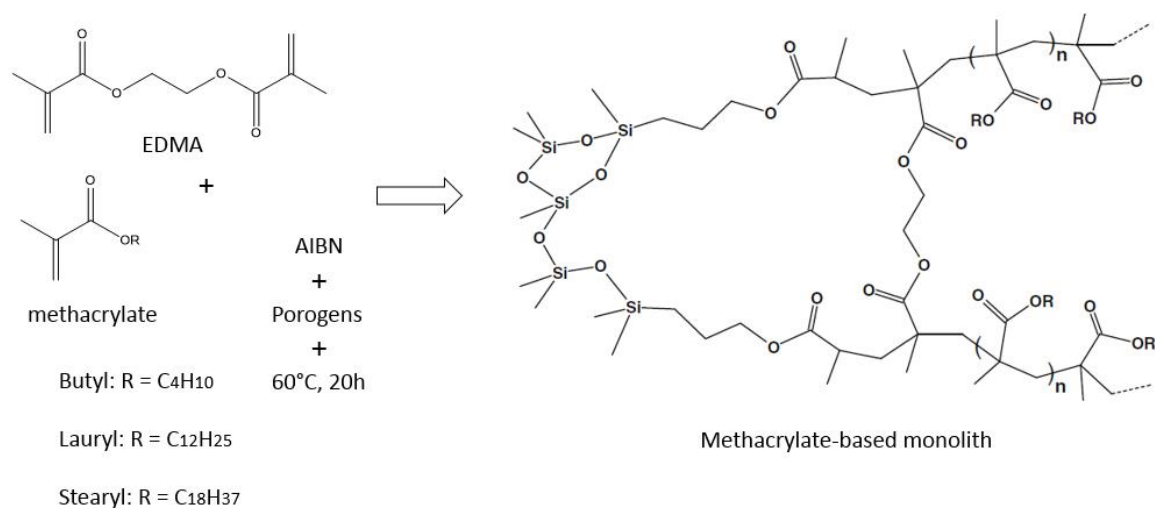
Polymers form cluster state or globule because of the unfavourable interaction with the solvent. Clusters are formed to reduce their contact with the solvent molecules [22], and they form porosity. Some polymerization parameters such as quantity of the porogenic solvents, percentage of cross linking monomer and ratio between the monomer and porogen directly affect the morphology and the porous properties of the monolith [18]. **Figure 5** shows a surface morphology of a PS-DVB monolith using a scanning electron microscope (SEM).



**Figure 5.** A SEM picture of PS-DVB monolith in cross section. Reprinted from [12].

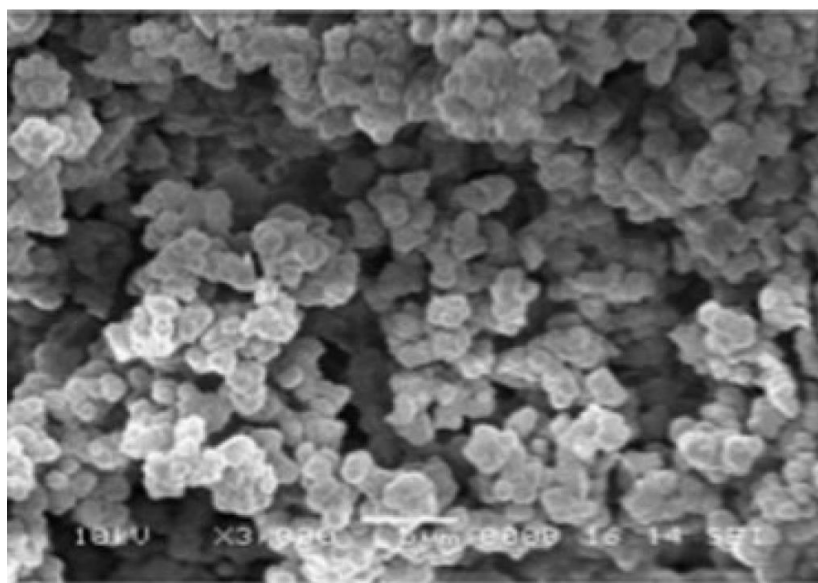
#### 1.6.2.2.2 methacrylate-based monoliths

Methacrylate-based monoliths are relatively polar and can be prepared by using butyl methacrylate (BMA) or other methacrylic acid esters as the monomer and ethylene dimethacrylate (EDMA) as the crosslinker [23]. The chemical structure of RP methacrylate-based monolith is shown in **Figure 6**.



**Figure 6.** The chemical structure of methacrylate-based monolith. Reprinted from [24].

Typical morphology of an acrylate-based monolith is shown in **Figure 7**.



**Figure 7.** A SEM picture of acrylate-based monolith. Reprinted it from [12].

## 1.7 Pre-column

Both particle packed and monolithic pre-columns are used for sample clean-up and enrichment in proteomics.

### 1.7.1 Packed and monolithic pre-columns in nano LC

Both particle packed and monolithic pre-columns have been used in miniaturized LC system for analysis of various samples. In general, packed particle pre-columns have larger ID than the monolithic.

## 1.8 Parameters important for monolithic structure

As mentioned, there are a number of experimental parameters which contributes to the final structure of the monolith. Functionality and structure of monolith can be controlled by choosing the right type of monomers and using the right degree of solvation of the monomers in porogenic solvents. Without altering the functionality, the porosity and pore size can be predicted and controlled by: 1. amount of crosslinker, 2. type and amount of porogen and 3. Polymerization temperature [25-27]

Although organic polymer monoliths have been used mainly for macromolecules in gradient elution mode due to a higher distribution of large macropores, adjustments of several experimental parameters have been employed to obtain columns suitable for fast and efficient isocratic separations of low molar mass (MM) compounds [28]. The polymerization parameters that affect the structure of a monolith are described in the following.

### 1.8.1 Monomer and crosslinker

A rigid and high mechanical strength monolith suitable for high pressure flow-through applications can be obtained using a high content of crosslinker [13]. By increasing the content of a crosslinker,

the chemical composition of the monolith changes as the crosslinking density of the monolithic backbone is increased [13]. Since DVB is more reactive than styrene, more crosslinkers are incorporated in the polymer backbone at the beginning of the copolymerization process and leads to a nuclei that are more densely crosslinked than those formed in a later stage [13]. Thus, by increasing the concentration of a crosslinker, the overall pore size decreased, and a higher number of smaller pores results [26, 29]. While a high distribution of smaller pores increases surface area, it also increases system backpressure. Therefore, a sufficient amount of crosslinker is essential in order to obtain enough surface area and a good permeability. According to Svec [30], the crosslinker in the polymerization should not exceed 30% weight (wt) of monomers in order to obtain a sufficiently good permeability.

### 1.8.2 Porogenic solvents

Porogens determine the overall pore size of the monolith without changing its chemical property [25]. They can be categorized either as good solvents or poor solvents according to the solvation of the polymer. Good solvents solvate the polymeric chains while the bad solvents do not [31]. The solvation effects contribute to different pore sizes in the final structure of the monoliths [27].

Large pores are formed by poorer solvents as they produce earlier start of the polymer phase separation [32]. Good solvents shift the overall pore size to small pore size because phase separation occurs late in the polymerization [27].

The formation of the macroporous morphology requires early phase separation of cross-linked nuclei. During polymerization the polymers separate from the solution because their MM or/and the cross-linked nuclei exceed the limited solubility in the mixture [29]. Precipitation of nuclei will grow to the size of globules and leads to a formation of a macroporous polymer as the polymerization proceeds further. Formation of larger globules consequently leads to a formation of large voids (pores) between them [29]. When a good solvent is used, it competes with monomers in the solvation of nuclei and as the local monomer concentration is lower, the globules became smaller [29].

By adjusting the porogen ratio between good and bad solvent, the macroporous properties can be optimized [13].

### 1.8.3 Polymerization temperature

The temperature of the polymerization affects the monolithic structure but not its chemical properties [32]. Temperature controls the porosity through reaction kinetic [27]. A higher temperature results in a larger number of free radicals. This gives rise to a larger number of growing nuclei [29]. As polymerization proceeds, formation of growing nuclei forms globule. This means that at higher temperature there is a greater number of growing polymeric nuclei which leads to a larger number of globules formed. The formation of a larger number of globules is compensated by their smaller size and smaller voids are created. Experimental findings conducted by Viklund et al. confirmed that higher temperature lead to a higher distribution of small pores for both the PS-DVB and the poly(glycidyl methacrylate-co-ethylene dimethacrylate) (GMA-EDMA) monolithic columns [29].

Moreover, temperature also affects the solvent quality that controls the phase separation of polymers from solution [29]. When only a poor solvent such as dodecanol for the polymerization of PS-DVB is used, the phase separation for a formation of a macroporous structure will occur when the nuclei reach a higher MM if a higher temperature is also used [29]. This is because the mixing of a polymer with a solvent is mostly an endothermic process, and so dissolution of the polymer will be promoted at elevated temperature [29]. Since the porogen effect is stronger than the temperature effect, a higher number of macropores will result as the temperature increases if only a poor solvent is used. On the other hand, when a mixture of a very good solvent such as toluene is used with a poor solvent such as decanol for the polymerization of PS-DVB, the pore size is again controlled by the nucleation rate, and it decreases as temperature increases [29]. The latter process is more common as a mixture of porogens rather than a sole porogen is mostly used.

Both UV and thermal initiations can be used to initiate polymerization. The rate of UV-initiated polymerization reaction, however, is much faster than the thermal, making a control of the polymerization rate difficult. A non-uniform layer growth of polymer may result if this rate is not carefully controlled [33]. When comparing UV initiation with thermal initiation, poorer homogeneity of monolithic structure may be obtained using the latter [23]. In this study thermal initiation was used as the polyimide coating on the capillary excluded the use of UV initiation.

#### 1.8.4 Initiator

Although there are several ways to initiate a polymerization process in monolithic synthesis, the most common practice is by using a radical initiator and initiating the reaction with heat [27]. 2'-azobis(2-methylbutyronitrile) (AIBN) is a radical initiator and is often used for monolith synthesis [34, 35]. The choice and the amount of initiator are important as the radical polymerization is a chain reaction. Higher amount of a radical initiator means a higher number of radicals which can initiate polymerization. According to Danquah and Forde [36], increasing initiator concentration (AIBN) from 0.5% (monomer w/w) to 1.5% (monomer w/w) resulted in the decrease of monolith pore size from 980 nm to 410 nm. The nature and the content of the initiator affect the polymerization rate, and this will therefore affect the structure and the properties of the monolithic material [37].

Each radical initiator have different rate of decomposition which can be expressed by its half-life( $t_{1/2}$ ). This means that different radical initiators require different temperatures at a given time in order to reduce their original amount by 50%. Arrhenius equation can be used to calculate the initiator half-life (**Equation 7**).

$$k_d = A \times e^{-E_a/RT} \text{ and } t_{1/2} = \ln 2 / k_d \quad (7)$$

Where  $k_d$  is the rate constant of the initiator dissociation in  $s^{-1}$ ,  $A$  is Arrhenius frequency factor in  $s^{-1}$ ,  $E_a$  is activation energy for the initiator dissociation in J/mole,  $R$  is 8.3142 J/mole·K,  $T$  is temperature in K and  $t_{1/2}$  is half-life in second.

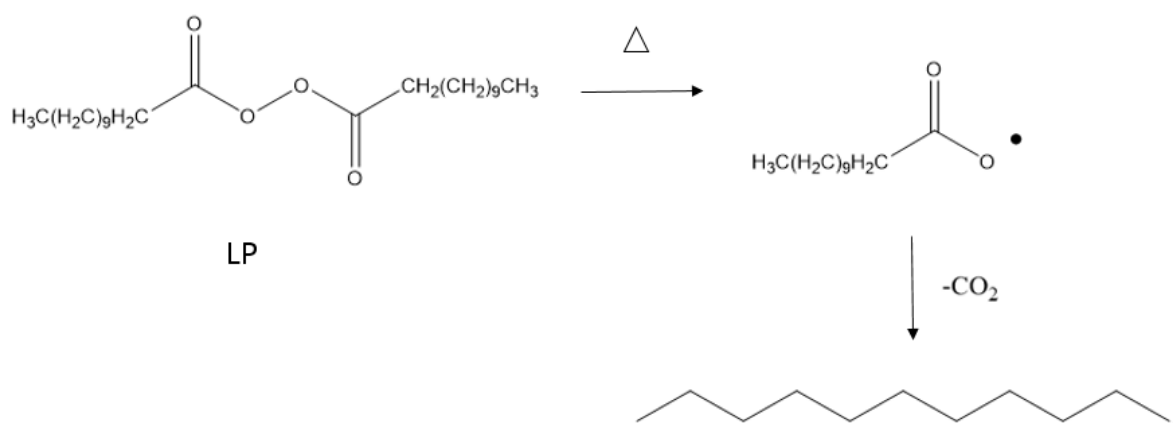
The residual concentration of the initiator can be calculated using **Equation 8**.

$$[I] = [I_0] \cdot e^{-k_d \cdot t} \quad (8)$$

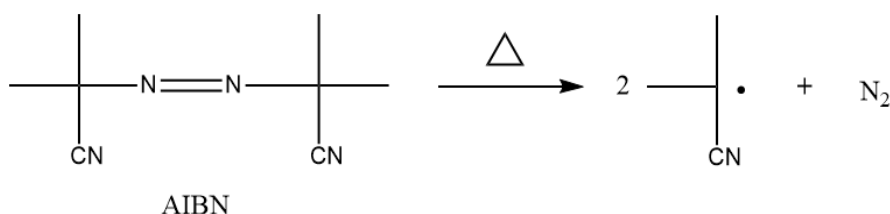
Where  $[I_0]$  is the original initiator concentration,  $[I]$  is the initiator concentration at time  $t$ , and  $t$  is the time measured from the start of decomposition in s.

When replacing one initiator with one that requires a higher temperature to reduce the original amount for the same length of time, e.g. replacing AIBN by with dibenzoyl peroxide (BPO), polymeric globules with larger pores will result when the same temperature is also used [35]. This is because

BPO has a slower decomposition rate than AIBN. This facilitates the diffusion of monomer in the polymerization process, and hence the formation of larger globules [35]. **Figures 8 and 9** show the breakdowns of LP and AIBN into radicals.



**Figure 8.** Breakdown of LP into radicals.



**Figure 9.** Breakdown of AIBN into radicals.

AIBN, 2,2'-azobis(2-methylbutyronitrile) (AMBN) and 1,1' azobis(cyclohexanecarbonitrile) (ABCN) are in the group of azo compound which have a general molecular formula of  $R-N=N-R'$ . At a high enough temperature, the loss of nitrogen gas will occur forming in carbon-centered radicals [38]. Lauroyl peroxide (LP) has the same decomposition mechanism to that of BPO which involves in a breakage of O-O bond and a loss of  $CO_2$ , and so the peroxide can be regarded as a carbon-centered  $CH_3[CH_2]_{10}$  radicals [39].



### 1.8.5 Polymerization time

Polymerization time changes the monolithic pore properties by influencing monomer conversion [40]. A higher crosslinker conversion for a short polymerization time is most likely to be the reason for an increase in monolith surface area with a decrease in polymerization time [40]. The effect of reaction time on the porous properties of monolithic columns for the separation of small molecules has been addressed by some groups. Trojer et al. prepared monolithic poly(4-methylstyrene-co-1,2-bis(4-vinylphenyl)ethane) capillary columns using polymerization times from 30 min to 24 h. The group found polymerization time over 45 min to gradually deteriorate the quality of separation. At 45 min, the highest column efficiency of 65,000 plates/m of alkylbenzoates was obtained. The separation quality became poor for columns with more than 2 h of polymerization and unacceptable at 12 and 24 h [41].

Svec and Frechet have found that the use of shorter reaction times than that required for complete monomer conversion was appropriate for preparation of monolith with larger flow through channels [42]. They suggested the reason to be termination of the polymerization process in the early stage. As in this stage the microglobles are smaller with looser assembling, their pore volume is larger [43]. As the polymerization reaction approaches completion, the pore volume decreases since a larger amount of polymer is formed within the same container volume. The pore volume will eventually reach the percentage of porogenic solvent in the polymerization mixture [43]. Maya and Svec found that the yield of polymer after 2.5 h of polymerization was lower than 50%, while the yield of the mixture polymerized for 15 h was in excess of 90%, and the yield reaches 100% at a polymerization time of 40 h. The surface area of the polymer obtained after 2.5 h was 75 m<sup>2</sup>/g and decreased to only 10 m<sup>2</sup>/g for a monolith polymerized for 40 h [43]. Nevertheless, sufficient polymerization time should be allowed to ensure maximum monomer conversion and monolith rigidity [40].

Increased polymerization times lead to larger heterogeneous globular structure [44] which lead to a larger A term and a lower column efficiency.

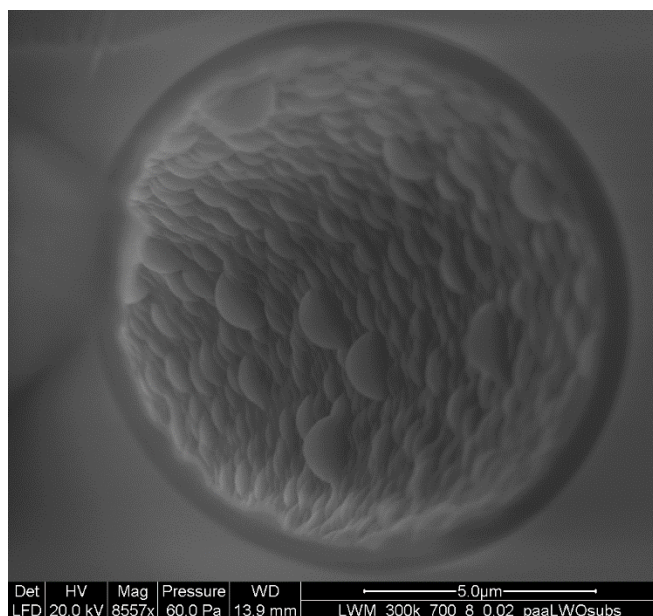
## 1.9 Analytical column

After sample enrichment, molecules are separated using an analytical column in a column switching system. Two types of analytical column were produced for use in this study. PS-DVB PLOT columns

were produced using the method described by Yue et al. [45] with modification between monomer to ethanol ratio according to Røgeberg et al. [46].

#### 1.9.1 PLOT columns

PS-DVB PLOT columns (**Figure 10**) can be prepared by a one-step polymerization and are used as analytical column in a RP mode. The open tubular structure gives 10  $\mu\text{m}$  ID columns a reasonably low backpressure even at several meters long. The thickness of the porous layer is about 0.75  $\mu\text{m}$  – 1  $\mu\text{m}$ , and it is reported to have sufficient capacity for the separation of proteins and peptides [46]. The thickness of the film can be adjusted by adjusting the monomers/porogen ratio. A thicker film leads to an increase in loading capacity while a thinner film leads to an increase in permeability and hence possibility to use a longer column. The narrow PLOT columns are used with a low flow rate (40 nl/min), and this hence increases the ionization efficiency for the MS. Røgeberg et al. [4] showed that intact proteins can be separated with good resolution, repeatabilities, and just a small amount of carry over using a 10  $\mu\text{m}$  PS-DVB PLOT analytical column. Using a solid phase extraction porous layer open tubular liquid chromatography mass spectrometry (SPE-PLOT LC-MS) setup, many proteins and peptides could be identified in just one single injection of an extract [46].



**Figure 10.** SEM image of a 10  $\mu\text{m}$  ID PS-DVB PLOT column.

## 1.10 Steps for preparation of analytical columns and pre-columns in the capillary format

In this thesis, PS-DVB and BMA-EDMA monoliths were investigated. BMA-EDMA monoliths were used for comparison.

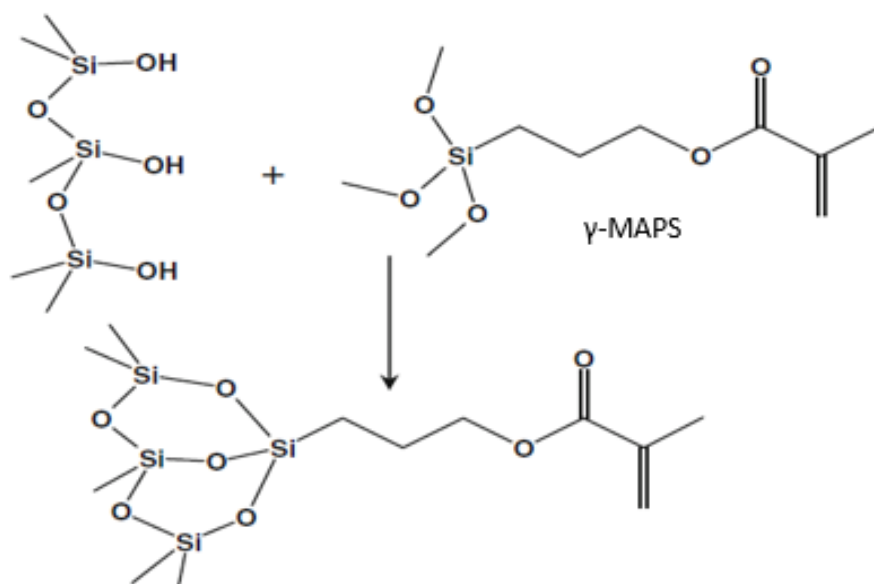
The preparation of organic polymer-based monolithic pre-columns and analytical columns consists of three steps: pre-treatment, silanization and polymerization.

### 1.10.1 Pre-treatment

A pre-treatment step involves filling a capillary with an alkaline solution to increase the density of silanol groups [47]. 1M NaOH solution is used. In this step, the siloxane groups inside the capillary wall are hydrolyzed by the base and become silanol groups which will then serve as anchors for vinyl groups used in the silanization step.

### 1.10.2 Silanization

In order to ensure a covalent attachment of the polymer to the capillary wall, a silanization step is performed prior to the polymerization. The capillary is treated with  $\gamma$ -(trimethoxysilyl) propyl methacrylate ( $\gamma$ -MAPS) in order to gain anchoring sites on the silanol groups for the grafting of the polymer during polymerization [47] (**Figure 11**). At elevated temperature, polymerization of the reagent via the vinyl group occurs. Therefore, an inhibitor 2,2-diphenyl-1-picrylhydrazyl hydrate (DPPH) was added to slow down this polymerization [47]. Gusev et al. [47] found that the use of the inhibitor DPPH gave the most stable polymer while a cleft between the monolith and the inner wall was found when the inhibitor was not used.



**Figure 11.** Silanization on capillary wall with  $\gamma$ -MAPS. Reprinted from [24].

### 1.10.3 Polymerization

A silanized capillary is filled with a polymerization mixture consisting of monomers, porogens and initiator. Heat is applied to initiate the polymerization. After the polymerization, the capillary is rinsed with a suitable organic solvent to remove the unreacted polymerization reagents.

### 1.11 Aim of study

The aim of this study was to prepare an efficient 50  $\mu\text{m}$  ID polymeric monolithic pre-columns for trapping of peptides and small molecules (MM  $\sim 1000$  g/mol) in a nano LC proteomic platform with PLOT analytical column. The effect of various parameters on monolithic structure was to be investigated. Different ratios of monomers/porogens, porogenic solvents, reaction temperature, initiator and reaction duration were varied in order to find the monolithic structure that gives a low backpressure and plate height for small molecules.

## 2. Experimental

### 2.1 Chemicals and solutions

Type 1 water was obtained from a Milli-Q ultrapure water purification system from Millipore (Bedford, MA, USA). Nitrogen gas (99.99%) was obtained from AGA (Oslo, Norway). HPLC grade acetonitrile (ACN) HiPerSolv was purchased from Chromanorm (Radnor, PA, USA). Ethanol was purchased from Arcus (Oslo, Norway). Toluene was purchased from Rathburn Chemicals (Walkerburn, UK). Sodium hydroxide pellets (99%) and 1-propanol were purchased from Merck (Darmstadt, Germany). Formic acid (FA) (50%), anhydrous N,N-dimethylformamide (DMF) (99.8%), 2,2-diphenyl-1-picrylhydrazyl (DPPH), 3-(trimethoxysilyl)propyl methacrylate ( $\gamma$ -MAPS) (98%), 2,2'-azobis(2-methylpropionitrile) (AIBN) (98%), 2,2'-azobis(2-methylbutyronitrile) (AMBN) (98%), 1,1'-azobis(cyclohexanecarbonitrile) (ABCN) (98%), lauroyl peroxide (LP) (97%), PSS-methacryl substituted (POSS) (Cage mixture, n = 8, 10, 12), lauryl methacrylate (LMA) (96%), poly(ethylene glycol) (PEG) (average MM 200), styrene (99%), divinylbenzene (DVB) (80% mixture of isomers), butyl methacrylate (BMA) (98%), ethylene dimethacrylate (EDMA) (98%), 1,4-butanediol (99%), 1-decanol (99%), Tris hydrochloride (Tris-HCL) (99%), LHRH (96%), DL-dithiothreitol (DDT), iodoacetamide (IAM), trifluoroacetic acid (TFA) and urea were purchased from Sigma Aldrich (St. Louis, MO, USA). Uracil was purchased from EMD Millipore (Billerica, MA, USA).

Recombinant APC (H00000324-Q01) and axin2 (H00008313-Q01) were purchased from Abnova (Tapei City, Taiwan). Glycogen synthase 3 $\beta$  (GSK3 $\beta$ ) were purchased from Life Technologies (Carlsbad, CA, USA) and beta-catenin (12-537) was purchased from Millipore (Billerica, MA, USA). Trypsin was purchased from Promega (Madison, WI, USA).

### 2.2 Preparation of samples and mobile phases

#### Toluene and Uracil

A 10 ml standard solution of uracil and toluene was made by diluting uracil (0.2 mg/ml) and 2,5  $\mu$ l toluene with type 1 water. The concentrations of toluene and uracil were 2.5% (v/v) and 10  $\mu$ g/ml.

## LHRH

A standard peptide solution was prepared by dissolving LHRH in water (with 5% ACN) to a final concentration of 0.2 mg/ml.

## Tryptic peptide mixture

The tryptic peptide mixture used in SPE-MS/MS and solid phase extraction porous layer open tubular tandem mass spectrometry (SPE-PLOT-MS/MS) systems was produced by Tore Vehus. A short sample preparation procedure is found in the **Appendix 6.1** Tryptic peptide mixture preparation.

## Mobile phases

Mobile phase A consisted of 0.1% (v/v) FA in water. Except for “Loadability on PS-DVB monolith” test where the mobile phase A also consisted of 4% ACN. Mobile phase B consisted of ACN and 0.1% FA.

## 2.3 Equipment and materials

### 2.3.1 Monolithic and PLOT columns preparation

A 2 – 20 µl Finnpiptette, a 10-100 µl Finnpiptette, and a 100-1000 µl Finnpiptette F2 from Thermo Scientific (Waltham, MA, USA) and a Mettler AE 166 delta range analytical balance from Mettler (Columbus, OH, USA) were used for solution and sample preparations. A 1 ml single use syringe was purchased from Becton Dickinson S.A. (Madrid, Spain) and was used for manual filling of polymerization solution. A laboratory-made pressure bomb system was used to fill and rinse capillary.

All polyimide-coated fused silica capillaries were purchased from Polymicro Technologies (Phoenix, AZ, USA). A GC 8000 series oven from SpectraLab Scientific (Markham, ON, Canada) and a Polaratherm Series 9000 oven from Selerity Technologies (Salt Lake City, UT, USA) were used for heating the capillaries during silanization and polymerization. Ultrasonication of polymerization mixtures was done using a model USC100T ultrasonic cleaning bath from VWR International (Leicestershire, England, UK).

After completed polymerization, a microscope with W10X/20 mm eyepiece magnification from Motic was used to check the presence/absence of polymers along the monolithic capillaries. Scanning electron microscope (SEM) images of the columns were taken using a FEI Quanta 200 FEG-ESEM (FEI, Hillsboro, OR, USA). The columns were cut to pieces of about 1 cm and placed on a holder with carbon tape inside the sample chamber. The images were taken using low vacuum mode with large field detector (LFD) and solid state detector (SSD).

### 2.3.2 Materials used during sample preparation of peptide mixture

An Acclaim PepMap100 (packed with 3 $\mu$ m C18, nanoViper) column was purchased from Thermo Scientific (California, USA). Bond Elut C18, 100 mg RP C18 cartridges was used to desalt a tryptic peptide mixture was purchased from Agilent (Santa Clara, CA, USA). SpeedVac (former Savant) was used to dry the mixture of the peptide sample was purchased from Thermo Fischer Scientific (Waltham, MA, USA).

### 2.3.3 LC-UV test systems

Easy-nLC-1000 (Proxeon, now Thermo Fisher Scientific, Waltham, MA, USA) pumps were used to conduct experiments for both LC-UV 1 and 2 systems. The UV detector used in LC-UV 1 was Knauer Wellchrom K-2600 equipped with a 40 nl flow cell was purchased from Artisan Technology group (IL, USA). A four-port VICI injector with a 50 nl internal loop from Valco Instruments (Houston, TX, USA) was used for manual injections of samples in the LC-UV 1 system. The Dionex detector used in LC-UV 2 system was purchased from Thermo Fischer Scientific (Waltham, MA, USA) and was equipped with an 11 nl flow cell.

A syringe pump (500  $\mu$ l) from Thermo Fischer Scientific (Waltham, MA, USA) was used for "Comparison of loadability on PS-DVB and BMA-EDMA monoliths". A 10  $\mu$ l syringe from SGE (Ringwood, VIC, Australia) was used for manual injections of samples in the LC-UV 1 system.



#### 2.3.4 SPE-MS/MS and SPE-PLOT-MS/MS test systems

The Easy-nLC pump-1000 (Proxeon) was used for “Comparison of pre-columns” (SPE-MS/MS) and “Compatibility testing with the PLOT system” (SPE-PLOT-MS/MS). 5  $\mu\text{m}$  ID PicoTip emitters (FS360-20-5-D-20-C7,  $5 \pm 1 \mu\text{m}$  tip) were used for both systems and was purchased from New Objective (Woburn, MA, USA).

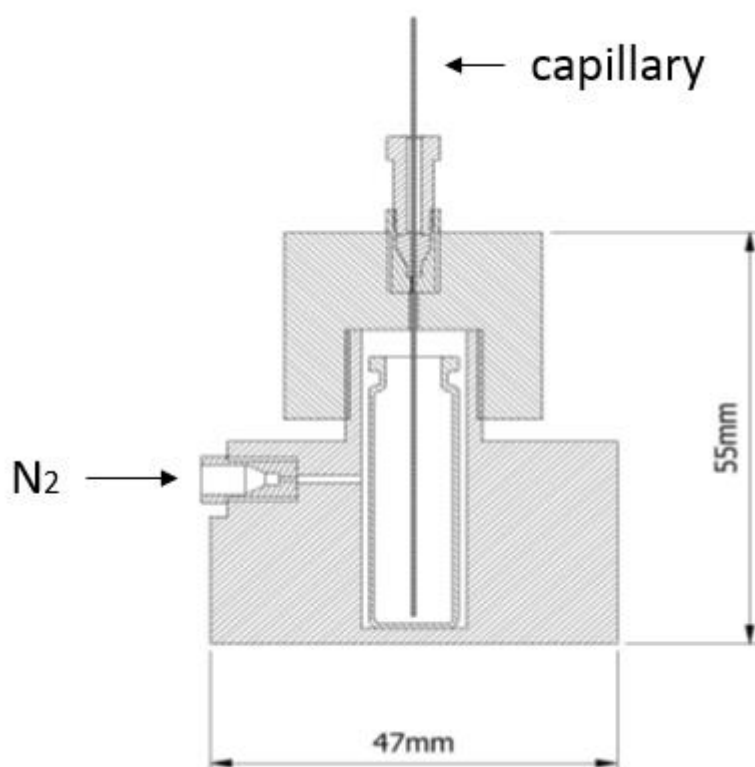
The PLOT column was connected to a silica PicoTip emitter with a PicoClear Union (PCU-360), both from New Objective (Woburn, MA, USA). For mass spectrometric detection, a Q-Exactive Orbitrap MS, purchased from Thermo Fischer Scientific (Waltham, MA, USA) was equipped with a nanospray ESI source and operated in positive ionization mode was used. **Table 2** shows the operating parameters of the MS for both the SPE-MS/MS and SPE-PLOT-MS/MS systems.

**Table 2.** Operating parameters of the MS

MS resolution	70,000
AGC target	1E6
Fill time	250 ms
Scan range	m/z 350-1850
MS/MS resolution	17,500
AGC target (MS/MS)	1E5
Fill time (MS/MS)	64 ms
Loop count	15
Isolation width	m/z 4.0
Normalized collision energy	25
Underfill	1 %
Dynamic exclusion	25 seconds
Fragmentation of ions with charge	2 - 6
Lock mass	m/z 445,12005

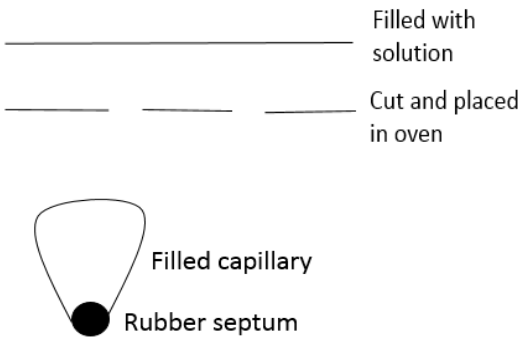

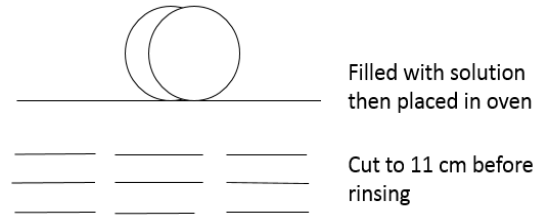
## 2.4 Monolithic pre-columns and PLOT columns preparation

A laboratory-made pressure bomb was used in most cases during column preparation for both pre-columns and analytical columns. A capillary was filled with a solution, rinsed and dried using this system. **Figure 12** illustrates the pressure bomb system.



**Figure 12:** Laboratory-made pressure bomb system used during columns preparation. A glass vial containing the appropriate liquid is placed inside the bomb where one end of the capillary is merged inside the vial. Nitrogen gas ( $\leq 200$  bar) is applied and forces the liquid through the entire capillary. Figure by Inge Mikalsen.

For monolithic columns, a 15 – 20 m long capillary was pre-treated, silanized, sealed, and kept in a refrigerator (up to two months) ready to be polymerized. A certain length of a silanized capillary was usually cut and filled (only the 25 cm polymerization length where a 75 cm capillary was filled and then cut to 25 cm pieces) with a polymerization mixture before placed in an oven. This refers to the polymerization length used. **Figure 13** describes all the polymerization lengths used in this study and the treatments performed after polymerization.

<p><b>25 cm polymerization length</b></p> 	<p>A 75 cm silanized capillary was filled with polymerization solution.</p> <p>It was then cut to 25 cm length. All ends were sealed before placed in an oven.</p> <p>After the polymerization, the ends inside the rubber septum was cut off. The column was rinsed with ACN. If the solution did not come through, a few centimetres of one or both end were cut (one at a time) until an opening was obtained.</p>
<p><b>30, 40 and 50 cm polymerization length</b></p> 	<p>A 30cm, 40cm, or 50cm silanized capillary was filled, sealed and polymerized.</p> <p>Rinsing step was performed as described for the 25 cm length.</p>
<p><b>1 m polymerization length</b></p> 	<p>A 1 m silanized capillary was filled, sealed and polymerized.</p> <p>The polymerized column was cut into ~ 10 - 11 cm length prior to rinsing. A clogged column was disposed.</p>

**Figure 13:** A short description of column preparation for each polymerization length used.

For PLOT columns, a 5.25 or 10.25 m capillary was pre-treated, silanized and polymerized. The pressure bomb was used for filling, rinsing, and drying of the capillary columns.

A short description of the pre-treatment, silanization, and polymerization steps and the chemicals used during columns preparation for both the monolithic and PLOT columns is found in the **Appendix 6.2**.

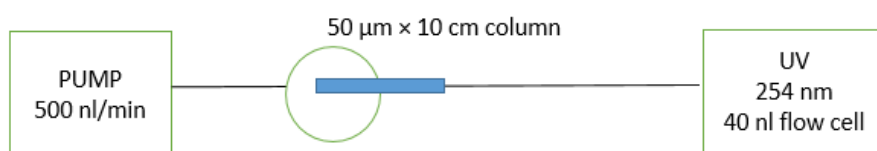
### Preparation of polymerization solution

The polymerization solutions were made freshly prior to producing of monolithic columns in every batch. The unused solution was discarded. Each chemical in the solution was weighed to the closest decimal on a four decimal places balance. The weighing of chemicals was always made in the order of; initiator, crosslinker, monomer, good solvent and bad solvent.

## 2.5 Test systems

Different test systems were used for efficiency testing of the monolithic column. **Figure 14 and 15** illustrates the setups of the LC-UV 1 & 2 systems. In the LC-UV 1 system, a column was inserted directly inside the 4-port injector (50 nl internal loop) while the other end was connected to an empty capillary (75  $\mu\text{m} \times 17\text{ cm}$ ) and to the detector. This system could only perform isocratic runs. The maximum backpressure was set to 300 bar. Manual pre-mixing of the MPs was required, and the injection volume was fixed to 50 nl. Toluene was the test analyte. The detector flow cell was 40 nl. In the LC-UV 2 system, auto-sampling and gradient elution were performed in “Loadability on PS-DVB monolith”. The length of the monolithic column was 10 cm for both systems. For “Comparison of loadability on PS-DVB and BMA-EDMA monoliths”, isocratic run and a 4 cm column were used. The detector flow cell in the LC-UV 2 system was 11 nl. **Figure 16** illustrates the setup of the SPE-MS/MS. **Figure 17** illustrates the setup of the SPE-PLOT-MS/MS. Both the SPE-MS/MS and SPE-PLOT-MS/MS systems were used for analysis of protein digest. The MS operating parameters for both systems are found in **Table 2**. **Tables 3 – 7** show the operating parameters (including column length and loading volume of sample) and sample used in each system.

### LC-UV 1 system

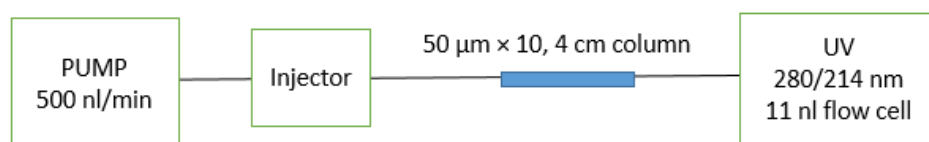


**Figure 14.** A setup of the LC-UV 1 test system.

**Table 3.** The experimental parameters used in the LC-UV 1 system for efficiency testing with toluene.

<b>MP A: water + 0.1% formic acid (FA)</b>		<b>MP B: ACN + 0.1% FA</b>	
<b>Mode and flow rate</b>		<b>A:B</b>	
Isocratic 500 nl/min		50:50	
<b>Sample and loading volume</b>	<b>Column dimension</b>	<b>UV wavelength (nm)</b>	
10 µg uracil & 2.5% v/v toluene	50 µm × 10 cm	254	

#### LC-UV 2 system



**Figure 15.** A setup of the LC-UV 2 test system for LHRH.

**Table 4.** The experimental parameters used for Loadability on PS-DVB monolith.

<b>MP A: 4% ACN + 0.1% formic acid (FA)</b>		<b>MP B: ACN + 0.1% FA</b>	
<b>Mode and flow rate</b>	<b>% B</b>	<b>Time (min)</b>	
Gradient 500 nl/min	0 – 36	10	
	36 – 95	5	
	95	5	
<b>Sample and loading volume</b>	<b>Column dimension</b>	<b>UV wavelength (nm)</b>	
200 ng/µl LHRH 1 µl loading	50 µm × 10 cm	280/214	

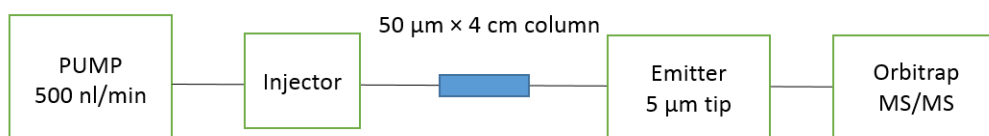
## SPE-UV

The setup of this system is the same as in LC-UV 2.

**Table 5.** The experimental parameters used for Comparison of loadability on PS-DVB and BMA-EDMA monoliths.

MP A: water + 0.1% formic acid (FA)		MP B: ACN + 0.1% FA
Mode and flow rate		A:B
Isocratic 500 nl/min		50:50
Sample and loading volume	Column dimension	UV wavelength (nm)
200 ng/ $\mu$ l LHRH 1 $\mu$ l loading volume	50 $\mu$ m $\times$ 4 cm	280/214

## SPE-MS/MS

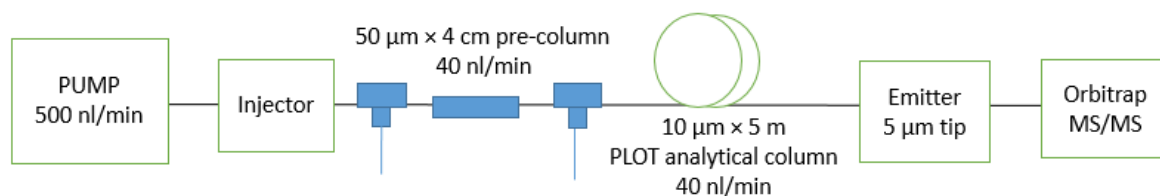


**Figure 16.** A setup of the SPE-MS/MS system for analysis of peptides.

**Table 6.** The experimental parameters used for analysis of tryptic peptides using the SPE-MS/MS system.

MP A: water + 0.1% formic acid (FA)		MP B: ACN + 0.1% FA	
Mode and flow rate	% B	Time (min)	
Gradient 500 nl/min	4 – 40	10	
	40 – 95	1	
	95	4	
Sample and loading volume		Column dimension	
1 ng/ $\mu$ l tryptic peptide mixture of recombinant AIXN2, APC, beta-catenin, GSK3beta and TNKS2 1 $\mu$ l, 3 $\mu$ l loading volume at 500 nl/min		50 $\mu$ m $\times$ 4 cm	

## SPE-PLOT-MS/MS



**Figure 17.** A setup of the SPE-PLOT-MS/MS system for analysis of peptides. The column switching system is not shown here (see **Figure 1** for more details).

**Table 7.** The experimental parameters used for Compatibility testing of pre-column with the PLOT system.

MP A: water + 0.1% formic acid (FA)		MP B: ACN + 0.1% FA	
Mode and flow rate	% B	Time (min)	
Gradient 500 nl/min	4 – 40	45	
	40 – 95	5	
	95	15	
Sample and loading volume		Column dimension	
1 ng/µl tryptic peptide mixture of recombinant AIXN2, APC, beta-catenin, GSK3beta and TNKS2 1 µl, 3 µl loading volume at 500 nl/min for 6 min		50 µm x 4 cm	

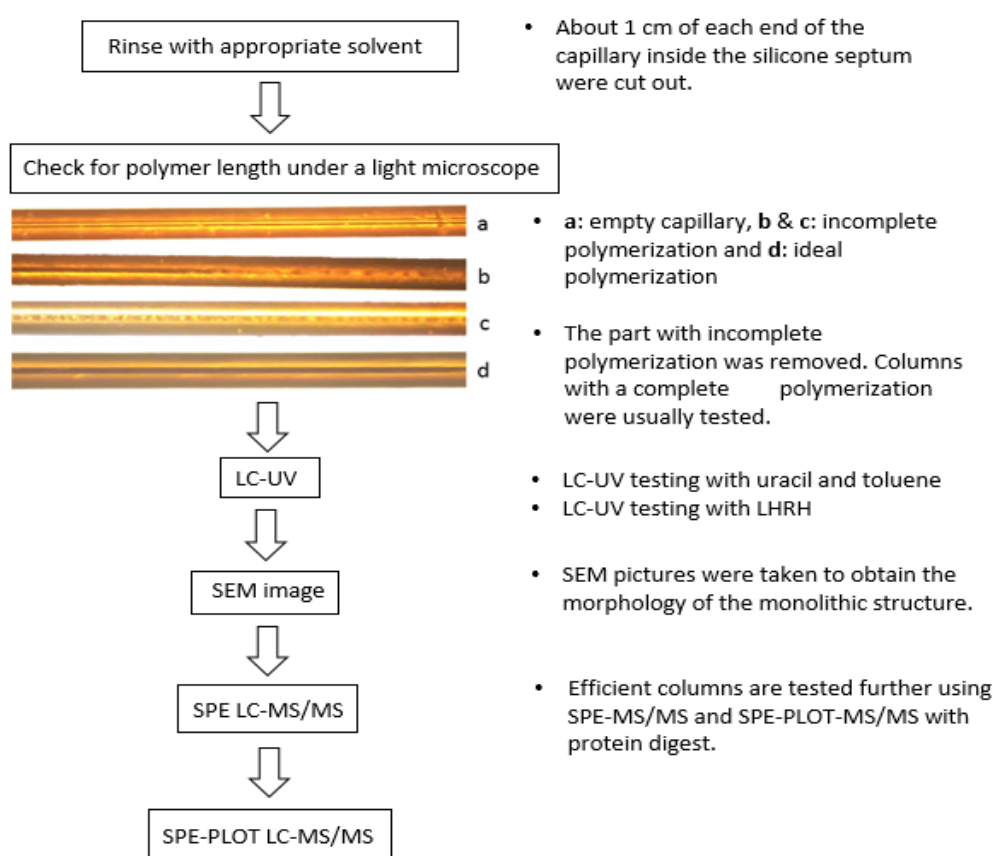
### Repeatability

The term repeatability in this study was defined as experiment undertaken in the same laboratory using the same testing instruments and polymerization conditions for production or testing of columns in different point in time or by different person.

### 3. Results and discussion

#### 3.1 Evaluation of pre-columns

There are several ways to discover if the polymerization conditions used to produce a monolithic column were appropriate or not. The initial steps of checking include: flushing a polymerized column with ACN to see if it is an open column, checking for the length of polymer under a light microscope, checking column's backpressure, testing by LC-UV with analyte and taking SEM pictures to observe the morphology. When flushing a column with ACN, a clogged column was cut until open as indicated by the presence of the solution at the outlet end. **Figure 18** shows a systematic description of the processes after a polymerization. In a later stage of testing, column with a good efficiency for toluene was to be tested with peptides. The results were to be compared with those obtained from BMA-EDMA monoliths.



**Figure 18.** A systematic description of the processes after a polymerization of a column.



### 3.2 Test system considerations

The reduction in column ID and length results in a reduction of column volume. When the column volume is small, the volume of the extra-column becomes large and significant. Extra-column band broadening is crucial to avoid in miniaturized system. The components that add up the extra-column band broadening are: the connection tubing before and after the column, that is, between the injector and the column, and from the column to the detector. The overall dispersion in the system is given by **Equation 9**.

$$\sigma_{v,\text{total}}^2 = \sigma_{v,\text{col}}^2 + \sigma_{v,\text{ext}}^2 \quad (9)$$

$\sigma_{v,\text{total}}$  is the total system volume,  $\sigma_{v,\text{col}}$  is the variance of the column and  $\sigma_{v,\text{ext}}$  is the variance of the extra-column volume.

For simplicity, the variances for extra-column band broadening were not calculated as they should be constant for all the columns tested. The columns were mounted directly in the injector (LC-UV 1 system) and the capillary tubing from column outlet to detector flow cell was the same throughout.

Two LC-UV test systems were used. Most testing were performed using the LC-UV 1 due to availability. The extra-column band broadening was most likely the highest for the LC-UV 1 system as couplings between column to the detector was done via a 75  $\mu\text{m}$  ID of 17 cm capillary and a larger flow cell of 40 nl was used.

#### LC-UV 1

This system was used to test all columns when toluene was the test analyte. Toluene was used in the simple LC-UV test system as it is a small hydrophobic molecule and has UV absorbance. Uracil was used to obtain the dead volume of the system as it should not have any interaction with the SP. For all the columns tested, the uracil  $w_{0.5}$  was measured to ensure that dead volume due to couplings is minimised and controlled. It was not possible to obtain the same uracil width for every column, but the discrepancy was kept small. The sample was in aqueous solution. As water has low elution strength, this will allow sample refocusing on the column.

Average plate height, pressure and k calculated from three consecutive injections of the sample for each column. The results are presented as the averages H, pressure and k calculated from all the columns made under the same polymerization conditions.

#### LC-UV 2

Extra-column band broadening was minimised by using very short and narrow capillaries before and after the column. LHRH was dissolved in water to allow refocusing on the column.

#### SPE-PLOT-MS/MS

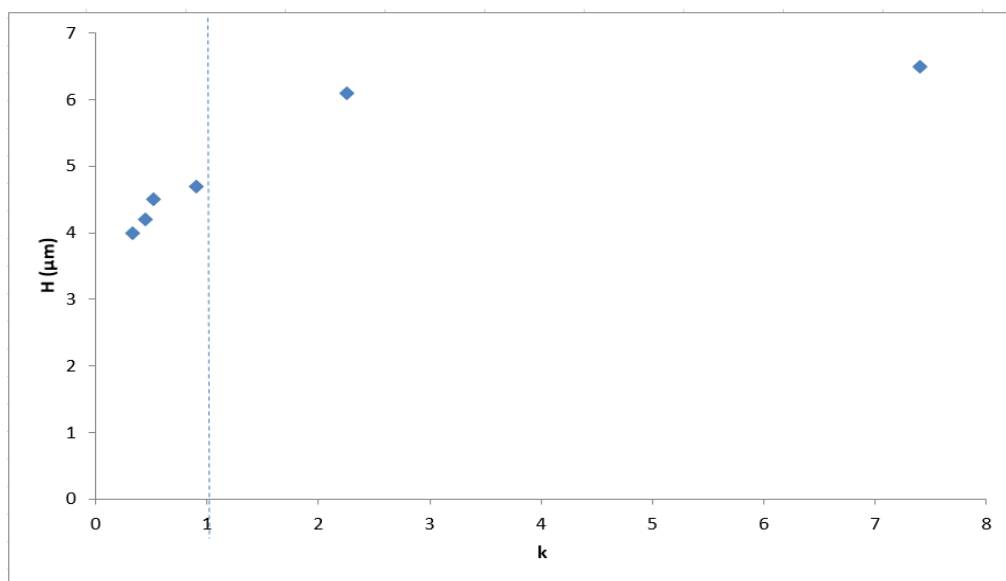
The flow rates from the LC pump, through pre-column and analytical column were chosen according to those found to be the optimal flow rates for the SPE-PLOT-MS/MS column switching system [45, 46].

#### Injection volume

The volume capacity of the column was calculated from its ID and its length. An approximate column volume of 196 nl was found to be the volume for an empty capillary of 50  $\mu\text{m}$  ID  $\times$  10 cm long. 60% of porogens were used. Hence, about 157 nl was assumed to be the volume capacity of the monoliths. The injection volumes used in both systems were smaller than the column volume capacity to avoid overloading. To avoid extra-column variance contribution from the injection volume, the analytes were in a less strong solvent as compared to that of the MP.

### 3.3 Effect of ACN concentration on k

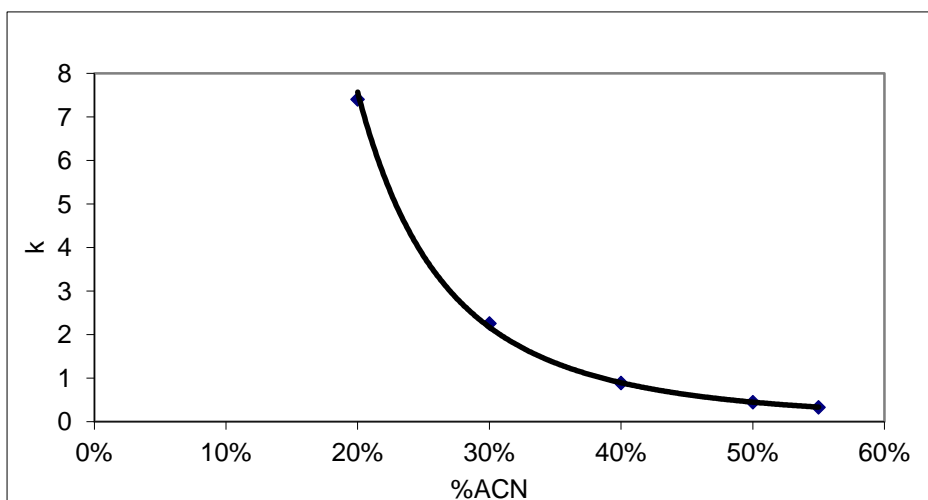
In a RP chromatographic system, k depends on the percentage of organic modifier, the SP material and to some extent the temperature. In order to verify that the columns function as RP columns, one BMA-EDMA monolith was used to investigate this effect. **Figure 19** shows a plot of H vs k (factor). The experiment was performed at room temperature.



**Figure 19.** A plot of  $H$  vs  $k$ . The experimental parameters and sample used are found in **Table 3** under LC-UV 1 test system. The column was made as described by Geiser et al. [48] but with LP as initiator and at 70°C overnight. The dotted lines indicate when  $k$  affects  $H$ .

$H$  increased mostly (factor of 1.3) when  $k$  increased by a factor of 2.5 (under 6.3 %ACN on  $k$  in the appendix). Hence, as long as the retention factor is less than 2, the results can be compared.

Therefore, the ACN concentration was kept at 50% for efficiency testing in this study. **Figure 20** shows a plot of  $k$  vs %ACN.



**Figure 20.** A plot of  $k$  vs % ACN. The experimental parameters and sample used are found in **Table 3** under LC-UV 1 test system. The same column as in **Figure 19** was used.

From this figure, it can be seen that when the percentage ACN is between 40 - 55%,  $k$  is lower than 2.  $k$  should be kept lower than 2 since when  $k > 2$ ,  $H$  greatly increased (**Figure 19**).

### 3.4 Choice of column ID and SP

#### 3.4.1 Column ID

A 50  $\mu\text{m}$  ID was chosen as it was the diameter used for BMA-EDMA and PS-DVB monolithic pre-columns for separation of biomolecules in a SPE-PLOT LC-MS system [45, 48]. When a 50  $\mu\text{m}$  ID is combined with a 10  $\mu\text{m}$  ID PLOT analytical column, it is thought to provide sufficient loading capacity and a column volume that is not too large to compromise the system efficiency. Although the column length of 4 cm was used in the column switching system, a 10 cm column was necessary for LC-UV testing due to couplings.

#### 3.4.2 PS-DVB and acrylate-based monoliths

PS-DVB was selected as it is the most commonly used SP amongst the organic polymer-based monolith for RP LC for biomolecule analysis [49]. Monolithic columns based on this material have also been utilized both for pre-concentration and analytical separation of peptides and proteins in column switching micro LC [49]. In this study, the PS-DVB monoliths were further developed based on a procedure described by Peroni et al. [50]. 1-decanol was used instead of dodecanol as dodecanol became solid when the room temperature was below 24°C experienced by the previous master student Lene Grutle [8]. The choice of the porogenic solvents selected was based on the solubility of the monomers to enable the polymer phase separation process and to support the formation of a macropores during polymerization [13]. Both dodecanol and 1-decanol can be categorized as bad solvents in the system.

Moreover, acrylate-based monoliths have been successfully used for various applications in the field of chromatography and with adjustable polarity and hydrophobicity [49]. BMA-EDMA monolithic columns are regarded as hydrophobic and were used in previous studies for enrichment of proteins and peptides and therefore chosen. The columns were made as described by Geiser et al. [48] with

small variations of temperature and reaction time, using 70°C overnight instead of 50°C for 72 h. LP was also tested.

PS-DVB-based monoliths are strongly hydrophobic [51] while methacrylate based monoliths are relatively hydrophobic. The hydrophobicity of PS-DVB monolith is higher compared with BMA-EDMA monolith [52].

### 3.5 Effect of polymerization parameters on PS-DVB monolithic structure

Various polymerization parameters were explored in order to fine-tune PS-DVB monolith pore size to effectively trap peptides in a nano LC column switching system.

Vaast et al. [13] reported that many monolithic columns have been prepared using the concentrations described by Svec and Fréchet of 40 wt% monomers, 60 wt% porogens and 1% wt% initiator with respect to monomer content [53]. These concentrations were chosen as a starting point. 50/50 ratio between monomer and crosslinker was chosen as this ratio gave a good outcome obtained by the previous master student Lene Grutle for development of PS-DVB monolithic pre-column [8].

H, pressure, and k are the three main parameters used to evaluate the monolithic columns.

#### 3.5.1 Percentage of good solvent

As described earlier, a good solvent dissolves polymers well, and this gives rise to the late phase separation and a monolith with a large surface area. However, a very high number of mesopores can result in high backpressure. Therefore, the right percentage of the good solvent, toluene, is crucial in order to acquire a monolith with sufficient surface area and a good permeability. The percentages of toluene and 1-decanol were varied to investigate the effects on the monolith porous structure.

**Table 8** shows the concentrations of the initiator, monomers and porogens used. Ratios between the two porogens were varied while the other parameters were kept constant.

**Table 8:** Concentrations of initiator, monomers and porogens used.

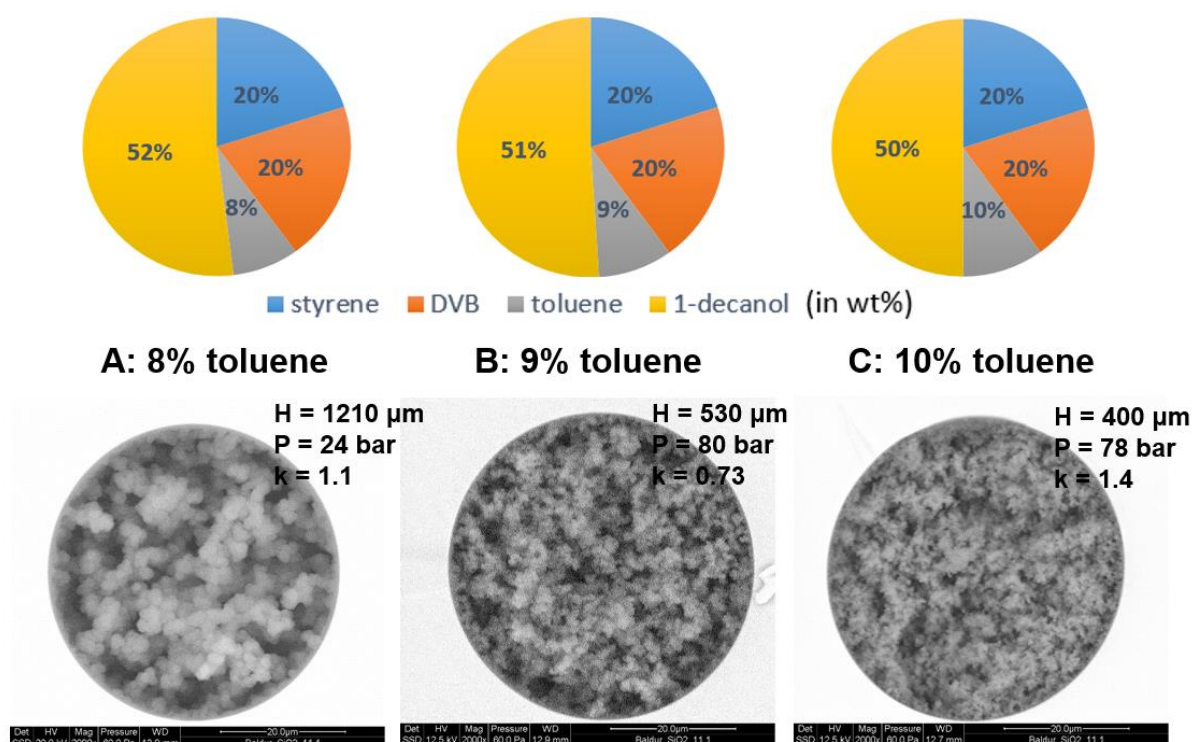
			Weight %	% wt
	Initiator	AIBN	1 <sup>1</sup>	
Monomers <sup>2</sup>	Monomer	Styrene	20	40
	Cross-linker	DVB	20	
Porogens	Good solvent	Toluene	5, 8, 9, 10	60
	Bad solvent	1-decanol	55, 52, 51, 50	

When 5% toluene was used, very little polymerization was obtained (data not shown) whereas 10% toluene resulted in many clogged columns (not open during rinsing) at 74°C. **Figure 21** shows columns' properties and morphologies obtained using 8 - 10% toluene.

---

<sup>1</sup> With respect to monomers

<sup>2</sup> Monomers = monomer and crosslinker



**Figure 21.** SEM pictures showing the effect of good solvent on monolithic structure. The chemical amounts used are found in the figure. 1wt% AIBN with respect to monomers, and at 74°C overnight<sup>3</sup> were used. The polymerization length was 25 cm. The experimental parameters and sample used are found in **Table 3** under LC-UV 1 test system.

By increasing the amount of good solvent by 1%, the overall globule size of the monolith became smaller, and higher efficiencies were obtained. H was the lowest and k was highest at 10% toluene which corresponds to the statement that a higher percentage of good solvent gives rise to a higher surface area. Conversely, the overall globule size and H were largest at 8% toluene. The plate height equation (introduction) suggests a high H when a particle size of a packed column is large, and this corresponds to a high H when monolith globule size is large. According to Vaast et al. the macroporous properties of the monolith affect the magnitude of the A-term [13]. Pressure and k were expected to increase with decreased H, but k was the lowest and pressure was the highest at 9% toluene. The higher pressure could be resulted from structural inhomogeneity of the monoliths. The cause of the lower k could not be determined.

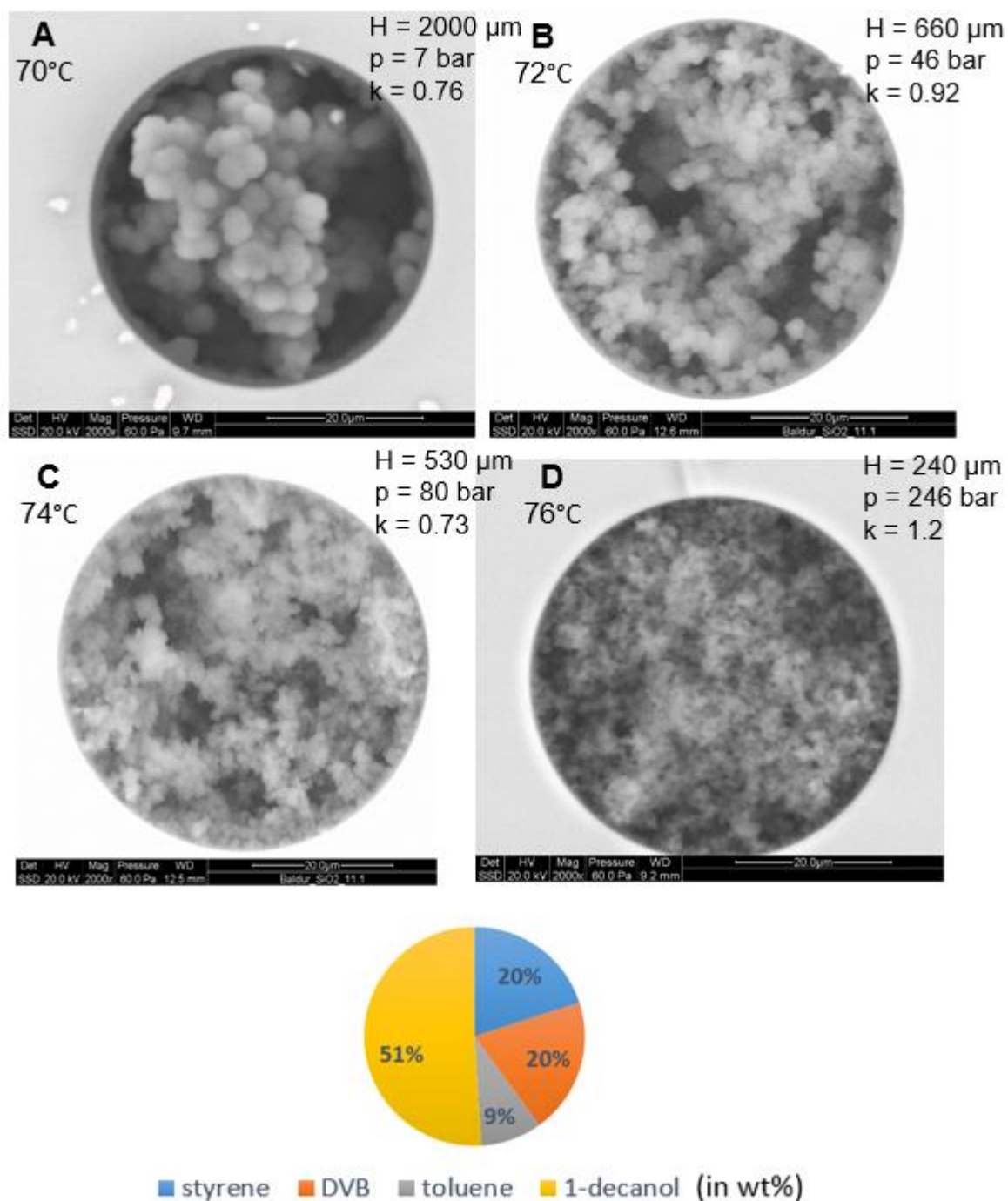
<sup>3</sup> overnight refers to the duration of 16 – 22 hours

*Although columns made with 10% toluene gave the best efficiency, many columns were either clogged or had too high backpressure ( $\geq 300$  bar). Therefore, 9% toluene was to be the starting amount of toluene used in further study.*

### 3.5.2 Temperature

In binary solvent system, high temperature gives rise to a larger number of globules which is compensated by its small size, and so a high number of smaller pores will result [29]. **Figure 22** shows SEM images and efficiencies of the columns made using different temperatures while the other polymerization conditions were kept constant.





**Figure 22.** SEM pictures of monolithic structures made using different temperatures. The amounts of chemical used for all the columns are shown in the figure. 1wt% AIBN with respect to monomers, and overnight were used. The polymerization length was 30 cm. The experimental parameters and sample used are found in **Table 3** under LC-UV 1 test system.

The SEM images show that when the temperature was increased by 2°C, the overall globule size of the monolith became smaller. *In other words, higher temperature used in a binary solvent system for*

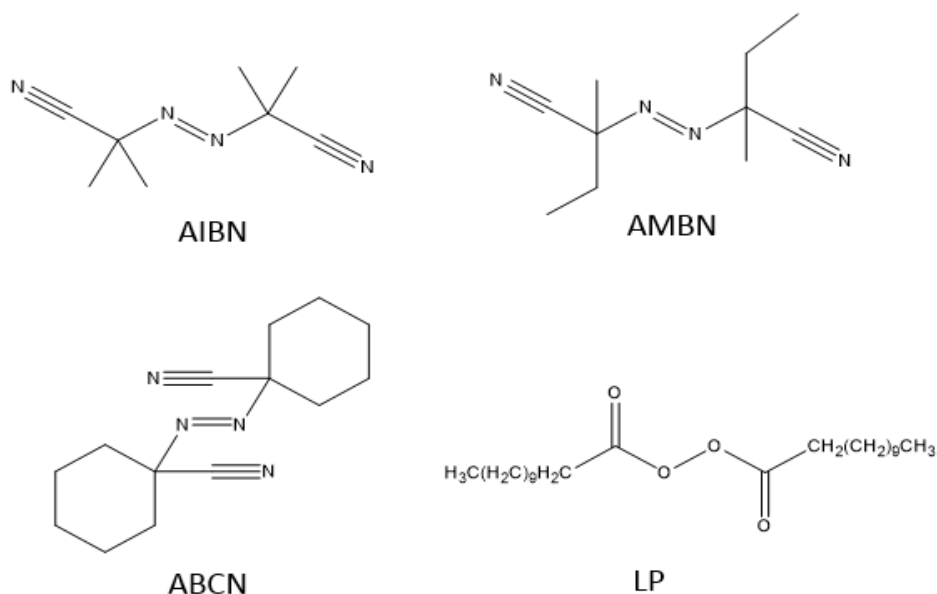
*production of monolith gave rise to a higher surface area monolith as found in many studies.*

Experimental findings conducted by Viklund et al. confirmed that higher temperature lead to a higher distribution of small pores for PS-DVB monolith [29]. This was also evident by the smallest H and the highest pressure obtained at the highest temperature. Higher temperature than 74°C resulted in many clogged columns or open columns with higher backpressures (pressure from 170 – 246 bar for a 10 cm column length). Optimal temperature required for a good monolithic structure may vary according to the type of the initiator used. When a change was made to one variable, adjustments of other variables may be needed to fine-tune the monolith structure. Although the overall globule size of the 74°C appears smaller than those of 70 and 72°C, k value was the lowest.

### 3.5.3 Thermal initiator

As mentioned, AIBN is the most used thermal initiator for preparation of various monolithic columns. It decomposes at a resonably low temperature, and it is soluble in organic solvent. Nevertheless, other thermal initiators can also be used to initiate polymerization. Due to difficulty in finding a supply of AIBN at a reasonable shipping rate at the time, the following initiators: AMBN, ACBN and LP were also tested for a possible replacement. **Figure 23** shows the chemical structures of the initiators. Their half-life temperatures for 10 hours are shown in **Table 9** and was used to give a general idea of a starting temperature to be tested. Using the same amount of each initiator (1 wt% with respect to monomers), each one was tested to find the optimised conditions for monolith with high efficiency and low backpressure. **Figures 24 - 31** show averages H and pressure of columns made with AIBN, AMBN, ABCN, and LP using different toluene percentages and temperatures. The ratio between the two monomers was kept constant at 50/50 and 40% wt between the monomers and porogens. Percentage between toluene and 1-decanol, temperature and the polymerization length (25 cm – 1 m (**Appendix 6.4**)) were varied. Different polymerization lengths were used to find the best technique which was easy to prepare and gave a good column efficiency. It could not be pinpointed that a certain polymerization length was the best for the all columns with repeatable outcomes. There was no trend to suggest that a certain part of the columnm, for example, inlet, middle or outlet gave better efficiency than the others (**Appendix 6.6**). Therefore, the average values of H, pressure and k were calculated and catagorised based on the parameters of initiator, temperature and percentage of toluene used.

The error bars show standard deviations (SD) of three or more columns made under the same polymerization conditions that could be tested.



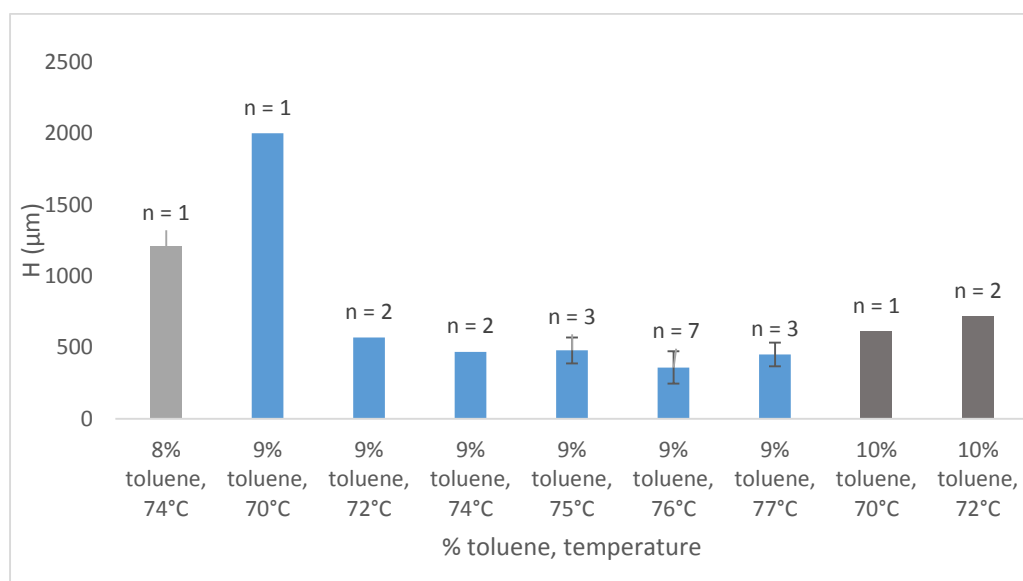
**Figure 23.** Chemical structure of the initiators tested.

**Table 9:** Half-life temperature ( $^{\circ}\text{C}$ ) for 10 hours polymerization of each initiator used. The information was obtained from Perkadox product data sheet.

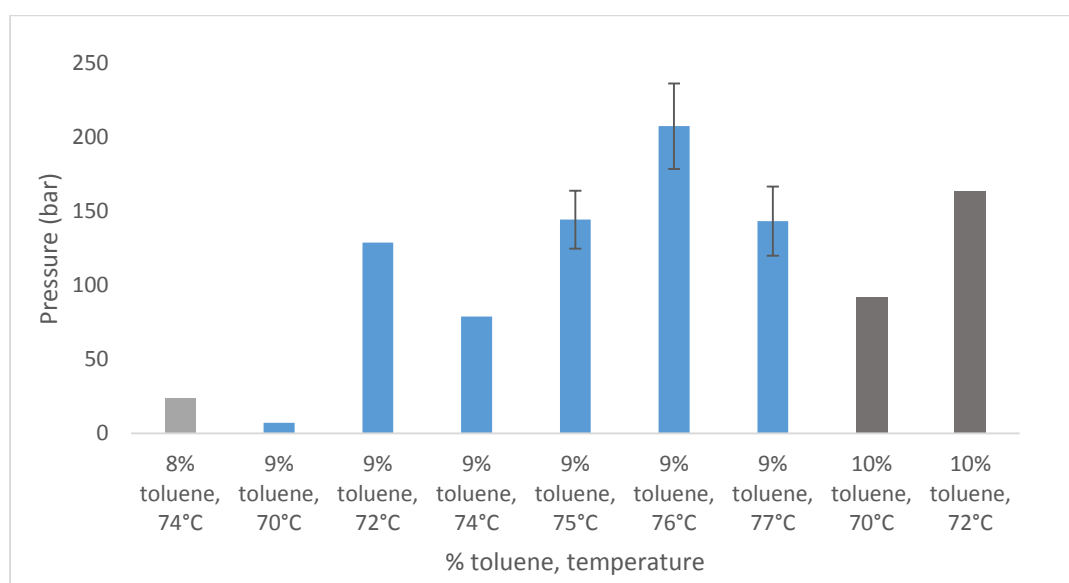
Initiator	Half-life temperature ( $^{\circ}\text{C}$ ) for 10 hours
LP	62
AIBN	64
AMBN	66
ABCN	85

When using a higher temperature, a shorter reaction time is required to decompose half of the initial amount. Other than temperature, the decomposition rate of a thermal initiator depends also on the solvent/monomer system used [54].

### 3.5.3.1 AIBN

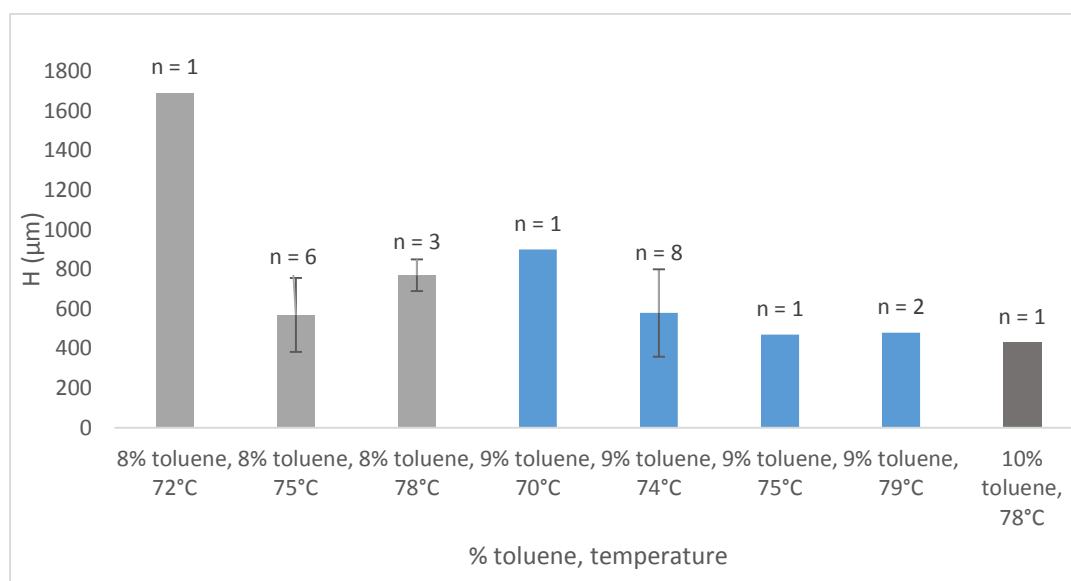


**Figure 24.** Plate height vs polymerization conditions of all columns made using AIBN. The polymerization solution contained: Initiator 1wt% with respect to monomers, 20% styrene, 20% DVB, X % toluene, (60 – X) % 1-decanol, and temperature used are as described. Overnight reaction time was used. The polymerization lengths used are found in **Appendix 6.4**. The experimental parameters and sample used are found in **Table 3** under LC-UV 1 test system. n indicates the number of column tested. SD error bars are given when  $n \geq 3$ .

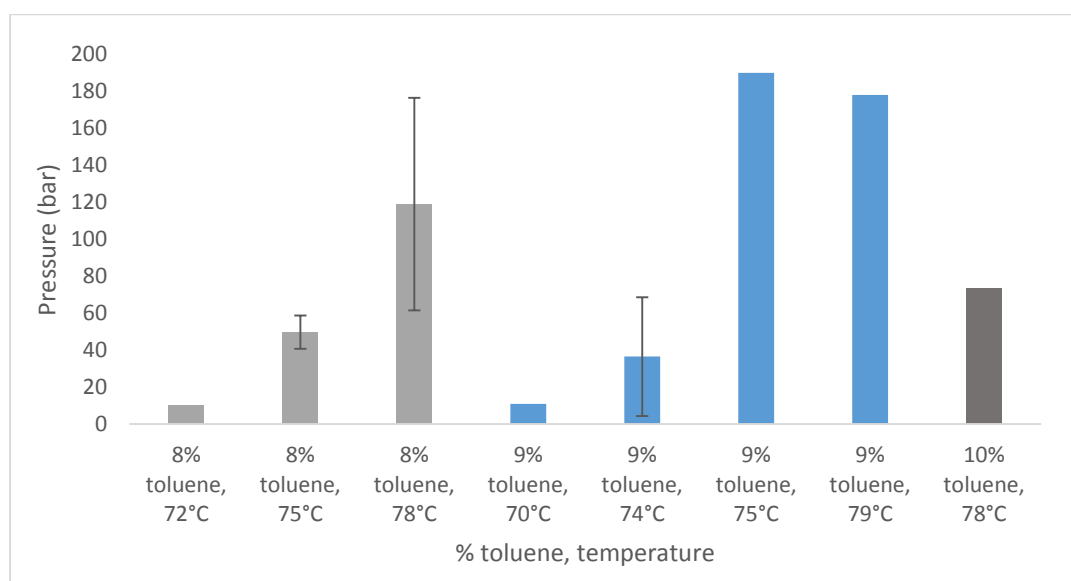


**Figure 25.** Pressure vs polymerization conditions of all columns made using AIBN. See **Figure 24** for all the details regarding polymerization conditions. The LC-UV parameters and sample used are found in **Table 3** under LC-UV 1 test system.

### 3.5.3.2 AMBN

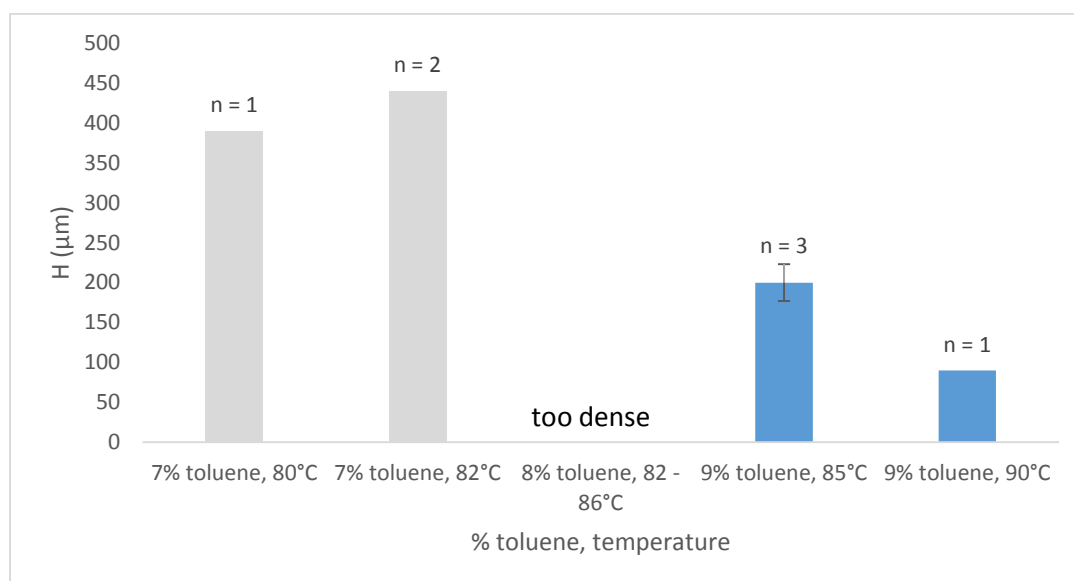


**Figure 26.** H vs polymerization conditions of all columns made using AMBN. See **Figure 24** for all the details regarding polymerization conditions. The LC-UV parameters and sample used are found in **Table 3** under LC-UV 1 test system.

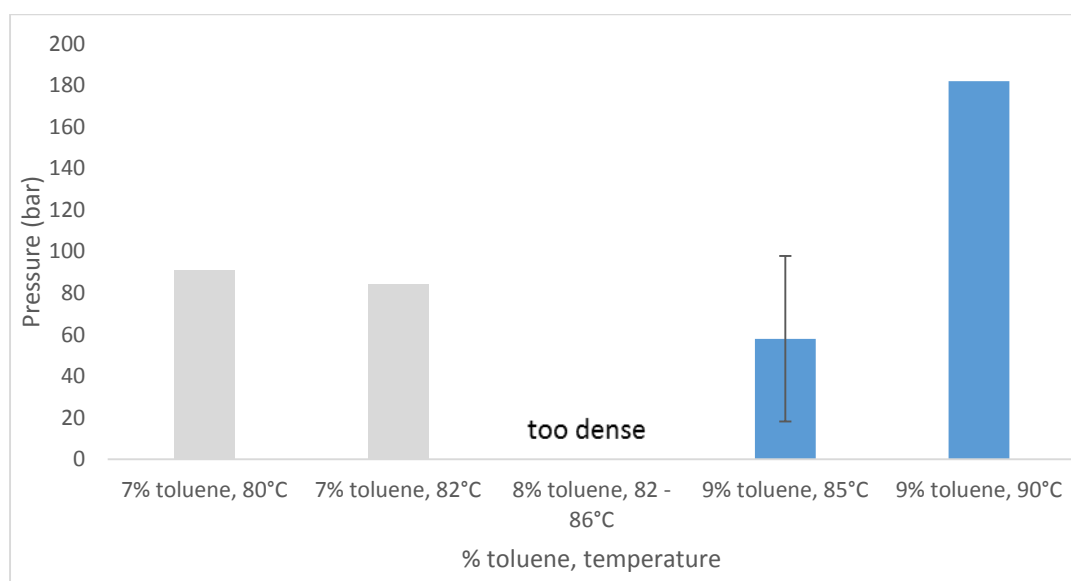


**Figure 27.** Pressure vs polymerization conditions of all columns made using AMBN. See **Figure 24** for all the details regarding polymerization conditions. The LC-UV parameters and sample used are found in **Table 3** under LC-UV 1 test system.

### 3.5.3.3 ABCN

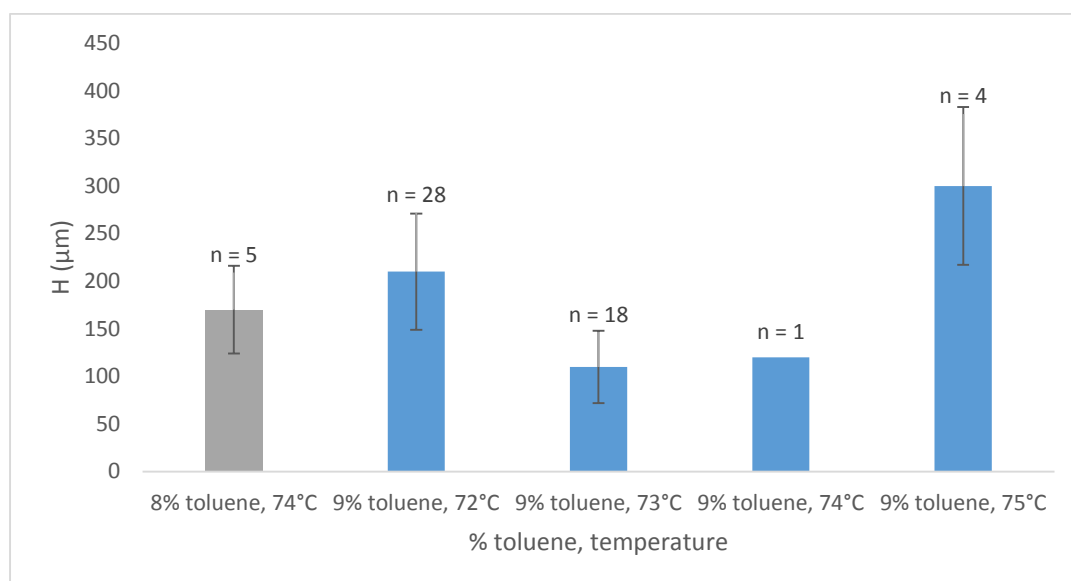


**Figure 28.** H vs polymerization conditions of all columns made using ABCN. See **Figure 24** for all the details regarding polymerization conditions. The LC-UV parameters and sample used are found in **Table 3** under LC-UV 1 test system.

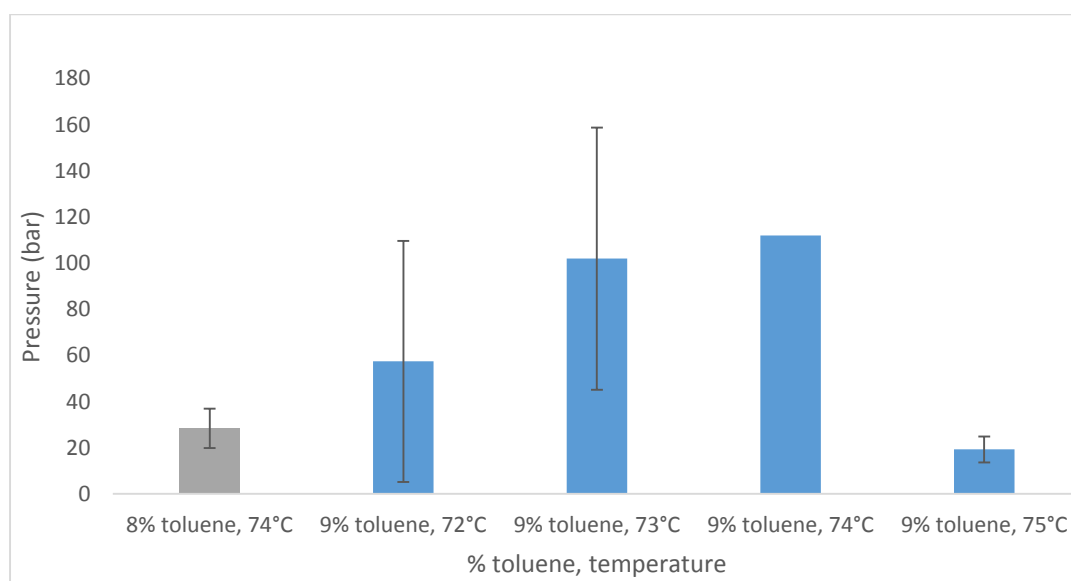


**Figure 29.** Pressure vs polymerization conditions of all columns made using ABCN. See **Figure 24** for all the details regarding polymerization conditions. The LC-UV parameters and sample used are found in **Table 3** under LC-UV 1 test system.

### 3.5.3.4 LP

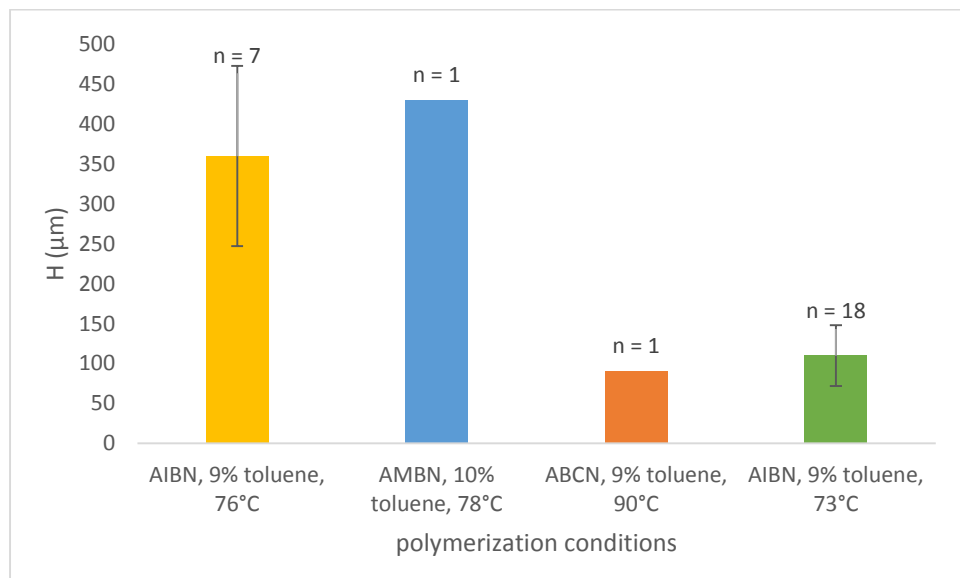


**Figure 30.** H values vs polymerization conditions of all columns made using LP. See **Figure 24** for all the details regarding polymerization conditions. The LC-UV parameters and sample used are found in **Table 3** under LC-UV 1 test system.



**Figure 31.** Pressure vs polymerization conditions of all columns made using LP. See **Figure 24** for all the details regarding polymerization conditions. The LC-UV parameters and sample used are found in **Table 3** under LC-UV 1 test system.

**Figure 32** show the best (average) H vs the polymerization conditions of each initiator. **Figure 33** shows morphologies of the columns made with the best polymerization conditions of each initiator.



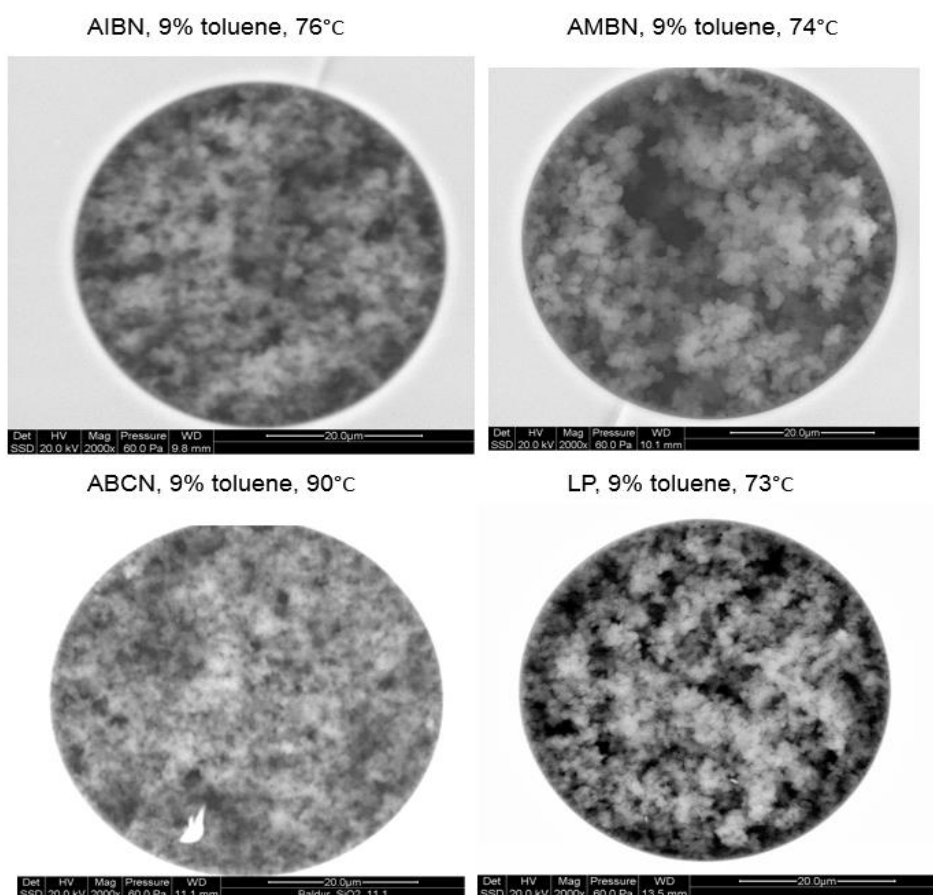
**Figure 32:** The best (average) H vs the polymerization conditions of each initiator. See **Figure 24** for all the details regarding polymerization conditions used. The LC-UV parameters and sample used are found in **Table 3** under LC-UV 1 test system. When n = 1 that was because the other columns made under the same polymerization conditions were either clogged or gave too high backpressure.

From **Figure 32**, it can be seen that the lowest H of 90 μm was obtained with ABCN. However, it was the only column with backpressure below 300 bar out of five columns made (in the same/different batch) using the same polymerization conditions. **Figures 28 – 29** show no results for 8% toluene at 82 – 86°C as all the columns made under these conditions were either clogged or gave too high backpressure. The polymerization conditions that gave the lowest H using ABCN did not give a repeatable outcome, and so ABCN was not further tested. If setting ABCN aside, the columns made with LP gave the lowest average H of 110 μm at reasonable backpressures. To this point, it was the best polymerization conditions found. Columns which give a better average efficiency may be obtained if a further fine-tuning of the polymerization conditions such as a use of different initiator concentration for LP was performed. An obstacle may be a difficulty in obtaining the conditions combining with the technique which give a good repeatability of a homogeneous monolith for every column in every batch. The efficiency was compared to that obtained by the previous master student Lene Grutle [8] and found it to be satisfactory. There was no correlation between efficiency



and backpressure found for any of the initiators used. Some columns that gave small H gave also lower pressure compared with columns that gave larger Hs gave also higher backpressures. Columns made with the same polymerization conditions but of different part, replicate or batch resulted in variation of H values. This was likely caused by the structural inhomogeneity. Retention factors,  $k$ , were similar for all initiators and they were in the range 0.78 – 1.8 with the average of around 1.2 for each initiator. There was no trend to suggest that increasing the good solvent concentration and/or temperature would increase or decrease  $k$  values.

*Since different initiators gave different efficiencies, it can be concluded that the column's efficiency is initiator dependent. The effect of the initiator type on monolith structure has not been indicated in other studies. It can be concluded that LP was the best initiator as many columns with small Hs at reasonable backpressures were obtained.*



**Figure 33.** SEM pictures of the columns made under the best polymerization conditions of each initiator.

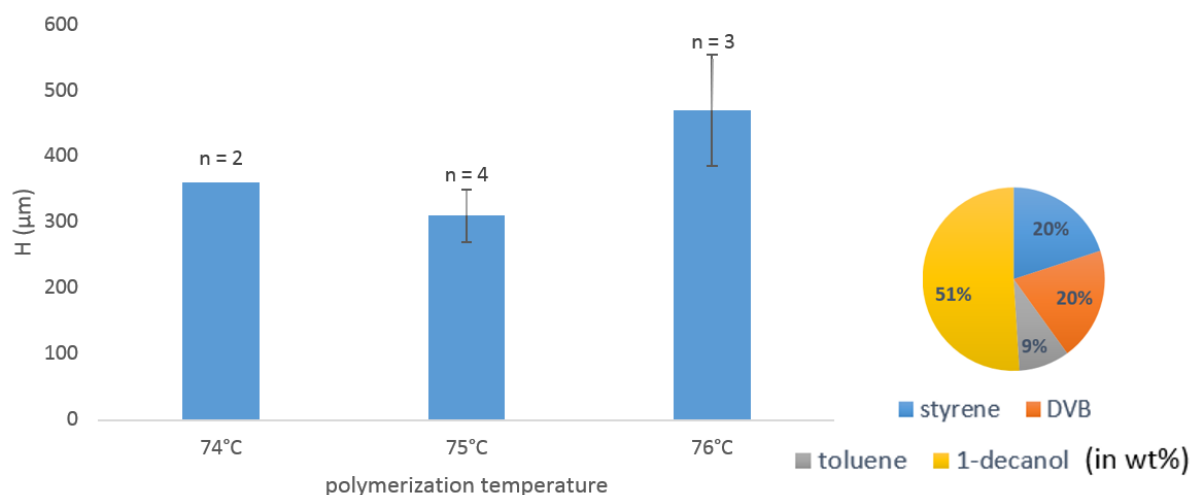
### 3.5.4 Initiator concentration

As an initiator concentration of 1 wt% of monomers weight was used to produce monolithic columns in many studies, 4.0 mg of each initiator (40% monomers) was used in earlier experiments. This amount, however, does give different amounts in millimoles (mmol) for different initiators. **Table 10** shows 4.0 mg amount in mmol of each initiator.

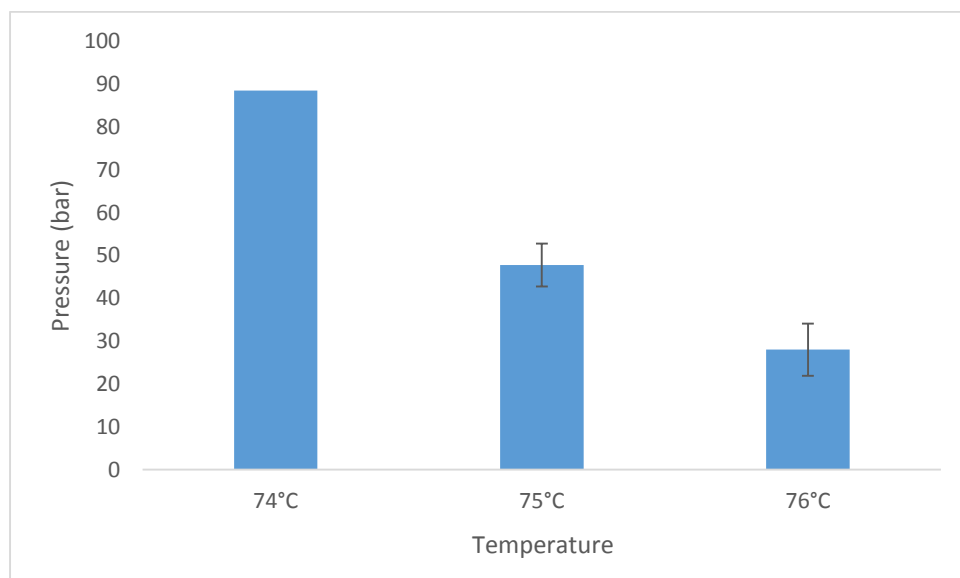
**Table 10.** Amount in mmol of 1 wt% initiator with respect to monomers.

Initiator	Molar mass (g/mol)	Mmol of 4.0 mg initiator
AIBN	164.21	0.0244
AMBN	192.30	0.0208
ABCN	244.34	0.0164
LP	398.62	0.0100

From the previous experiment, LP was considered the most promising initiator followed by AIBN. 0.01 mmole amount (~2 mg) of AIBN corresponding to the 0.0100 mmol amount of LP was investigated in order to see if the amount (mmol) or type of initiator would give a different in efficiency or backpressure. **Figure 34 - 35** show average H and pressure of columns made with 2 mg AIBN using different temperatures. The amounts of the chemical used was based on those that gave the best average efficiency in the previous experiment.



**Figure 34.**  $H$  vs polymerization temperature of columns made using 2.0 mg AIBN. The chemical contents and temperature used are shown in the figure. 50 cm polymerization length was used. The LC-UV parameters and sample used are found in **Table 3** under LC-UV 1 test system.  $n$  indicates the number of column tested. SD error bars are given when  $n \geq 3$ .

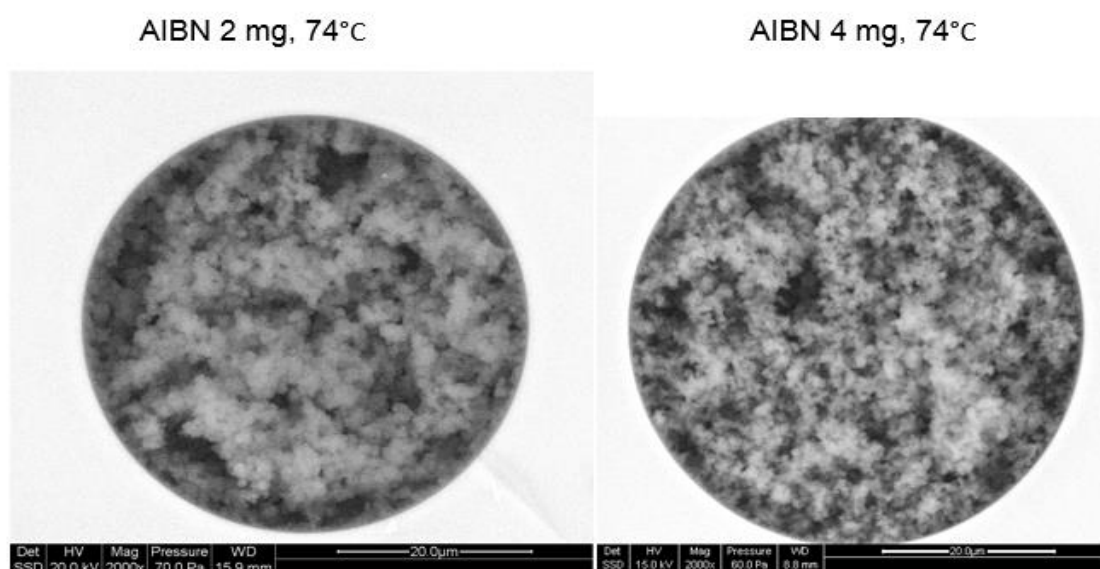


**Figure 35.** Pressure vs polymerization temperature of columns made using 2.0 mg AIBN. See under **Figure 34** for all the details regarding polymerization conditions. The LC-UV parameters and sample used are found in **Table 3** under LC-UV 1 test system.

From **Figure 34**, it can be seen that the smallest average H of 310  $\mu\text{m}$  was obtained when using 2 mg AIBN. This value is not greatly lower than 360  $\mu\text{m}$  (lowest average H of AIBN) which was obtained with using 4 mg AIBN.

*Hence, using 2.0 mg or 4.0 mg of AIBN did not greatly affect column efficiency. This confirms that LP was a better initiator than AIBN when the same amount in mmol was used.*

**Figure 36** shows the monoliths morphologies produced with 2 and 4 mg AIBN, respectively. The SEM images revealed that 4 mg AIBN gave overall smaller pores. This could be attributed to an increase in number of free radicals. According to Danquah and Forde [36], increasing initiator concentration (AIBN) from 0.5% (monomer w/w) to 1.5% (monomer w/w) resulted in the decrease of monolith pore size from 980 nm to 410 nm. Monolith with a larger surface area should give smaller H, but inhomogeneity of the monoliths may be the reason for the slightly larger average H with 4 mg AIBN. Experiments conducted by Vaast et al. lead them to conclude that the structural inhomogeneity of smaller macropore size can be caused by formation of domain of larger agglomerates composed of very small globules [13]. k values were similar for both the amounts, and this did not confirm that the surface area of 4.0 mg AIBN was larger.



**Figure 36.** SEM pictures of monoliths produced using 2 and 4 mg AIBN. Polymerization solution used are as described in **Figure 34**. The reaction temperature was 74°C overnight.

### 3.5.5 Monomer to porogen ratio

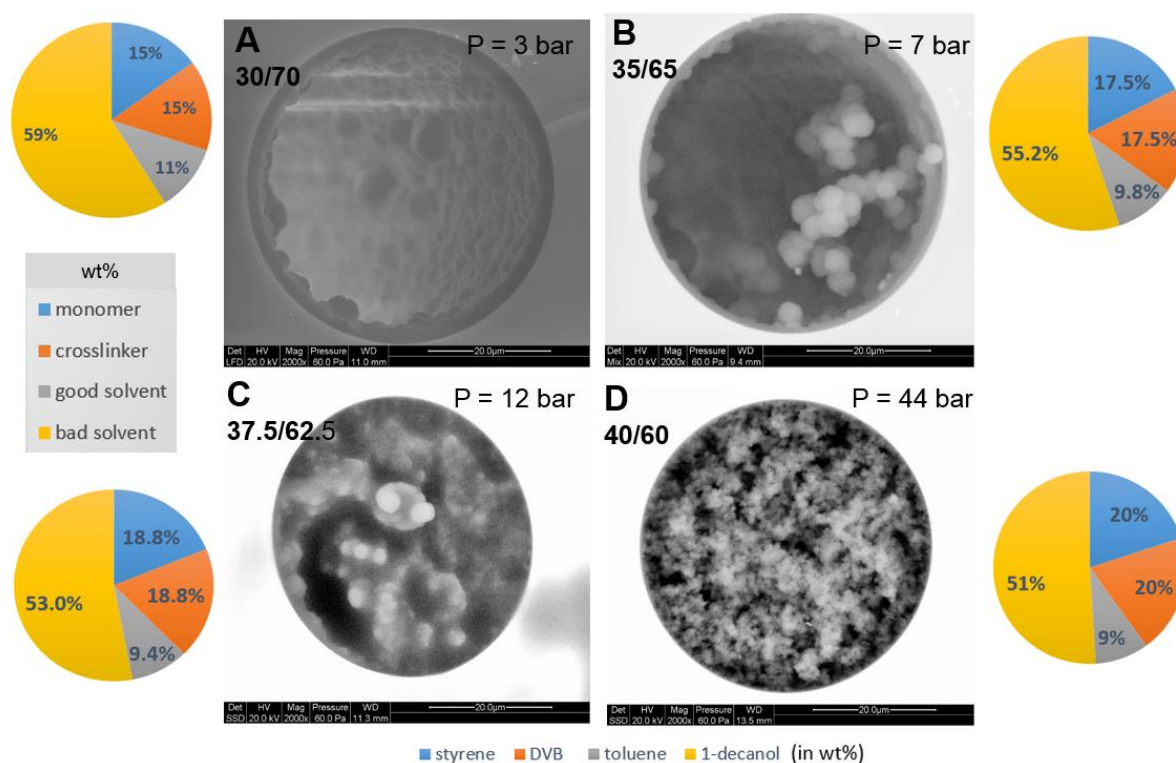
An optimal ratio between monomer and porogen is crucial for a good permeability and rigidity of the monolithic structure. Yuanyuan et al. suggested the monomer/porogen ratio to not exceed 50% to obtain good permeability, and to not be too low to obtain a good surface density and rigidity [55]. In order to find-tune the ratio that gives the best monolith with a rigid structure and reasonable backpressure, different percentages of monomers/porogens were investigated. **Table 11** shows the ratios between monomers and porogens used.

**Table 11.** Percentages of monomers to porogens tested.

<b>Monomers</b> Styrene/DVB (50/50) w/w	30	35	37.5	40
<b>Porogens</b> Toluene/ 1-decanol (15/85) w/w	70	65	62.5	60

The ratios between each monomer and porogen were kept constant at 50/50 and 15/85 respectively, while the ratios between monomers and porogens were varied.

**Figure 37** shows SEM images of monolithic columns made with the described monomers/porogens ratios. Other polymerization conditions used was based on the columns with a low average H obtained from the previous experiments. When 30/70 of monomers/porogen was used, a PLOT structure was obtained. By increasing the ratio of monomers/porogens, the number of globules increased. At 40/60 ratio, a complete monolithic structure was obtained. Due to a reasonable high backpressure and a complete structure of monolith formed, not more than 40/60 was further tested. This ratio was then used further in this study.



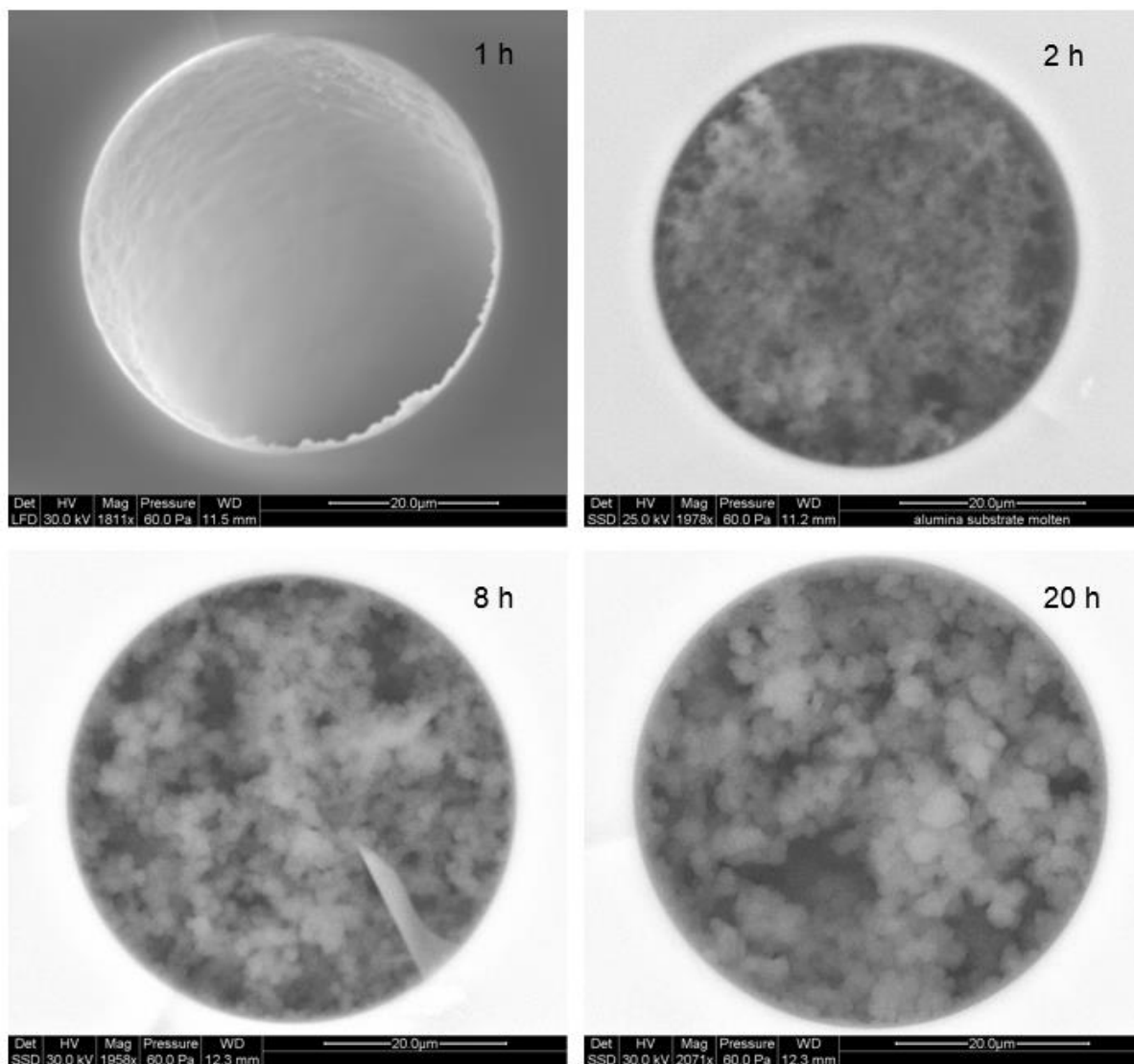
**Figure 37.** SEM pictures of PS-DVB columns of different monomers/porogens ratios. The chemical contents used are shown in the figure. At 73°C overnight and column polymerization length of 50 cm were used. The LC-UV parameters used are found in **Table 3** under LC-UV 1 test system.

*From the SEM images and the pressure testing, it can be concluded that the monomer/porogen ratio of 40/60 as used in many studies for production of monolithic columns provided the best monolithic structure at a reasonable backpressure.*

### 3.5.6 Reaction time

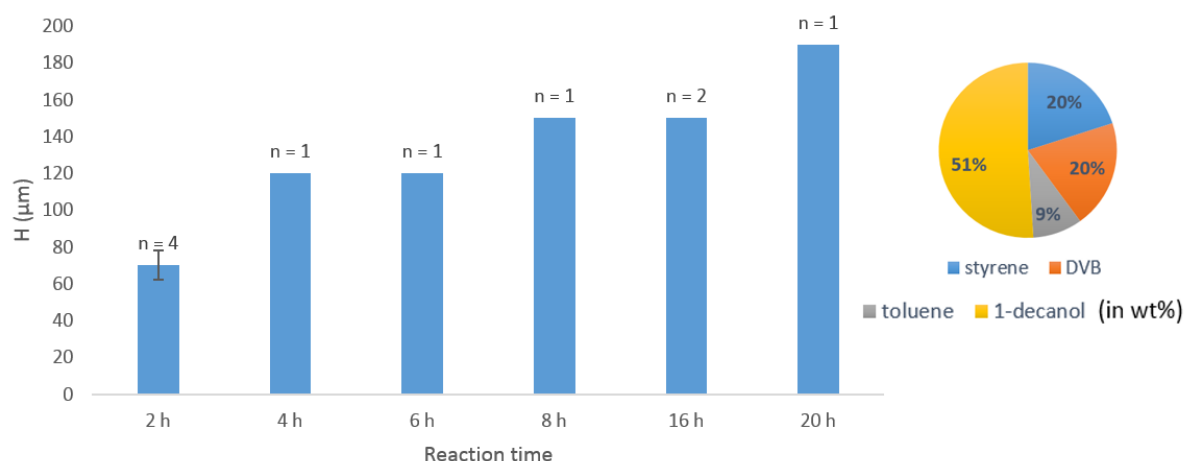
In some studies, reaction time was found to be the parameter which causes a major change in efficiency and permeability of the monoliths [41-43, 56]. Hence, effect of reaction time was also examined. Using the polymerization conditions (other than the temperature) which gave the most efficient monoliths (**Figure 32** see discussion about why ABCN was not chosen), reaction times of 1, 2, 4, 6, 8, 16, 20 and 24 h were investigated. Reaction temperature of 72°C was chosen instead of 73°C since it gave a much lower average pressure. **Figure 38** shows SEM images of the monolithic columns of some reaction times which show major differences in the structures. **Figure 39 – 41** show

averages H, pressure and k at different reaction times. Two replicates were made for 2 h reaction time since a short reaction time yielded monoliths with a high surface area in some studies.

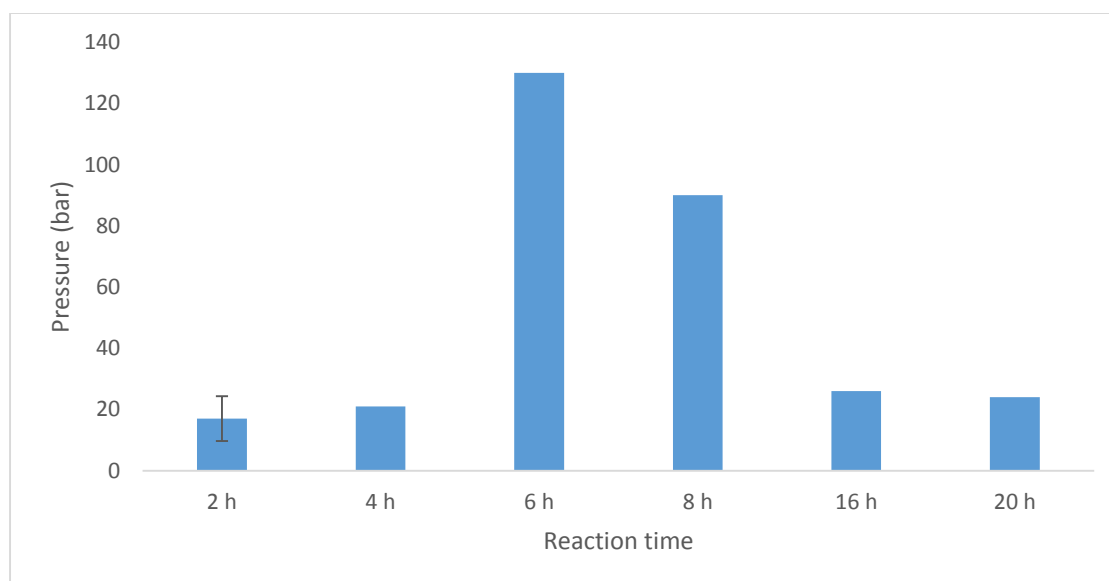


**Figure 38.** SEM images of the monolithic columns using different reaction times. The polymerization conditions used are described in the next figure (**Figure 39**).

From the SEM images, it is clear that a minimum reaction time of 2 h is required at 72°C in order to obtain a monolithic structure in a 50 μm ID capillary column. The SEM images show that the overall globule size of 2 h reaction time appears to be the smallest, and this should indicate the highest surface area.

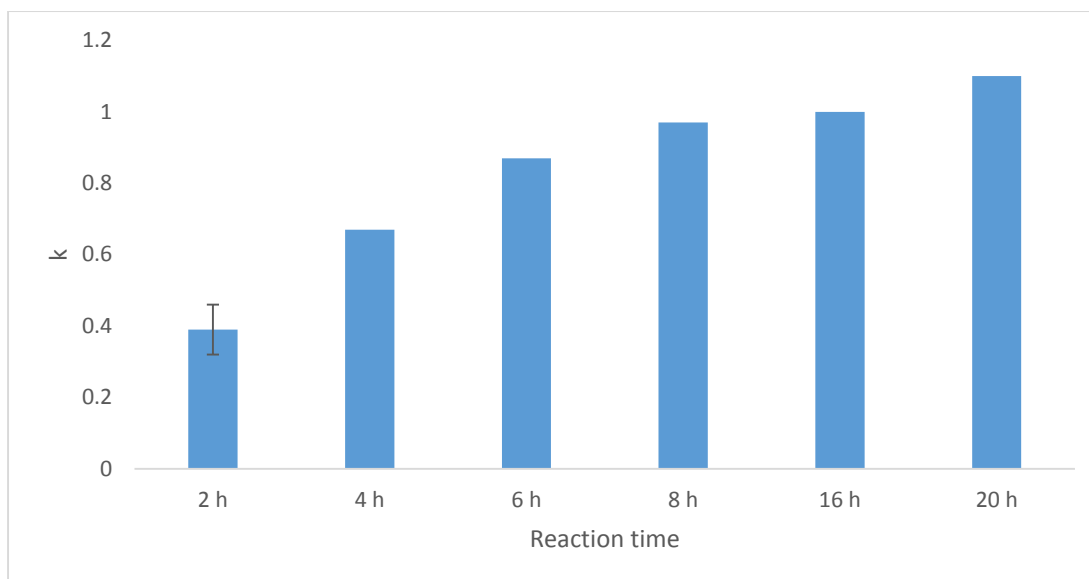


**Figure 39.**  $H$  vs reaction time. The conditions that gave good efficiency for LP (1 wt% with respect to monomers) from pervious experiments were used (shown in figure). Reaction times are as stated ( $72^\circ\text{C}$ ). The polymerization length was 30 cm. The experimental parameters and sample used are found in **Table 3** under LC-UV 1 test system.  $n$  indicates the number of column tested. SD error bars are given when  $n \geq 3$ .



**Figure 40.** Pressure vs reaction time. Polymerization conditions used are described in **Figure 39**. The experimental parameters and sample used are found in **Table 3** under LC-UV 1 test system.  $n$  indicates the number of column tested. SD error bars are given when  $n \geq 3$ .





**Figure 41:** k vs reaction time. Polymerization conditions used are described in **Figure 39**. The experimental parameters and sample used are found in **Table 3** under LC-UV 1 test system. n indicates the number of column tested. SD error bars are given when  $n \geq 3$ .

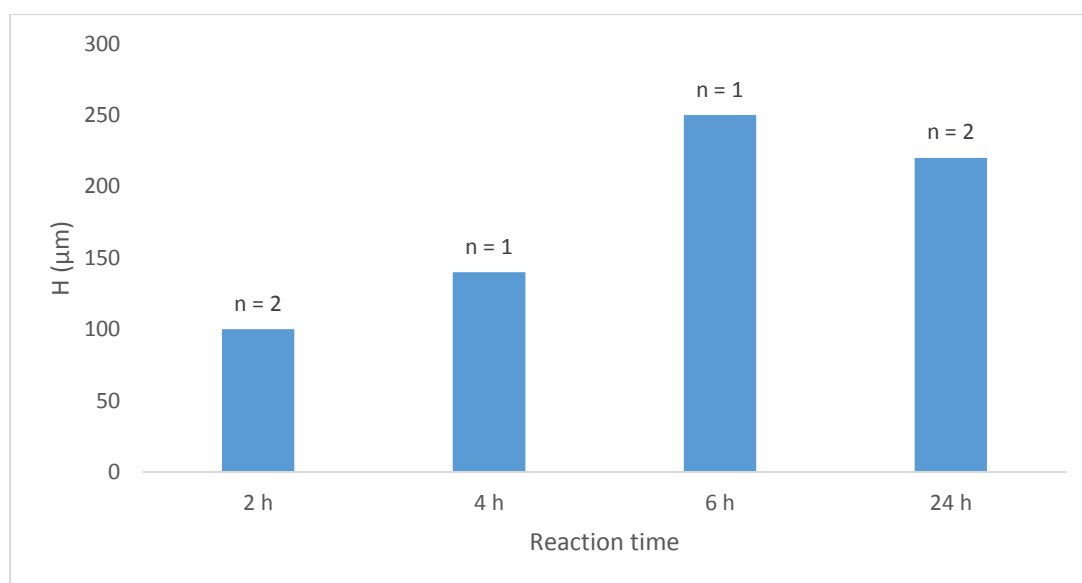
From **Figure 39**, it can be seen that H increased with increased reaction time. A higher crosslinker conversion for short polymerization time is most likely to be the reason for an increase in monolith surface area with a decrease in polymerization time [40]. According to Maya and Svec [43] increasing polymerization time lead to decreasing surface area of the monolithic structure in their findings. Moreover, the backpressures were also lowest at 2 h. Greiderer et al. concluded that shortening the polymerization time increased surface area as the amount of mesopore increased, and the permeability was also increased [56]. Increased polymerization times lead to larger heterogeneous globular structure, growth of polymer material at the column wall and three-dimensional inter-adherence [44] which may be responsible for higher H (larger A term) and backpressure.

*The surface area and permeability were maximised at 2 h reaction time as the lowest Hs and backpressures were obtained. These properties deteriorated as the reaction time increased.*

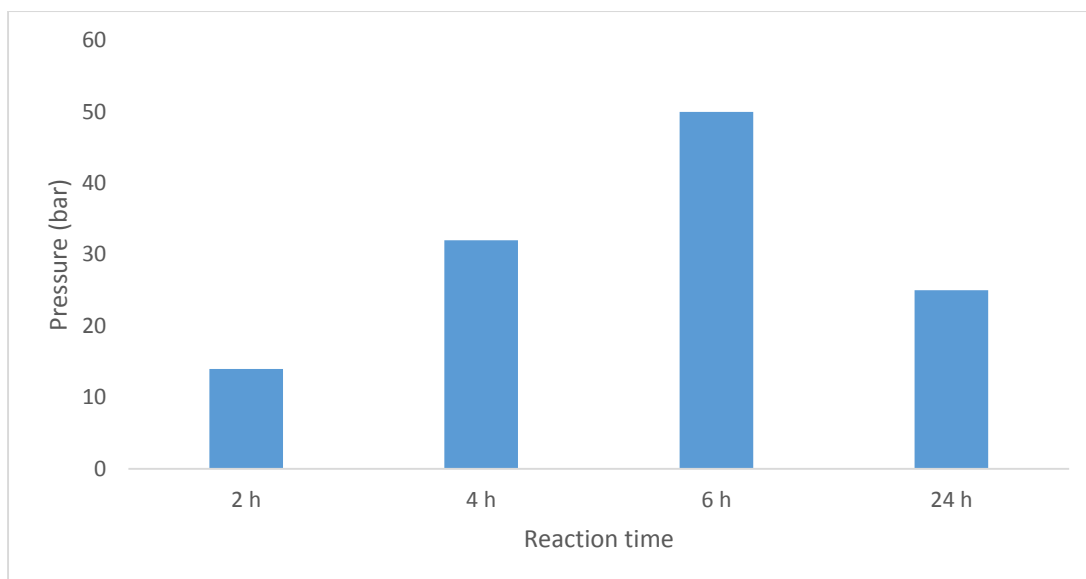
The lowest k and pressure obtained from the 2 h reaction time did not confirm that the monolith had the highest surface area. k value increased with increased reaction time (**Figure 41**). According to Bruchet et al. high retention factors illustrate the high surface area of the monolith [57]. Vaast et

al. stated that by reducing the size of the globules, the plate height will decrease at the expense of column permeability [13]. Therefore, a higher surface area monolith was expected to give smaller  $H$ , and higher pressure and  $k$  which was not obtained. The cause of this variation could not be determined. Nevertheless, the main purpose of this study was to find a monolith that gives a low  $H$  for small molecule at a reasonable backpressure to be tested further with peptides which was achieved here.

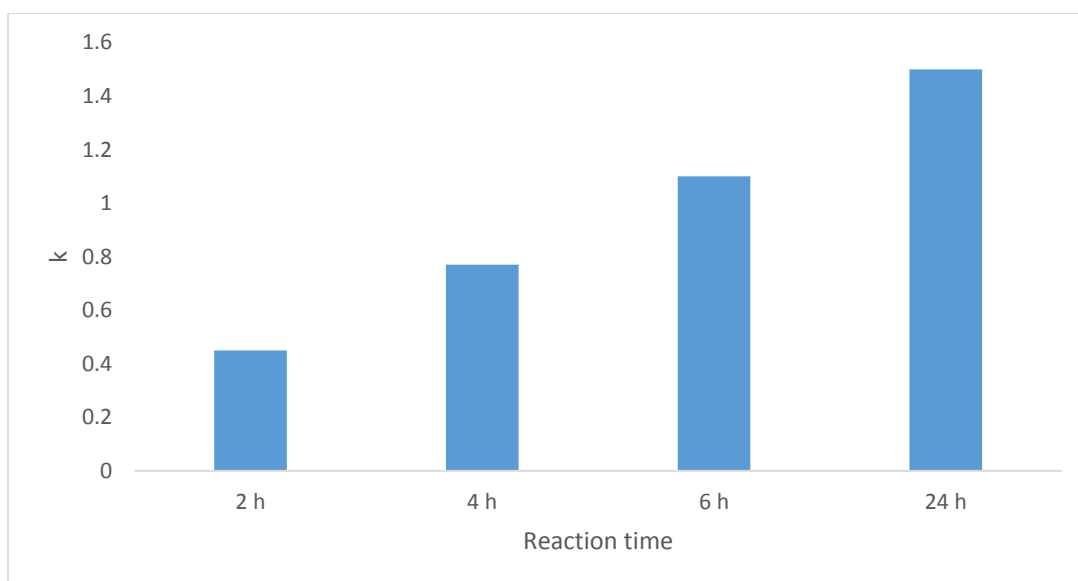
The experiment was repeated using manual filling of the polymerization solution by a syringe instead of the bomb system to see if this would improve the homogeneity of the monolithic structure. 72°C reaction temperature was chosen since it gave satisfactory  $H$  values in the previous experiment. Due to clogged columns of some of the reaction times, only columns of 2, 4, 6 and 24 h reaction times were obtained. **Figures 42 – 44** show averages  $H$ , pressure, and  $k$ , respectively.



**Figure 42.**  $H$  vs reaction time (manual filling used). Polymerization conditions used are described in **Figure 39**. 30 cm polymerization length was used. The experimental parameters and sample used are found in **Table 3** under LC-UV 1 test system.

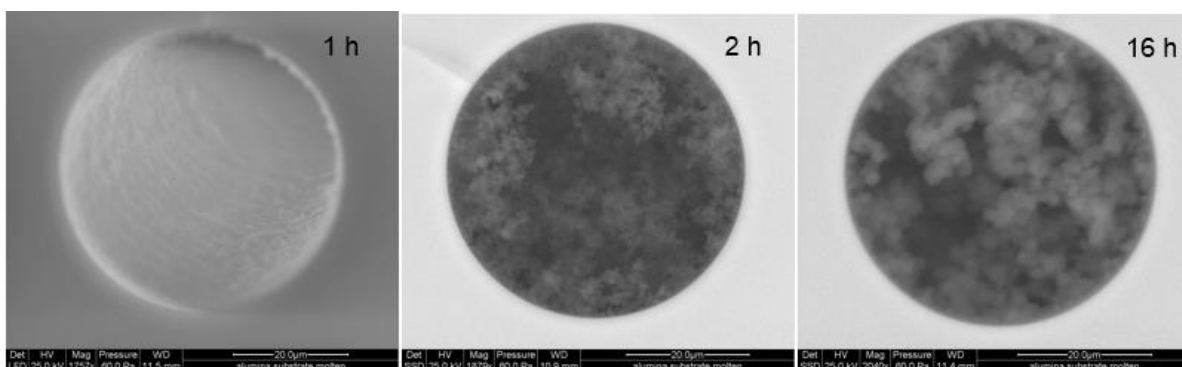


**Figure 43.** Pressure vs reaction time (manual filling used). Polymerization conditions used are described in **Figure 39**. The experimental parameters and sample used are found in **Table 3** under LC-UV 1 test system.



**Figure 44.** k vs reaction time (manual filling used). Polymerization conditions used are described in **Figure 39**. The experimental parameters and sample used are found in **Table 3** under LC-UV 1 test system.

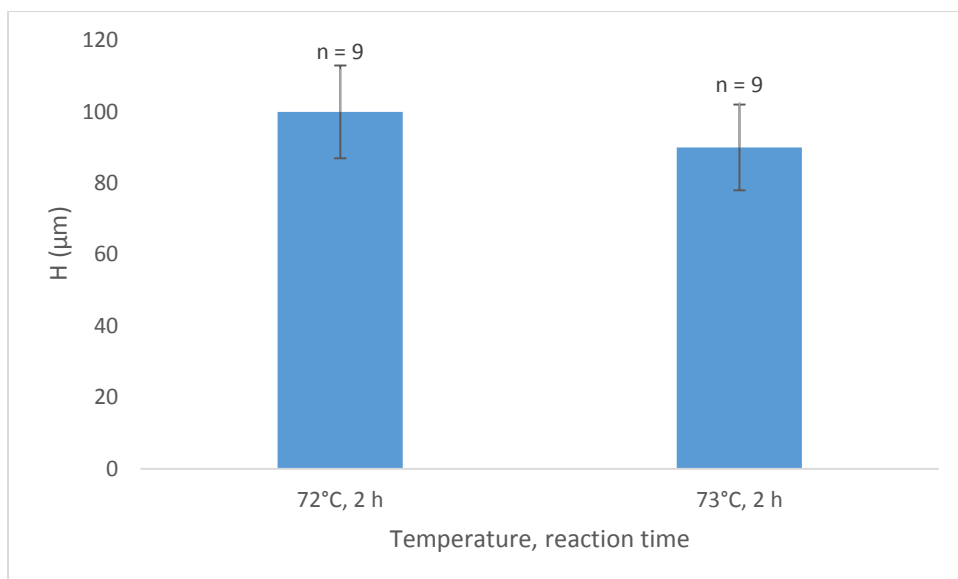
**Figure 45** shows SEM images of the monolithic columns of some reaction times that show major differences in the structures.



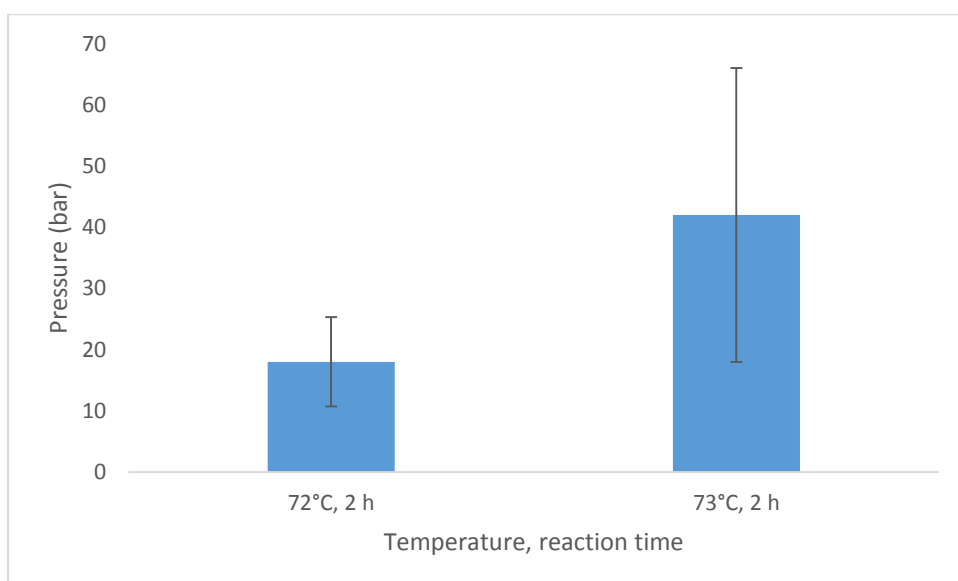
**Figure 45.** SEM images of PS-DVB monoliths prepared with different reaction times. Polymerization conditions used are described in **Figure 39**. Manual filling of polymerization solution was performed.

The 2 h reaction time still gave the lowest plate heights and the lowest backpressures. Longer reaction time gave increase plate heights and larger overall globule size. Uneven distribution of large voids in the monoliths (**Figure 45**) suggest structure inhomogeneity. Therefore, columns filled using a syringe did not improve homogeneity of the monolith structure.

Since LP (1% wt of monomers), 20% styrene, 20% DVB, 9% toluene, 51% 1-decanol at 72°C, and 2 h polymerization times gave the lowest average plate height and backpressure, these polymerization conditions were repeated to test for repeatability. 73°C reaction temperature was also used to see the effect on monolithic properties. A polymerization length of 33 cm was used so that three parts of the column could be tested ( $3 \times \sim 10$  cm). Different parts of each replicate (inlet, mid and outlet) were also noted (**Appendix 6.6**). Three replicates were prepared for both temperatures. **Figures 46 - 47** show averages H and pressure of each reaction temperature.



**Figure 46.** H vs reaction time (column repeatability testing). Chemical contents used are described in **Figure 39** using 72 and 73°C polymerization temperature for 2 h. The experimental parameters and sample used are found in **Table 3** under LC-UV 1 test system. n indicates the number of column tested. SD error bars are given when  $n \geq 3$ .



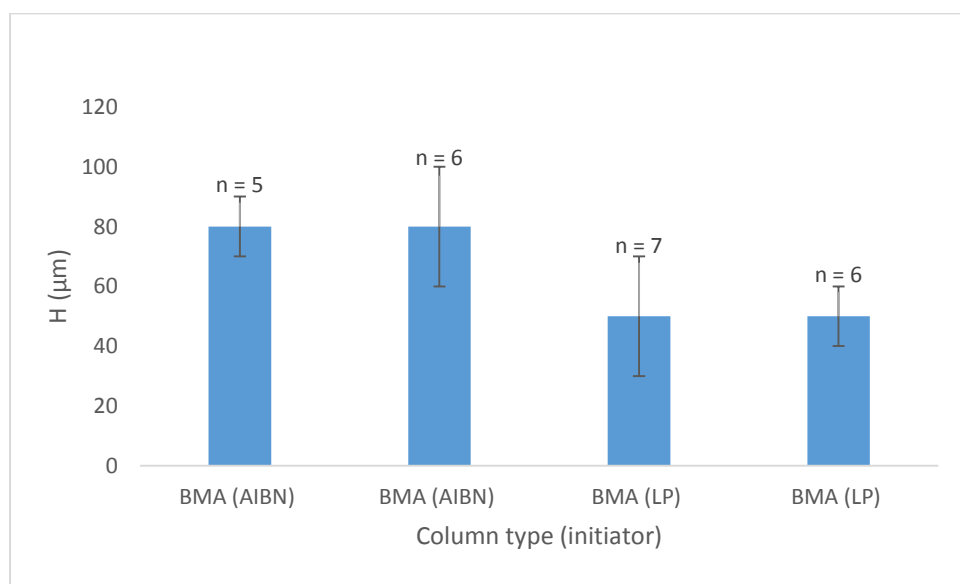
**Figure 47.** Pressure vs reaction time (column repeatability testing). Chemical contents used are described in **Figure 39** using 72 and 73°C polymerization temperature for 2 h. The experimental parameters and sample used are found in **Table 3** under LC-UV 1 test system. n indicates the number of column tested. SD error bars are given when  $n \geq 3$ .

Similar plate heights and pressures were obtained from this batch compared with the two previous batches. This shows that these polymerization conditions can produce monolithic columns with similar properties, and hence the repeatability is promising. From **Figure 46**, it can be seen that the difference of 1°C almost did not affect the efficiency. The average pressure is, however, double as high with 73°C. Hence, control of temperature is also important to obtain repeatable columns.

Percentage relative standard deviation (%RSD) of H for all the columns (3 batches) produced under the conditions described in **Figure 39** is 16% (**Appendix 6.7**) which was considered acceptable.

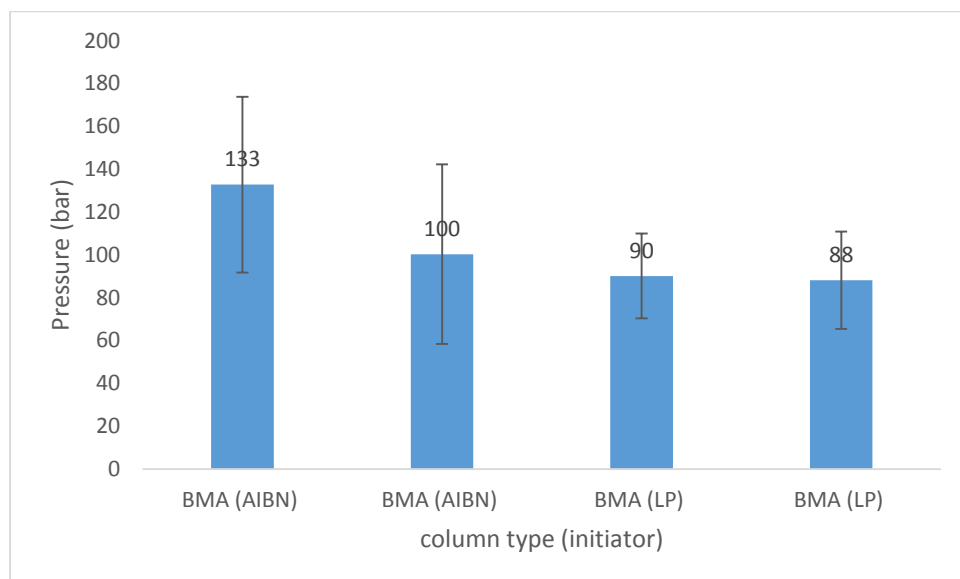
### 3.6 BMA-EDMA monolith

For comparison, BMA-EDMA monolithic columns (50  $\mu\text{m} \times 10\text{ cm}$ ) were produced using the procedure described by Geiser et al. [48]. Temperature of 70°C and overnight reaction time were used instead of what is described. AIBN was used as in the original procedure, but LP was also investigated since it gave good results for PS-DVB monoliths. **Figures 48 – 49** show the averages H and pressure of BMA-EDMA monoliths made with AIBN (two different batches) and LP (two replicates of one batch).



**Figure 48.** H of BMA-EDMA columns made using AIBN or LP. Only the first batch (1<sup>st</sup> column) of BMA-EDMA (AIBN) was produced using a 60 cm polymerization length whereas the rest was produced

using 1 m. The second batch (2<sup>nd</sup> column) of BMA-EDMA (AIBN) columns was produced by Ole Kristian Brandtzæg. The LC-UV parameters and sample used are found in **Table 3** under LC-UV 1 test system. n indicates the number of column tested. SD error bars are given when n ≥ 3.



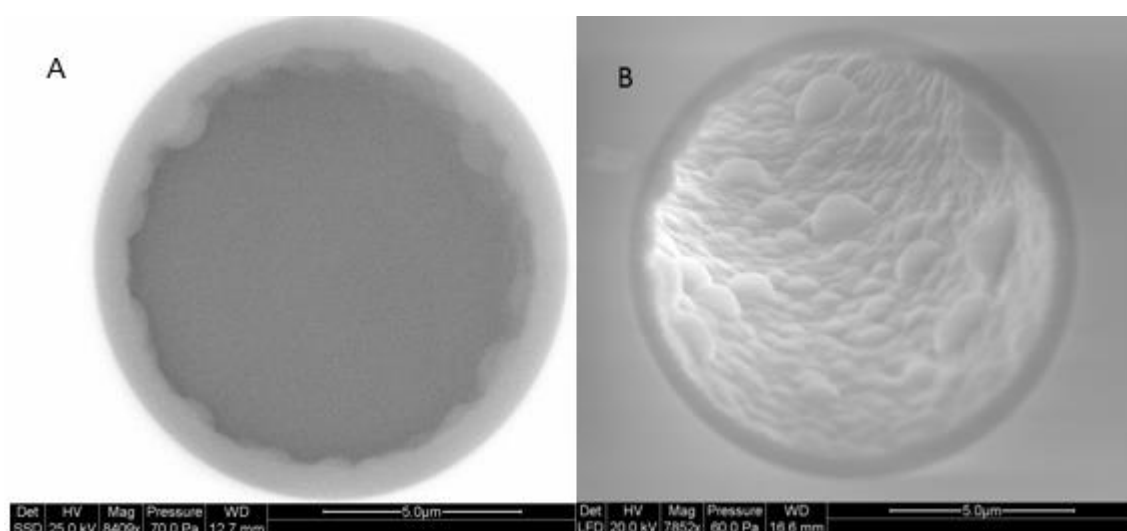
**Figure 49.** Pressure of BMA-EDMA columns made using AIBN or LP as initiator. The LC-UV parameters and sample used are found in **Table 3** under LC-UV 1 test system. n indicates the number of column tested. SD error bars are given when n ≥ 3.

The BMA-EDMA monolithic columns made using LP gave better average efficiencies than those made using AIBN. Pressures and k values (**Appendix 6.8**) were quite similar for all the columns. The average H of the best polymerization conditions found for PS-DVB monoliths was about double as high as the average H obtained from the BMA-EDMA columns both using LP. The average pressure of the PS-DVB was, however, much lower (see under Reaction time). The k values were similar for both the PS-DVB (2 h reaction time) and BMA-EDMA columns.

*BMA-EDMA monolithic columns made with LP gave lower average H for toluene than the most effective PS-DVB monoliths but with a much higher backpressure. The average H of effective PS-DVB monoliths on toluene was 90 μm.*

### 3.7 PLOT analytical column

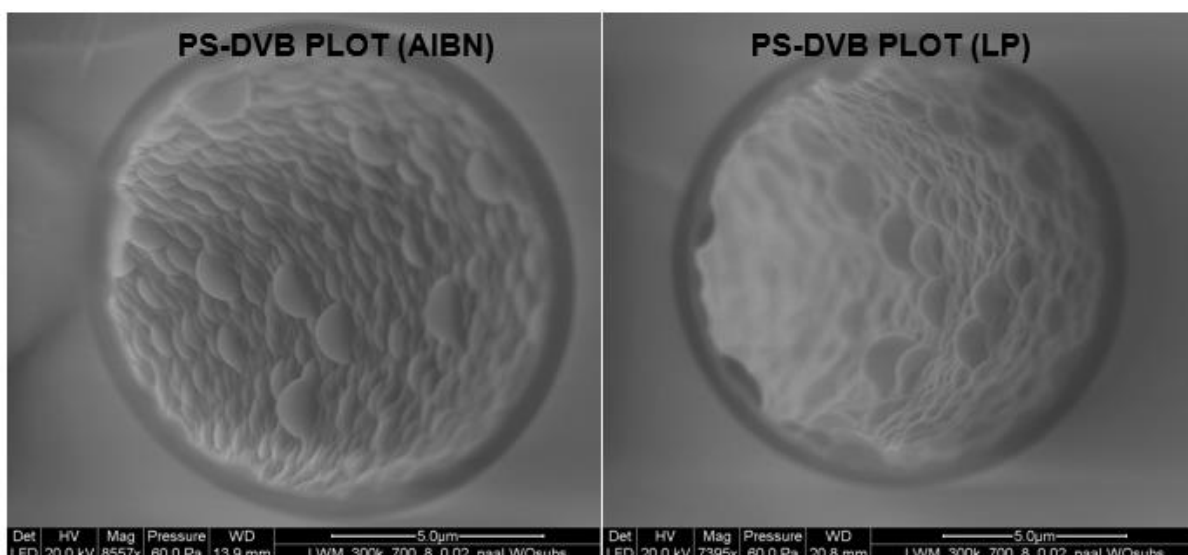
PLOT analytical columns were produced as described by Yue et al. [45] with small change with monomer/ethanol ratio as described by Røgeberg et al. [46]. 5 m long columns were produced. A longer column of 10 m was later successfully produced. An increase in porogen/monomer ratio led to a decrease in film thickness as shown in **Figure 50**. This result is in agreement with experimental finding conducted by Røgeberg et al. [46]. AIBN was used as in the original procedure and LP was also tested. **Figure 50** shows morphologies of PS-DVB PLOT made with AIBN and LP.



**Figure 50.** SEM images of PS-DVB PLOT columns. A: 40% monomer/60% ethanol. B: 30% monomers/70% ethanol. Other polymerization conditions are as described by Røgeberg et al. [46].

The PLOT column was to be used with a pre-column for peptide analysis. **Figure 51** shows PS-DVB PLOT columns made with AIBN and LP respectively. Both columns appear to have the same surface morphologies.



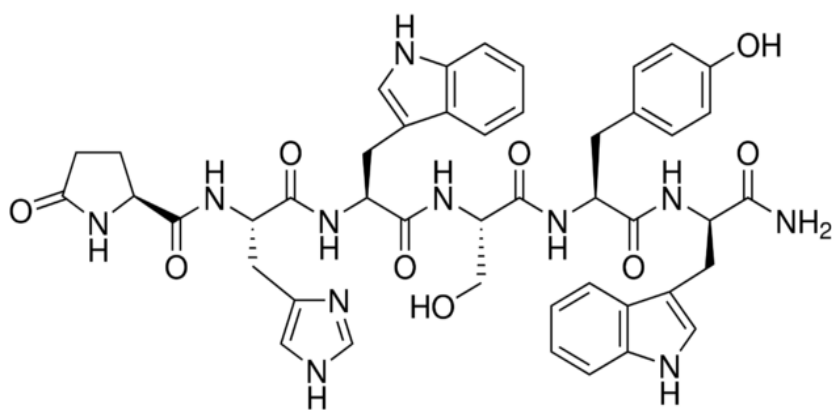


**Figure 51.** SEM images of PS-DVB PLOT columns. The columns length was ~5.25 m. AIBN (left) and LP (right) were used as an initiator. The polymerization conditions used (30% monomers/70% ethanol) are as described by Røgeberg et al. [46].

*This concludes that LP is a possible replacement for AIBN for production of PS-DVB PLOT columns. However, comparison of columns performance did not undergo.*

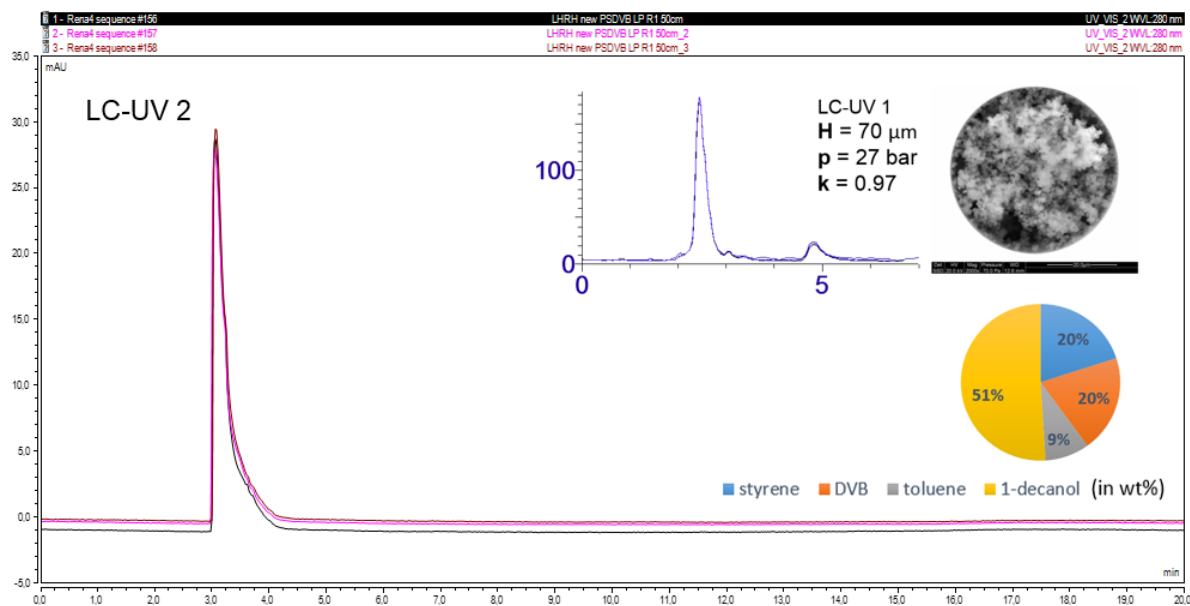
### 3.8 Trapping of peptides on monolithic column.

The monolithic columns were tested for their ability to serve as a trapping column in a column switching system for proteomics. LHRH fragment with MM less than 1000 g/mol was selected as a test analyte. **Figure 52** shows the structure of LHRH.



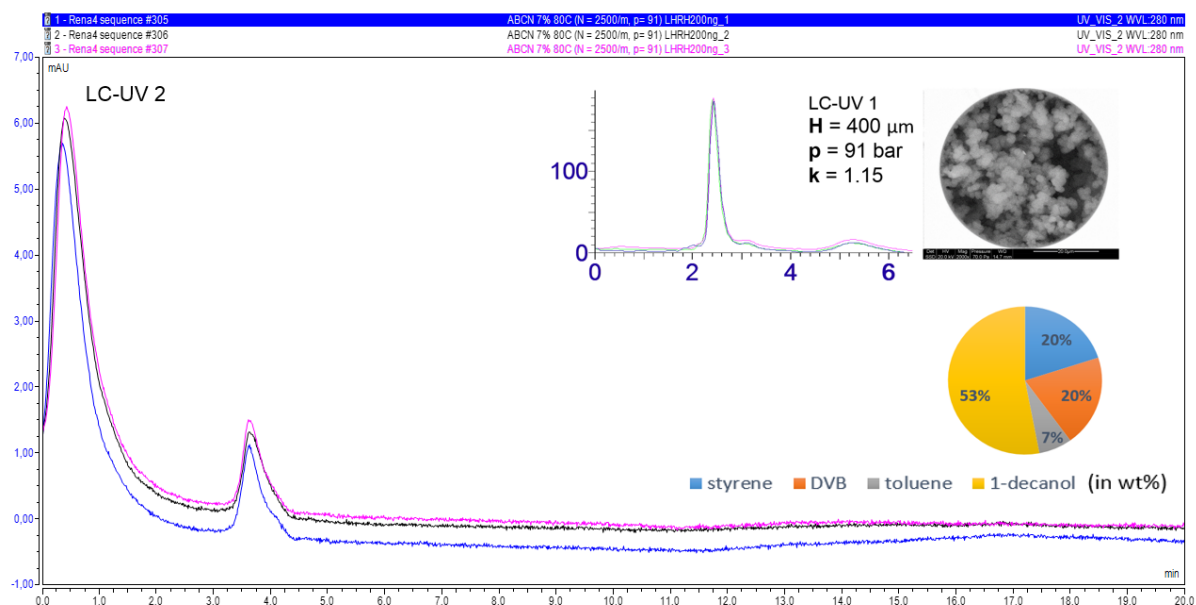
**Figure 52.** Structure of LHRH. [D-Trp<sup>6</sup>]-LHRH Fragment, 1-6. MM: 887.94 g/mol

A PS-DVB column that gave a plate height of 70  $\mu\text{m}$  for toluene in LC-UV 1 system was tested with LHRH. **Figure 53** shows chromatograms of three injections of 1  $\mu\text{L}$  (200 ng) LHRH using gradient elution.



**Figure 53.** Chromatogram of LHRH on PS-DVB monolithic column. Chemical contents used are described in the figure with 1 wt% LP (with respect to monomers), at 73°C overnight. 50 cm polymerization length was used. The LC-UV parameters and sample used are found in **Table 4** under LC-UV 2 test system.

Peak tailing was likely caused by column overloading of the analyte. From the chromatograms, it can be seen that the column was able to trap the analyte, and the gradient system eluted LHRH as a narrow peak. A column that gave quite poor efficiency was also tested for comparison. **Figure 54** shows chromatograms of three injection of 1  $\mu$ l (200 ng) LHRH on a PS-DVB that gave H of 400  $\mu$ m for toluene in the LC-UV 1 system.



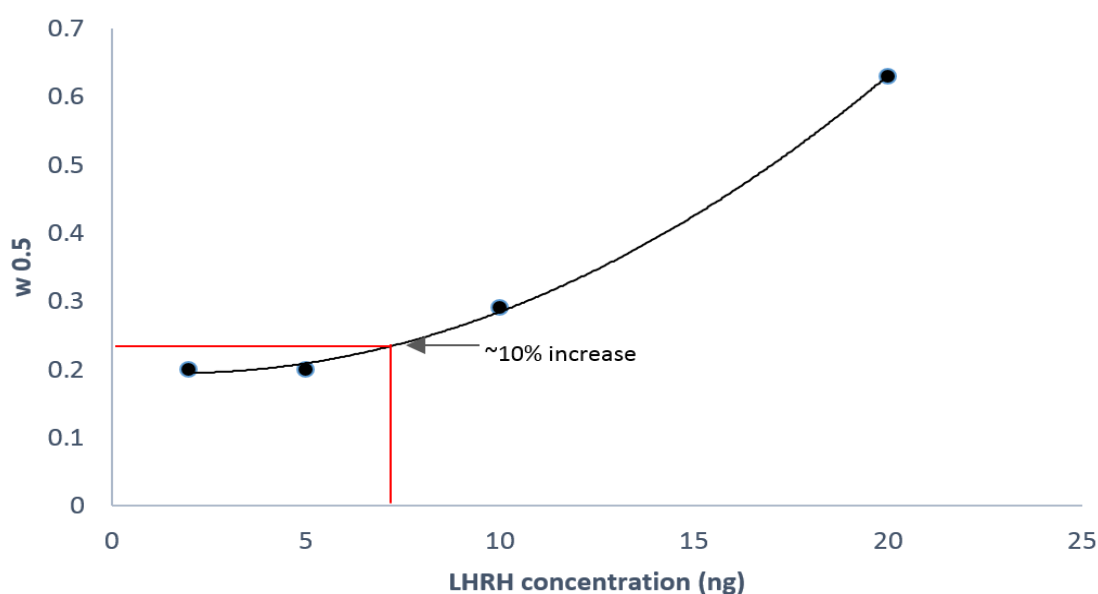
**Figure 54.** Chromatogram of LHRH on PS-DVB monolithic column. Chemical contents used are described in the figure with 1 wt% ABCN (with respect to monomers), at 80°C overnight. The LC-UV parameters and sample used are found in **Table 4** under LC-UV 2 test system.

The chromatograms in **Figures 53 and 54** show that the column that gave a good efficiency for small molecule gave also a narrow elution peak for LHRH without a breakthrough. Breakthrough, loss of the analyte as the SP could not retain it well enough, occurred when an inefficient column was used (**Figure 54**) (MP A contained 4% ACN for these testing). A larger elution band was also obtained with this column.

*It can be concluded that a column with a good efficiency for toluene is likely to be a good trapping column for LHRH.*

### 3.9 Loadability on PS-DVB monolith

It is important to know the approximate loading capacity of the column for the analyte in order to avoid breakthrough or peak tailing. **Figure 55** shows the  $w_{0.5}$  of different LHRH concentrations using a selected PS-DVB column.

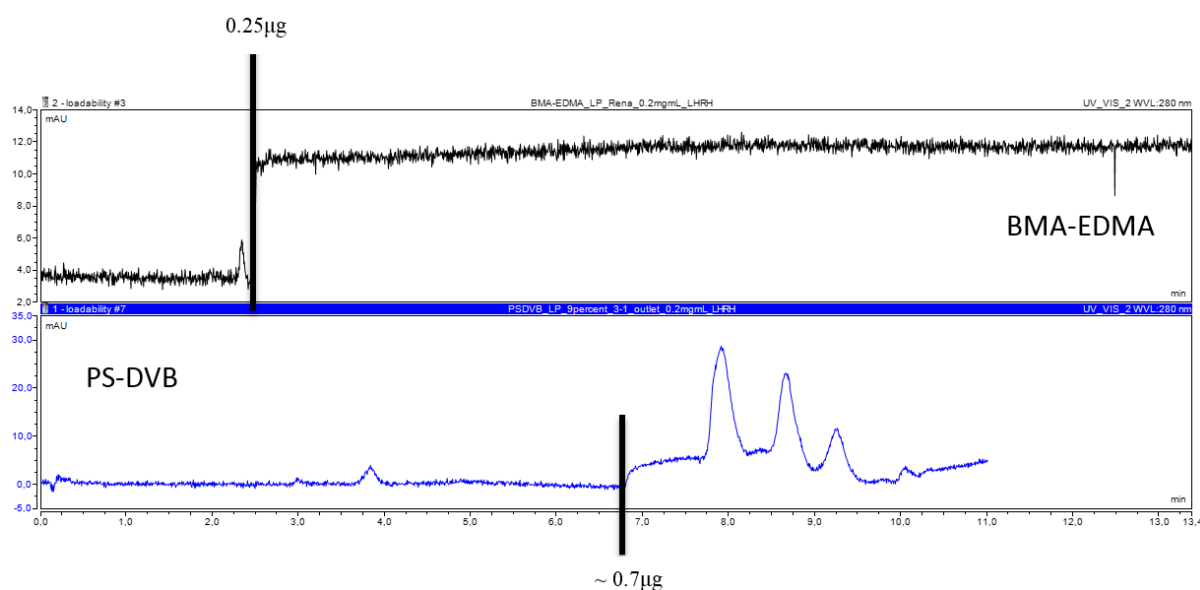


**Figure 55.** Peak width at half height vs concentration of LHRH. The column used was the same column as described in **Figure 53**. The experimental parameters and sample used are found in **Table 4** under LC-UV 2 test system.

A higher than 10% increase of peak width indicates an overloading. From this figure, the loading capacity of this column for LHRH is suggested to be in the range of 5 – 7 ng.

### 3.10 Comparison of loadability on BMA-EDMA and PS-DVB monoliths

High loadability is important for a proper trapping of peptides. Continuous infusion of sample until breakthrough occurs can be used to determine loadability of a column [58]. The loadability was tested for both BMA-EDMA and PS-DVB monolithic columns (**Figure 56**) using the SPE-UV system.



**Figure 56.** Comparison of loadability on BMA-EDMA and PS-DVB monoliths. 50  $\mu\text{m}$   $\times$  4 cm BMA-EDMA and efficient PS-DVB were used. BMA-EDMA monolith was produced by Tore Vehus using the standard procedure but with 3 h polymerization. The chemical compositions used for PS-DVB monolith are as described in **Figure 39** at 73°C for 16 h. The experimental parameters and sample used are found in **Table 5** under SPE-UV test system. The test was carried out by Tore Vehus.

0.2 mg/ml LHRH was infused onto each column using a syringe pump at a constant flow rate of 500 nl/min with a low-eluting MP (2% ACN in 0.1% TFA). Column breakthrough (i.e. mass loading capacity) was defined as a signal increase of over a period of time. For the BMA-EDMA column, the loading capacity was estimated to be 0.25  $\mu\text{g}$ , whereas the PS-DVB column could retain 0.7  $\mu\text{g}$  before breakthrough was observed. Calculations of column volumes are found in **Appendix 6.10**.

*The PS-DVB monolith has a better loading capacity than the BMA-EDMA monolith for LHRH. This suggests that it might be a better trapping column for small relatively hydrophobic molecules.*

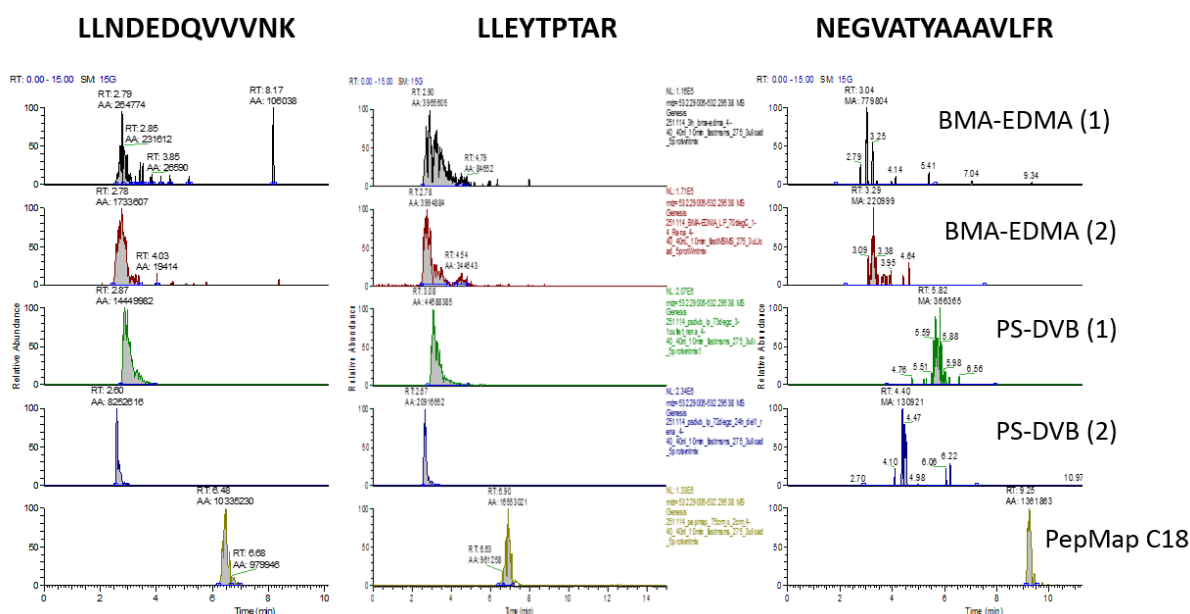
### 3.11 Comparison of pre-columns

Efficient PS-DVB monolithic column was to be compared with BMA-EDMA monolithic column for trapping capacity of tryptic peptides prior to testing with the PLOT system.

Different columns were tested using the SPE-MS/MS system and a tryptic peptide mixture. **Figure 57** shows chromatograms of some of the peptides (for simplicity) eluting from each column. **Table 12** shows the peptide sequences, their MM and mass over charge ( $m/z$ ) found. Structures of amino acid side chains are found in **Appendix 6.11**. **Figure 58** shows peak areas of selected peptides.

**Table 12:** Peptides sequences, their MM and  $m/z$  found

Peptide sequence	LLNDEDQVVVNK	ATVGLIR	LLEYTP TAR	NEGVATYAAAVLFR	VTPFNYNPSPR
MM	1385.52	728.89	1063.24	1481.68	1291.44
$m/z$	693.36743	365.23462	532.29285	741.39429	646.32507

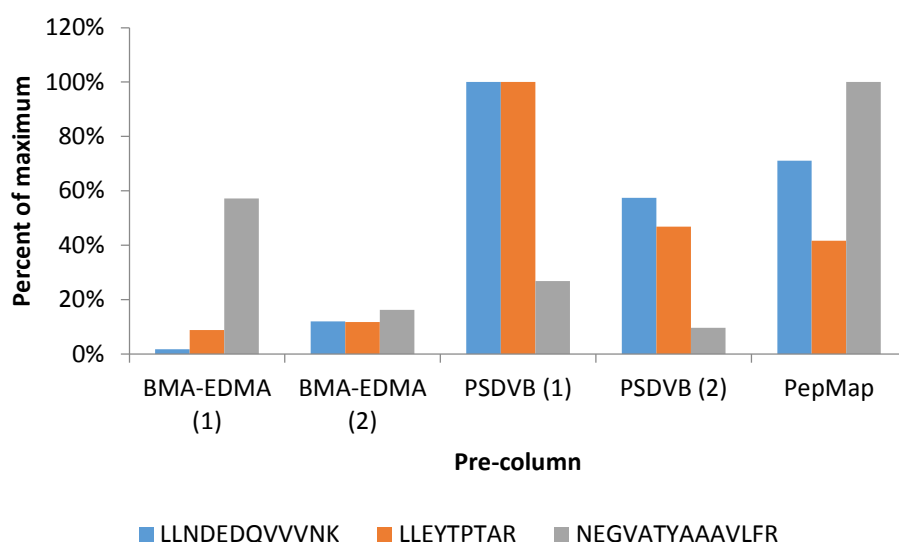


**Figure 57.** Chromatograms of tryptic peptides on various SPE columns. BMA-EDMA (1) was made by Tore Vehus using the standard procedure but with 3 h polymerization. BMA-EDMA (2) was made using the standard procedure but with LP and 70°C overnight. PS-DVB (1) and (2) was made using the chemical compositions as described in **Figure 39** at 73°C, 2 h and 16 h polymerization times, respectively. All monolithic columns were 50  $\mu$ m x 40 mm. PepMap C18 column dimension was

75µm × 20 mm. The operating parameters and the sample used are described in **Table 6** under SPE-MS/MS. The test was carried out by Tore Vehus.

Similar retention times were obtained on both the BMA-EDMA and PS-DVB monoliths. The retention time for the third peptide on the PS-DVB (1) was slightly long. This may indicate a higher affinity of the SP on the peptide. According to Vaast et al. a larger number of small globules led to a larger retention due to a larger surface area accessible for the interaction with peptides [13]. The commercial C18 packed column gave the longest retention time. Since this study focuses on monolithic pre-columns, particle packed pre-column was not used for comparison. When comparing only the monolithic columns, the PS-DVB monoliths gave larger peak areas for the first two peptides (**Figure 58**). This implies that they have a better trapping capacity for the peptides. The PS-DVB monoliths also gave better peak shapes, and this suggests a better refocusing on the pre-column. Between the two BMA-EDMA monolithic columns, the one made with LP gave better peak shapes. Thus, columns that gave good efficiency for toluene gave better peak shapes for peptides.

*Out of all the monolithic columns tested, the PS-DVB (1) gave overall the largest peak areas with the best peak shapes. This implies that the PS-DVB (1) may be the best monolithic column for trapping of the peptides. However, the compatibility with the used analytical column has to be investigated.*

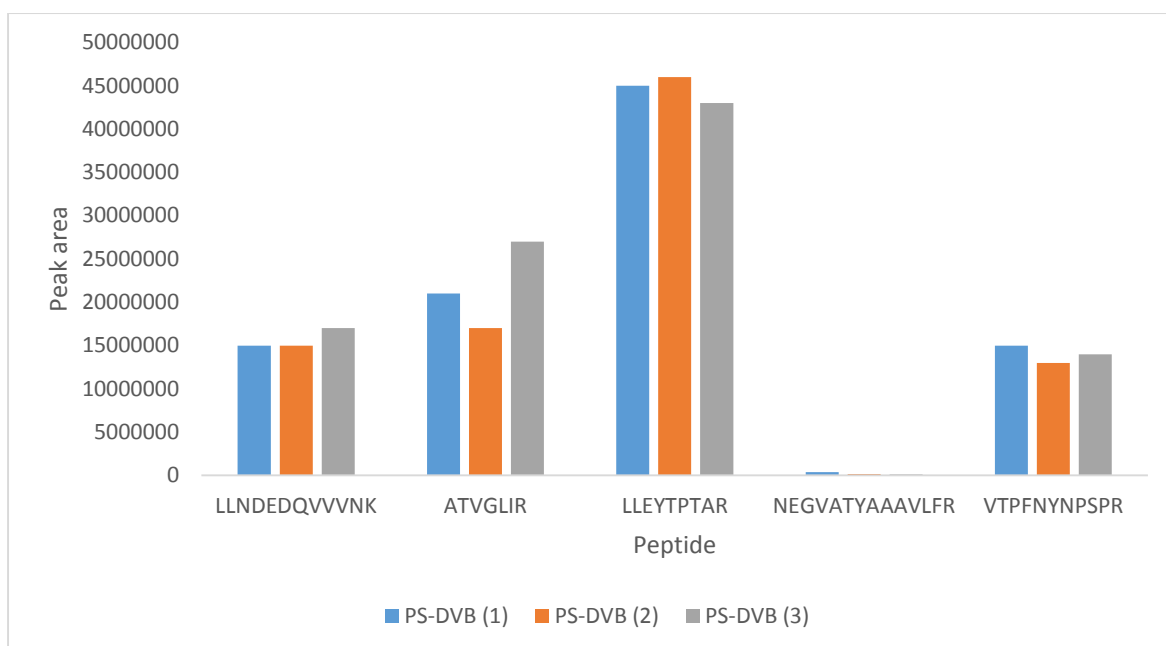


**Figure 58.** Peak areas of peptides. The columns polymerization conditions used are as described in **Figure 57**. The operating parameters and the sample used are described in **Table 6** under SPE-MS/MS. The test was carried out by Tore Vehus.

### 3.12 PS-DVB monolith trapping repeatability

Three PS-DVB monolithic columns were tested for trapping repeatability using the SPE-MS/MS system and the tryptic peptide mixture. **Figure 59** shows the peak areas of each peptide. The peak area values are found in **Appendix 6.9**.



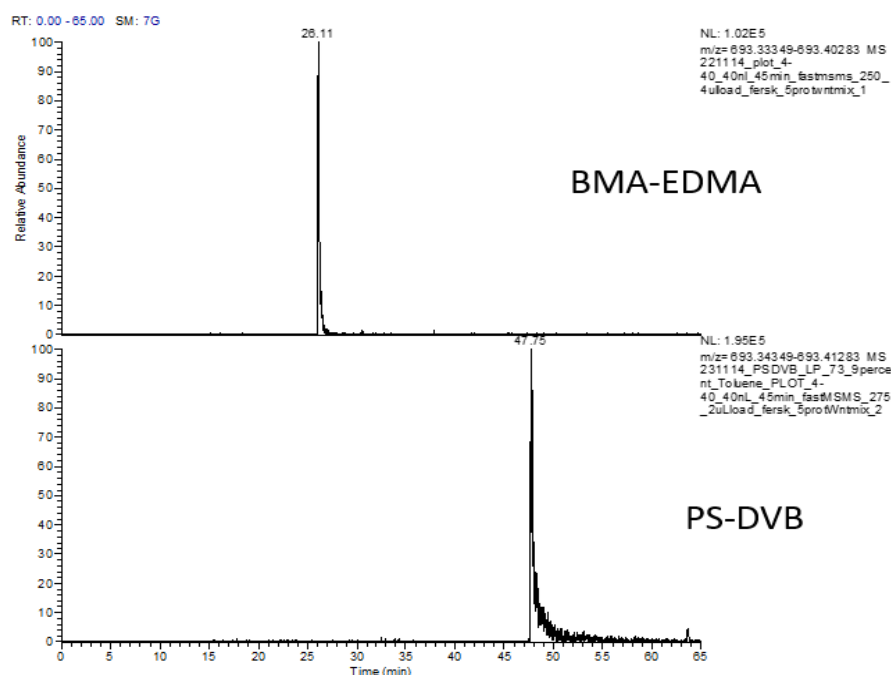


**Figure 59.** Peak area of peptides on the different PS-DVB pre-column (same batch). Column polymerization conditions used are as described in **Figure 39** (using 2 h reaction time). The operating parameters and the sample used are described in **Table 6** under SPE-MS/MS. The test was carried out by Tore Vehus.

The %RSD of peak area for three peptides were lower generally than 7, but the highest %RSD was 59 (NEGVATYAAVLFR) (**Appendix 6.9**). Thus, the trapping repeatability of the PS-DVB columns was sufficiently good for four out of five peptides.

### 3.13 Compatibility testing of pre-columns with the PLOT system

The PS-DVB and BMA-EDMA monolithic pre-columns were tested (individually) with a PLOT analytical column using the SPE-PLOT-MS/MS system and the tryptic peptide mixture to investigate its applicability in the system. **Figure 60** shows the chromatograms.



**Figure 60.** Testing of monolithic pre-columns with PLOT analytical column. 50  $\mu\text{m}$   $\times$  4 cm BMA-EDMA (1) and PS-DVB (1) were used. **Figure 57** describes the polymerization conditions used for the production. The operating parameters and the sample used are described in **Table 7** under SPE-PLOT-MS/MS. The test was carried out by Tore Vehus.

The PS-DVB monolithic pre-column (50  $\mu\text{m}$   $\times$  4 cm) used in combination with a PS-DVB PLOT analytical column (10  $\mu\text{m}$   $\times$  ~5 m) gave longer retention time and larger peak width compared with that of the BMA-EDMA pre-column (**Figure 60**). The retention time of the PS-DVB monolith was expected to be similar to that obtained with BMA-EDMA since similar retention times were obtained from both columns in the SPE-MS/MS system (**Figure 57**). The cause of this outcome is unknown and requires a further investigation. Due to time constraint and system availability, a further testing did not undergo. For a development of any columns, it is important to test the column using the whole system as different results can be obtained.

## 4. Conclusion

The developed PS-DVB monolithic pre-column ( $50\mu\text{m} \times 10\text{ cm}$ ) gave a good efficiency ( $H = 90\text{ }\mu\text{m}$ ) for toluene, and it gave a better trapping capacity for peptides than the BMA-EDMA monolith. LP was found to be the best initiator as the columns made with 1wt% (with respect to monomers) LP gave the best efficiency. When the ratio between monomers to porogens was lower than 40/60, monoliths with very open structures were obtained. Hence a 40/60 ratio was selected. Increasing the percentage of the good porogenic solvent led to monoliths with a higher surface area and backpressure. Increased temperature also led to monoliths with overall smaller globules and higher column backpressure. A short reaction time of 2 hours gave monolithic columns with the lowest plate height and backpressure. The efficient PS-DVB monolith gave a sufficiently good column repeatability (16% RSD) with toluene. Columns with a high efficiency did not always give higher backpressure or  $k$  value. The efficient PS-DVB monoliths gave similar retention times for peptides compared with the BMA-EDMA monoliths using the SPE-MS/MS system. Larger peak areas and better peak shapes obtained with the PS-DVB monoliths from this system implied that the columns (two tested) have a better trapping capacity and efficiency compared with the BMA-EDMA monoliths. When used in combination with a PLOT analytical column for peptides in SPE-PLOT-MS/MS system, a longer  $t_R$  than expected ( $\sim 48\text{ min}$ ) was obtained. The  $t_R$  was expected to be similar to that obtained with BMA-EDMA monolith since similar retention times were obtained from both types of column in the SPE-MS/MS system.



## 5. Bibliography

1. R. Soares, C. Franco, E. Pires, M. Ventosa, R. Palhinhas, K. Koci, A. Martinho de Almeida, A. Varela Coelho **(2012)**. Mass spectrometry and animal science: Protein identification strategies and particularities of farm animal species. *Journal of Proteomics*, 75, 4190-4206.
2. A. Zotou **(2012)**. An overview of recent advances in HPLC instrumentation. *Central European Journal of Chemistry*, 10, 554-569.
3. G. Mitulović, K. Mechtler **(2006)**. HPLC techniques for proteomics analysis - A short overview of latest developments. *Briefings in Functional Genomics and Proteomics*, 5, 249-260.
4. M. Rogeberg, S. R. Wilson, T. Greibrokk, E. Lundanes **(2010)**. Separation of intact proteins on porous layer open tubular (PLOT) columns. *Journal of Chromatography A*, 1217, 2782-2786.
5. J. P. C. Vissers **(1999)**. Recent developments in microcolumn liquid chromatography. *Journal of Chromatography A*, 856, 117-143.
6. F. Mansion, P. Chiap, V. Houbart, J. Crommen, A. C. Servais, M. Fillet **(2011)**. Optimization of micro-HPLC peak focusing for the detection and quantification of low hepcidin concentrations. *Journal of Separation Science*, 34, 1820-1827.
7. Y. Saito, K. Jinno, T. Greibrokk **(2004)**. Capillary columns in liquid chromatography: between conventional columns and microchips. *Journal of Separation Science*, 27, 1379-1390.
8. L. Grutle **(2013)** Thesis for the Master's in chemistry. Department of Chemistry, Faculty of mathematics and natural sciences, University of Oslo.
9. O. Núñez, H. Gallart-Ayala, C. P. B. Martins, P. Lucci **(2012)**. New trends in fast liquid chromatography for food and environmental analysis. *Journal of Chromatography A*, 1228, 298-323.
10. F. Gritti, G. Guiochon **(2014)**. Mass transport of small retained molecules in polymer-based monolithic columns. *Journal of Chromatography A*, 1362, 49-61.
11. Y. V. Kazakevich, R. LoBrutto **(2007)**. *HPLC for Pharmaceutical Scientists*. New Jersey: John Wiley & Sons, Inc.
12. J. Rozenbrand, W. P. Van Bennekorn **(2011)**. Silica-based and organic monolithic capillary columns for LC: Recent trends in proteomics. *Journal of Separation Science*, 34, 1934-1944.
13. A. Vaast, H. Terry, F. Svec, S. Eeltink **(2014)**. Nanostructured porous polymer monolithic columns for capillary liquid chromatography of peptides. *Journal of Chromatography A*, 1374, 171-179.
14. F. Svec **(2004)**. Organic polymer monoliths as stationary phases for capillary HPLC. *Journal of Separation Science*, 27, 1419-1430.

15. R. D. Arrua, T. J. Causon, E. F. Hilder **(2012)**. Recent developments and future possibilities for polymer monoliths in separation science. *Analyst*, 137, 5179-5189.
16. Wang, P.G. **(2010)**. *Monolithic Chromatography and Its Modern Applications*. Arizona: ILM Publications.
17. C. G. Huber, C. Schley, N. Delmotte **(2005)** Chapter 2 *Capillary high-performance liquid chromatography for proteomic and peptidomic analysis*, in *Comprehensive Analytical Chemistry*. Oxford: Wilson & Wilson's.
18. F. Svec **(2004)**. Preparation and HPLC applications of rigid macroporous organic polymer monoliths. *Journal of Separation Science*, 27, 747-766.
19. C. Stassen, G. Desmet, K. Broeckhoven, L. Van Lokeren, S. Eeltink **(2014)**. Characterization of polymer monolithic columns for small-molecule separations using total-pore-blocking conditions. *Journal of Chromatography A*, 1325, 115-20.
20. K. Marcus, H. Schafer, S. Klaus, C. Bunse, R. Swart, H. E. Meyer **(2007)**. A new fast method for nanoLC-MALDI-TOF/TOF-MS analysis using monolithic columns for peptide preconcentration and separation in proteomic studies. *Journal of Proteome Research*, 6, 636-43.
21. C. W. Huck, R. Bakry, G. K. Bonn **(2005)**. Polystyrene/Divinylbenzene Based Monolithic and Encapsulated Capillary Columns for the Analysis of Nucleic Acids by High-Performance Liquid Chromatography-Electrospray Ionisation Mass Spectrometry. *Engineering in Life Sciences*, 5, 431-435.
22. R. Wang, Z. G. Wang **(2012)**. Theory of polymers in poor solvent: Phase equilibrium and nucleation behavior. *Macromolecules*, 45, 6266-6271.
23. K. Štulík, V. Pacáková, J. Suchánková, P. Coufal **(2006)**. Monolithic organic polymeric columns for capillary liquid chromatography and electrochromatography. *Journal of Chromatography B*, 841, 79-87.
24. Z. Alothman, A. Aqel, H. Al Abdelmoneim, A. Yacine Badjah-Hadj-Ahmed, A. Al-Warthan **(2011)**. Preparation and Evaluation of Long Chain Alkyl Methacrylate Monoliths for Capillary Chromatography. *Chromatographia*, 74, 1-8.
25. J. Urban, P. Jandera **(2008)**. Polymethacrylate monolithic columns for capillary liquid chromatography. *Journal of Separation Science*, 31, 2521-2540.
26. M. R. Buchmeiser **(2007)**. Polymeric monolithic materials: Syntheses, properties, functionalization and applications. *Polymer*, 48, 2187-2198.
27. E. B. Anderson, M. R. Buchmeiser **(2012)**. Catalysts Immobilized on Organic Polymeric Monolithic Supports: From Molecular Heterogeneous Catalysis to Biocatalysis. *ChemCatChem*, 4, 30-44.
28. J. Urban, V. Škeříková **(2014)**. Effect of hypercrosslinking conditions on pore size distribution and efficiency of monolithic stationary phases. *Journal of Separation Science*, 37, 3082-3089.

29. C. Viklund, F. Svec, J. M. J. Fréchet, K. Irgum (1996). Monolithic, "molded", porous materials with high flow characteristics for separations, catalysis, or solid-phase chemistry: Control of porous properties during polymerization. *Chemistry of Materials*, 8, 744-750.
30. F. Svec (2012). Quest for organic polymer-based monolithic columns affording enhanced efficiency in high performance liquid chromatography separations of small molecules in isocratic mode. *Journal of Chromatography A*, 1228, 250-262.
31. R. D. Arrua, M. C. Strumia, C. I. Alvarez Igarzabal (2009). Macroporous Monolithic Polymers: Preparation and Applications. *Materials*, 2, 2429-2466.
32. V. F. Samanidou, E. G. Karageorgou (2011). An overview of the use of monoliths in sample preparation and analysis of milk. *Journal of Separation Science*, 34, 2013-2025.
33. D. A. Collins, E. P. Nesterenko, B. Paull (2014). Porous layer open tubular columns in capillary liquid chromatography. *Analyst*, 139, 1292-1302.
34. P. Jandera, J. Urban, V. Škeříková, P. Langmaier, R. Kubíčková, J. Planeta (2010). Polymethacrylate monolithic and hybrid particle-monolithic columns for reversed-phase and hydrophilic interaction capillary liquid chromatography. *Journal of Chromatography A*, 1217, 22-33.
35. F. Svec, J. M. J. Fréchet (1995). Temperature, a simple and efficient tool for the control of pore size distribution in macroporous polymers. *Macromolecules*, 28, 7580-7582.
36. M. K. Danquah, G. M. Forde (2008). Preparation of macroporous methacrylate monolithic material with convective flow properties for bioseparation: Investigating the kinetics of pore formation and hydrodynamic performance. *Chemical Engineering Journal*, 140, 593-599.
37. C. Zheng, Y. P. Huang, Z. S. Liu (2013). Synthesis and theoretical study of molecularly imprinted monoliths for HPLC. *Analytical and Bioanalytical Chemistry*, 405, 2147-2161.
38. E. T. Denisov, T. G. Denisova, T. S. Pokidova (2005). *Handbook of free radical initiator*. New Jersey: John Wiley & Sons, Inc.
39. M. You, C. Lin, M. Liu, Y. Chou, C. Shu (2009) Thermal decomposition of lauroyl peroxide BY TGA-FTIR. Paper No.: 25-7470940.
40. E. Grushka, N. Grinberg (2012). *Advances in Chromatography*. Northwestern: Taylor & Francis.
41. L. Trojer, C. P. Bisjak, W. Wieder, G. K. Bonn (2009). High capacity organic monoliths for the simultaneous application to biopolymer chromatography and the separation of small molecules. *Journal of Chromatogr A*, 1216, 6303-6309.
42. F. Svec, J. M. J. Frechet (1995). Kinetic Control of Pore Formation in Macroporous Polymers. Formation of "Molded" Porous Materials with High Flow Characteristics for Separations or Catalysis. *Chemistry of Materials*, 7, 707-715.
43. F. Maya, F. Svec (2014). A new approach to the preparation of large surface area poly(styrene-co-divinylbenzene) monoliths via knitting of loose chains using external

crosslinkers and application of these monolithic columns for separation of small molecules. *Polymer*, **55**, 340-346.

44. I. Nischang, I. Teasdale, O. Bruggemann **(2011)**. Porous polymer monoliths for small molecule separations: advancements and limitations. *Analytical and Bioanalytical Chemistry*, **400**, 2289-2304.
45. G. Yue, Q. Luo, J. Zhang, S. I. Wu, B. L. Karger, G. Yue, Q. Luo, J. Zhang, S. L. Wu, B. L. Karger **(2007)**. Ultratrace LC/MS proteomic analysis using 10-microm-i.d. Porous layer open tubular poly(styrene-divinylbenzene) capillary columns. *Analytical chemistry*, **79**, 938-946.
46. M. Rogeberg, T. Vehus, L. Grutle, T. Greibrokk, S.R. Wilson, E. Lundanes **(2013)**. Separation optimization of long porous-layer open-tubular columns for nano-LC-MS of limited proteomic samples. *Journal of Separation Science*, **36**, 2838-2847.
47. I. Gusev, X. Huang, C. Horváth **(1999)**. Capillary columns with in situ formed porous monolithic packing for micro high-performance liquid chromatography and capillary electrochromatography. *Journal of Chromatography A*, **855**, 273-290.
48. L. Geiser, S. Eeltink, F. Svec, J. M. J. Fréchet **(2007)**. Stability and repeatability of capillary columns based on porous monoliths of poly(butyl methacrylate-co-ethylene dimethacrylate). *Journal of Chromatography A*, **1140**, 140-146.
49. R. Bakry, C. W. Huck, G. K. Bonn **(2009)**. Recent applications of organic monoliths in capillary liquid chromatographic separation of biomolecules. *Journal of Chromatographic Science*, **47**, 418-431.
50. D. Peroni, D. Vanhoutte, F. Vilaplana, P. Schoenmakers, S. de Koning, H. G. Janssen **(2012)**. Hydrophobic polymer monoliths as novel phase separators: Application in continuous liquid-liquid extraction systems. *Analytica Chimica Acta*, **720**, 63-70.
51. D. Corradini, E. Eksteen, R. Eksteen, P. Schoenmakers, N. Miller **(2011)**. *Handbook of HPLC*. New York: Marcel Dekker, Inc.
52. D. Peroni, D. Vanhoutte, F. Vilaplana, P. Schoenmakers, S. de Koning, H. G. Janssen **(2012)**. Hydrophobic polymer monoliths as novel phase separators: application in continuous liquid-liquid extraction systems. *Analytica Chimica Acta*, **720**, 63-70.
53. Q. C. Wang, F. Svec, J. M. J. Frechet **(1993)**. Macroporous polymeric stationary-phase rod as continuous separation medium for reversed-phase chromatography. *Analytical Chemistry*, **65**, 2243-2248.
54. S. Ebnesajjad **(2012)**. *Polyvinyl Fluoride: Technology and Applications of PVF*. Amsterdam: Elsevier Science.
55. L. Yuanyuan, A. Pankaj, H. D. Tolley, L. L. Milton **(2012)**. Organic Monolith Column Technology for Capillary Liquid Chromatography. *Advances in Chromatography*, **50**, 237-280.
56. A. Greiderer, L. Trojer, C. W. Huck, G. K. Bonn **(2009)**. Influence of the polymerisation time on the porous and chromatographic properties of monolithic poly(1,2-bis(p-vinylphenyl))ethane capillary columns. *Journal of Chromatography A*, **1216**, 7747-7754.



57. A. Bruchet, V. Dugas, C. Mariet, F. Goutelard, J. Randon **(2011)**. Improved chromatographic performances of glycidyl methacrylate anion-exchange monolith for fast nano-ion exchange chromatography. *Journal of Separation Science*, 34, 2079-2087.
58. R. Hahn, R. Schlegel, A. Jungbauer **(2003)**. Comparison of protein A affinity sorbents. *Journal of Chromatography B*, 790, 35-51.
59. A. Voronkov, D. D. Holsworth, J. Waaler, S. R. Wilson, B. Ekblad, H. Perdreau-Dahl, H. Dinh, G. Drewes, C. Hopf, J. P. Morth, S. Krauss **(2013)**. Structural basis and SAR for G007-LK, a lead stage 1,2,4-triazole based specific tankyrase 1/2 inhibitor. *Journal of Medical Chemistry*, 56, 3012-3023.

## 6. Appendix

### 6.1 Tryptic peptide mixture preparation

The poly-ADP-ribosylation polymerization (PARP)-domain of human tankyrase2 (TNKS2) was produced by Tore Vehus as described by Voronko et al. [59].

The tryptic peptide mixture was produced by Tore Vehus. In short, 10 µg of each standard protein was digested with trypsin by dissolving it in 1 mL 8 M urea and in 50 mM Tris-HCl pH 8.0. The samples were reduced in 5 mM DDT at 37°C for 30 minutes and alkylated with 15 mM IAM for 15 minutes in the dark. Trypsin was added to a protein:enzyme ratio of 1:20, and incubated over night at 37°C. The digested standards were desalted using SPE on RP C18 cartridges with type 1 water and eluted in 1 mL 80 % ACN from Radnor 0.1 % FA (v/v) and dried with SpeedVac. Each standard was reconstituted in 0.1 % (v/v) TFA to a final concentration of 10 µg/ml. A set of external standard mixtures (ExSMix) containing 1, 0.5, 0.1, 0.05, 0.01, 0.005, 0.001, 0.0005 and 0.0001 µg/ml of each protein standard were prepared by appropriate dilution with 0.1 % (v/v) TFA.

### 6.2 Column preparation steps

PRE-TREATMENT	SILANIZATION
1) The capillary is filled with 1M NaOH	1) The silanization solution is prepared by mixing the following compounds: 0.0050 g DPPH, 0.3135 g γ-MAPS and 0.6608 g DMF
2) Both ends of the capillary are plugged with a rubber septum	2) The capillary is filled with the silanization solution
3) The capillary is left in room temperature overnight	3) Both ends of the capillary are plugged with a rubber septum
4) The capillary is rinsed with type I water until neutrality is obtained as indicated by pH indicator strips	4) The capillary is placed in an oven at 110 °C for 6 hours
5) The capillary is rinsed with ACN for ~30 min	5) The capillary is rinsed with ACN for ~30 min
6) The capillary is dried with N2 for ~1 hour	6) The capillary is dried with N2 for ~30 min

<b>POLYMERIZATION: 10 <math>\mu</math>m i.d. PS-DVB PLOT columns</b>	<b>POLYMERIZATION: 50 <math>\mu</math>m i.d. PS-DVB monolithic columns</b>
1) The polymerization solution is prepared by mixing the following compounds: 0.0050 g AIBN, 0.1818 g styrene, 0.1828 g DVB, 0.7434 g EtOH	1) The appropriate amount of each chemical of the polymerization mixture is pipetted transferred into a glass vial and weighed. The amount is adjusted if necessary
2) The polymerization mixture is homogenized by ultrasonication for 5 min	2) The polymerization mixture is homogenized by ultrasonication for 5 min
3) The capillary is filled with the polymerization solution	3) The capillary is filled with the polymerization solution
4) Both ends of the capillary are plugged with a rubber septum	4) Both ends of the capillary are plugged with a rubber septum
5) The capillary is placed in an oven at 74°C for 16 hours	5) The capillary is placed in an oven using appropriate temperature and reaction time
6) The capillary is rinsed with ACN for ~1 hour	6) The capillary is rinsed with ACN
7) The capillary is dried with N <sub>2</sub> for ~30 min	7) The capillary is dried with N <sub>2</sub>

### 6.3 %ACN on k

% ACN	p (bar)	N	H ( $\mu$ m)		tR	k	
60%	104	22373	4.5		3.6	0.52	
55%	100	24800	4.0	0.9	3.1	0.33	0.6
50%	103	24009	4.2	1.1	3.4	0.45	1.4
40%	107	21196	4.7	1.1	4.7	0.90	2.0
30%	107	16276	6.1	1.3	8.4	2.26	2.5
20%	98	15479	6.5	1.1	22.3	7.40	3.3

## 6.4 Thermal initiator

polymerization conditions	H (μm)	P (bar)	k	Length (cm) polymerized	Batch #
AIBN					
*5% toluene, 70°C	-	-	-	25	1
*10% toluene, 70, 85 and 80°C	-	-	-	25	2
*7% toluene, 70 and 74°C	-	-	-	25	3
*columns were not tested due to clogging or incomplete monolithic structure					
8% toluene, 74°C	1210	24	1.2	25	4
9% toluene, 70°C	2000	7	0.76	25	5
9% toluene, 72°C	660	46	0.92		
9% toluene, 72°C	470	212	0.85	25	6
9% toluene, 74°C	530	80	0.73	25	5
9% toluene, 74°C	400	78	1.4	25	6
9% toluene, 75°C	640	128	1.2	25	5
9% toluene, 75°C, part 1	440	174	1.4	40	9
9% toluene, 75°C, part 2	490	155	1.3		
9% toluene, 75°C, part 1	430	133	1.2	30	10
9% toluene, 75°C, part 2	420	132	1.2		
	H <sub>avg</sub>	H <sub>SD</sub>	H <sub>%RSD</sub>		
	480	91	19		
		H (μm)	P (bar)	k	Length (cm) polymerized
9% toluene, 76°C, rep. 1	390	230	1.2	40	9
9% toluene, 76°C, rep. 1, part 1	360	218	1.0	30	9
9% toluene, 76°C, rep. 1, part 2	170	215	1.0		
9% toluene, 76°C, rep. 1, part 1	480	170	1.0		
9% toluene, 76°C, rep. 1, part 2	450	170	1.0		
9% toluene, 76°C, rep. 2, part 1	410	204	0.96		
9% toluene, 76°C, rep. 2, part 2	240	246	1.2		
	H <sub>avg</sub>	H <sub>SD</sub>	H <sub>%RSD</sub>		
	360	110	32		

	H (μm)	P (bar)	k	Length (cm) polymerized	Batch #
9% toluene, 77°C, rep. 1, part 1	360	148	1.2	30	10
9% toluene, 77°C, rep. 1, part 2	520	118	1.2		
9% toluene, 77°C, rep. 2	480	164	1.2		
	H <sub>avg</sub>	H <sub>SD</sub>	H <sub>%RSD</sub>		
	450	83	18		
		H (μm)	P (bar)	k	Length (cm) polymerized
10% toluene, 70°C	610	92	0.86	25	6
10% toluene, 72°C, rep. 1, part 1	760	58	1.2	40	8
10% toluene, 72°C, rep. 1, part 2	680	270	1.2	40	8
Polymerization conditions	H (μm)	P (bar)	k	Length (cm) polymerized	Batch #
AMBN					
8% toluene, 72°C	1690	10	1.1	30	4
8% toluene, 75°C, rep. 1, part 1	280	36	0.78	25	1
8% toluene, 75°C, rep. 1, part 2	380	57	0.82		
8% toluene, 75°C, rep. 2, part 1	680	48	1.2		
8% toluene, 75°C, rep. 2, part 2	680	59	1.2		
8% toluene, 75°C, rep. 3, part 1	700	43	1.6		
8% toluene, 75°C, rep. 3, part 2	680	55	1.2		
	H <sub>avg</sub>	H <sub>SD</sub>	H <sub>%RSD</sub>		
	570	190	33		
		H (μm)	P (bar)	k	Length (cm) polymerized
8% toluene, 78°C	760	118	1.1	30	4
8% toluene, 78°C, rep. 1, part 1	690	177	1.2	30	5
8% toluene, 78°C, rep. 1, part 2	850	62	1.1		
	H <sub>avg</sub>	H <sub>SD</sub>	H <sub>%RSD</sub>		
	770	80	10		
		H (μm)	P (bar)	k	Length (cm) polymerized

9% toluene, 70°C	900	11	1.3	30	10
9% toluene, 74°C, rep. 1, part 1	210	39	1.3	25	3
9% toluene, 74°C, rep. 1, part 2	450	46	1.8		
9% toluene, 74°C	380	108	1.4	50	8
9% toluene, 74°C, rep. 1, part 1	860	41	1.5	50	9
9% toluene, 74°C, rep. 1, part 2	660	19	1.4		
9% toluene, 74°C, rep. 1, part 3	550	16	1.3		
9% toluene, 74°C, rep. 1, part 1	730	11	1.3	30	10
9% toluene, 74°C, rep. 1, part 2	800	12	1.2		
	H <sub>avg</sub>	H <sub>SD</sub>	H <sub>%RSD</sub>		
	580	220	39		
		H (μm)	P (bar)	k	Length (cm) polymerized
9% toluene, 75°C	470	190	0.80	25	2
9% toluene, 79°C, rep. 1, part 1	580	175	1.6	25	3
9% toluene, 79°C, rep. 1, part 2	370	181	1.3		
10% toluene, 78°C	430	73	1.1	30	7
Polymerization conditions	H (μm)	P (bar)	k	Length (cm) polymerized	Batch #
ABCN					
7% toluene, 80°C	390	91	1.2	50	5
7% toluene, 82°C, rep. 1, part 1	400	78	1.1		
7% toluene, 82°C, rep. 1, part 2	470	91	1.2		
9% toluene, 85°C, rep. 1	210	37	1.5	25	1
9% toluene, 85°C, rep. 2, part 1	170	33	1.5		
9% toluene, 85°C, rep. 2, part 2	210	104	1.2		
	H <sub>avg</sub>	H <sub>SD</sub>	H <sub>%RSD</sub>		
	200	23	12		
		H (μm)	P (bar)	k	Length (cm) polymerized
9% toluene, 90°C	90	182	1.3	25	1
Polymerization conditions	H (μm)	P (bar)	k	Length (cm) polymerized	Batch #

LP					
8% toluene, 74°C, rep. 1, part 1	180	19	1.3	50	2
8% toluene, 74°C, rep. 1, part 2	130	28	0.79		
8% toluene, 74°C, rep. 2, part 1	130	36	1.2		
8% toluene, 74°C, rep. 2, part 2	150	38	1.2		
8% toluene, 74°C, rep. 2, part 3	240	21	1.1		
	H <sub>avg</sub>	H <sub>SD</sub>	H <sub>%RSD</sub>		
	170	50	28		
		H (μm)	P (bar)	k	Length (cm) polymerized
9% toluene, 72°C, rep. 1, part 1	80	80	1.5	25	1
9% toluene, 72°C, rep. 1, part 2	110	91	1.1		
9% toluene, 72°C, rep. 1, part 1	220	35	1.1	100	4
9% toluene, 72°C, rep. 1, part 2	250	27	1.2		
9% toluene, 72°C, rep. 1, part 3	130	35	1.2		
9% toluene, 72°C, rep. 2, part 1	220	230	1.4		
9% toluene, 72°C, rep. 2, part 2	270	30	1.3		
9% toluene, 72°C, rep. 3, part 1	170	55	1.3		
9% toluene, 72°C, rep. 3, part 2	180	41	1.2		
9% toluene, 72°C, rep. 3, part 3	190	17	1.2		
9% toluene, 72°C, rep. 3, part 4	190	154	1.2		
9% toluene, 72°C, rep. 3, part 5	300	116	1.3		
9% toluene, 72°C, rep. 1, part 1	300	55	1.2	100	5
9% toluene, 72°C, rep. 1, part 2	290	70	1.2		
9% toluene, 72°C, rep. 1, part 3	190	28	1.2		
9% toluene, 72°C, rep. 2, part 1	170	30	0.94		
9% toluene, 72°C, rep. 2, part 2	210	26	1.1		
9% toluene, 72°C, rep. 2, part 3	260	170	1.3		
9% toluene, 72°C, rep. 2, part 4	250	75	1.2		
9% toluene, 72°C, rep. 2, part 5	310	45	1.2		
9% toluene, 72°C, rep. 1, part 1	230	34	1.2	33	7
9% toluene, 72°C, rep. 1, part 2	280	24	1.2		
9% toluene, 72°C, rep. 1, part 3	280	24	1.2		

9% toluene, 72°C, rep. 2, part 1	170	16	0.98		
9% toluene, 72°C, rep. 2, part 2	190	16	1		
9% toluene, 72°C, rep. 2, part 3	120	17	0.97		
9% toluene, 72°C, rep. 3, part 1	220	35	1.3		
9% toluene, 72°C, rep. 3, part 2	220	32	1.2		
	H <sub>avg</sub>	H <sub>SD</sub>	H <sub>%RSD</sub>		
	210	60	28		
		H (μm)	P (bar)	k	Length (cm) polymerized
9% toluene, 73°C, rep. 1, part 1	80	92	1.1	30	3
9% toluene, 73°C, rep. 1, part 2	80	71	0.99		
9% toluene, 73°C, rep. 2, part 1	120	44	0.99		
9% toluene, 73°C, rep. 2, part 2	80	31	1.0	50	3
9% toluene, 73°C, rep. 3, part 1	70	27	0.97		
9% toluene, 73°C, rep. 3, part 2	90	30	0.92		
9% toluene, 73°C, rep. 1, part 1	180	210	0.83	100	5
9% toluene, 73°C, rep. 1, part 2	130	90	0.92		
9% toluene, 73°C, rep. 1, part 3	140	97	0.92		
9% toluene, 73°C, rep. 1, part 4	190	209	1.1		
9% toluene, 73°C, rep. 2, part 1	160	170	0.94		
9% toluene, 73°C, rep. 2, part 2	150	109	1.3		
9% toluene, 73°C, rep. 1	120	166	1.5	30	6
9% toluene, 73°C, rep. 2, part 1	100	94	1.3		
9% toluene, 73°C, rep. 2, part 2	80	126	1.4		
9% toluene, 73°C, rep. 3	100	75	1.3		
9% toluene, 73°C, rep. 4, part 1	80	74	1.4		
9% toluene, 73°C, rep. 4, part 2	70	120	1.4		
	H <sub>avg</sub>	H <sub>SD</sub>	H <sub>%RSD</sub>		
	110	38	34		
		H (μm)	P (bar)	k	Length (cm) polymerized
9% toluene, 74°C	120	112	1.1	50	3
9% toluene, 75°C	260	14	1.1	30	3



9% toluene, 75°C, rep. 1, part 1	240	17	1.1	40	3
9% toluene, 75°C, rep. 1, part 2	420	27	1.1	40	3
9% toluene, 75°C	270	19	1.1	50	3
	<b>H<sub>avg</sub></b>	<b>H<sub>SD</sub></b>	<b>H<sub>%RSD</sub></b>		
	<b>300</b>	<b>80</b>	<b>28</b>		

## 6.5 Initiator amount

Polymerization conditions	H (μm)	P (bar)	k	Length (cm) polymerized	Batch #
AIBN (2 mg)					
9% toluene, 74°C, part 1	280	102	1.2	50	1
9% toluene, 74°C, part 2	440	75	1.2		
9% toluene, 75°C, part 1	360	53	1.2	50	1
9% toluene, 75°C, part 2	310	49	1.2		
9% toluene, 75°C, part 3	320	48	1.2		
9% toluene, 75°C, part 4	260	41	1.1		
	H <sub>avg</sub>	H <sub>SD</sub>	H <sub>%RSD</sub>		
	310	40	13		
		H (μm)	P (bar)	k	Length (cm) polymerized
9% toluene, 76°C, part 1	460	24	1.2	50	1
9% toluene, 76°C, part 2	390	25	1.2		
9% toluene, 76°C, part 3	560	35	1.2		
	H <sub>avg</sub>	H <sub>SD</sub>	H <sub>%RSD</sub>		
	470	90	18		
		H (μm)	P (bar)	k	Length (cm) polymerized

## 6.6 Reaction time

Polymerization conditions	H (μm)	P (bar)	k	Length (cm) polymerized	Batch #
LP, 9% toluene, 72°C					
2 h, rep. 1, part 1	70	14	0.31	30	1
2 h, rep. 1, part 2	70	13	0.36		
2 h, rep. 2, part 1	80	28	0.44	30	1
2 h, rep. 2, part 2	80	13	0.46		
	H <sub>avg</sub>	H <sub>SD</sub>	H <sub>%RSD</sub>		
	80	10	8		
Polymerization conditions	H (μm)	P (bar)	k	Length (cm) polymerized	Batch #
4 h	120	21	0.67	30	1
6 h	120	130	0.87	30	1
8 h	150	90	0.97	30	1
16 h, part 1	150	27	0.95	30	1
16 h, part 2	150	24	1.1		
20 h	190	24	1.1	30	1

Polymerization conditions	H (μm)	P (bar)	k	Length (cm) polymerized	Batch #
<b>LP, 9% toluene, 72°C</b>					
2 h, part 1	110	14	0.45	30	2
2 h, part 2	90	14	0.45		
4 h	140	32	0.77	30	2
6 h	250	50	1.1	30	2
24 h, part 1	230	25	1.5	30	2
24 h, part 2	220	25	1.4		

Polymerization conditions	H (μm)	P (bar)	k	Length (cm) polymerized	Batch #
<b>LP, 9% toluene, 72°C, 2 h</b>					

Rep. 1, outlet	120	37	0.51	33	3
Rep. 1, mid	110	17	0.48	33	3
Rep. 1, inlet	90	20	0.54	33	3
Rep 2, outlet	100	14	0.52	33	3
Rep 2, mid	90	14	0.50	33	3
Rep 2, inlet	100	19	0.51	33	3
Rep 3, outlet	90	17	0.50	33	3
Rep 3, mid	80	14	0.49	33	3
Rep 3, inlet	80	14	0.48	33	3
	<b>H<sub>avg</sub></b>	<b>H<sub>SD</sub></b>	<b>H<sub>%RSD</sub></b>		
	<b>100</b>	<b>10</b>	<b>14</b>		
	<b>H (μm)</b>	<b>P (bar)</b>	<b>k</b>	<b>Length (cm) polymerized</b>	<b>Batch #</b>
<b>LP, 9% toluene, 73°C, 2 h</b>					
Rep. 1, outlet	90	97	0.57	33	3
Rep. 1, mid	110	39	0.58	33	3
Rep. 1, inlet	100	39	0.58	33	3
Rep 2, outlet	100	23	0.57	33	3
Rep 2, mid	90	27	0.59	33	3
Rep 2, inlet	110	72	0.60	33	3
Rep 3, outlet	70	23	0.59	33	3
Rep 3, mid	90	27	0.59	33	3
Rep 3, inlet	90	33	0.59	33	3
	<b>H<sub>avg</sub></b>	<b>H<sub>SD</sub></b>	<b>H<sub>%RSD</sub></b>		
	<b>90</b>	<b>10</b>	<b>13</b>		

## 6.7 Column repeatability (PS-DVB monolith)

Polymerization conditions	n = 15	H <sub>avg</sub>	H <sub>SD</sub>	H <sub>%RSD</sub>
LP, 9% toluene, 72°C, 2 h 3 batches		90	10	16
		P <sub>avg</sub>	P <sub>SD</sub>	P <sub>%RSD</sub>
		17	6.7	38
		k <sub>avg</sub>	k <sub>SD</sub>	k <sub>%RSD</sub>
		0.47	0.1	13

## 6.8 BMA-EDMA monolith

Polymerization conditions	H (μm)	P (bar)	k	Length (cm) polymerized	Batch #
BMA-EDMA (AIBN)					
Part 1	70	204	0.48	60	1
Part 2	80	131	0.47		
Part 3	90	106	0.47		
Part 4	80	107	0.45		
Part 5	70	116	0.47		
	H <sub>avg</sub>	H <sub>SD</sub>	H <sub>%RSD</sub>		
	90	10	13		

Polymerization conditions	H (μm)	P (bar)	k	Length (cm) polymerized	Batch #
<b>BMA-EDMA (AIBN) made by Ole Kristian Brandtzæg</b>					
Part 1	100	23	0.47	100	1
Part 2	50	125	0.48		
Part 3	60	113	0.47		
Part 4	70	112	0.46		
Part 5	80	87	0.46		
Part 6	110	142	0.48		

	<b>H<sub>avg</sub></b>	<b>H<sub>SD</sub></b>	<b>H<sub>%RSD</sub></b>	
	<b>80</b>	<b>20</b>	<b>30</b>	

Polymerization conditions	H (μm)	P (bar)	k	Length (cm) polymerized	Batch #
BMA (LP) rep. 1					
Part 1	80	106	0.58	100	1
Part 2	60	83	0.56		
Part 3	40	85	0.56		
Part 4	40	90	0.56		
Part 5	40	124	0.56		
Part 6	60	81	0.56		
Part 7	60	62	0.54		
	H <sub>avg</sub>	H <sub>SD</sub>	H <sub>%RSD</sub>		
	50	20	28		
		H (μm)	P (bar)	k	Length (cm) polymerized
BMA (LP) rep. 2					
Part 1	30	108	0.65	100	2
Part 2	40	108	0.59		
Part 3	50	73	0.58		
Part 4	50	67	0.59		
Part 5	60	63	0.56		
Part 6	70	110	0.58		
	H <sub>avg</sub>	H <sub>SD</sub>	H <sub>%RSD</sub>		
	50	10	28		

## 6.9 Trapping repeatability of PS-DVB monoliths

Name	LLNDEDQVVVNK	ATVGLIR	LLEYTP TAR	NEGVATYAAAVLFR	VTPFNYNPSPR
3-1 Outlet	1.50E+07	2.10E+07	4.50E+07	3.70E+05	1.50E+07
3-1 Inlet	1.50E+07	1.70E+07	4.60E+07	1.50E+05	1.30E+07
3-3 Inlet	1.70E+07	2.70E+07	4.30E+07	1.40E+05	1.40E+07
Average	1.60E+07	2.20E+07	4.40E+07	2.20E+05	1.40E+07
SD	1.10E+06	5.20E+06	1.60E+06	1.30E+05	9.40E+05
% RSD	6.9	24	3.6	59	6.5

## 6.10 Comparison of loadability calculations

Volume on column = time breakthrough  $\times$  flow rate

### BMA-EDMA

$$2.5 \text{ min} \times 500 \text{ nL/min} = 1250 \text{ nL} = 1.25 \text{ }\mu\text{L}$$

$$0.2 \text{ mg/mL LHRH} = 0.2 \text{ }\mu\text{g}/\mu\text{L} \rightarrow 0.2 \text{ }\mu\text{g}/\mu\text{L} \times 1.25 \text{ }\mu\text{L} = 0.25 \text{ }\mu\text{g}$$

### PS-DVB

$$6.75 \text{ min} \times 500 \text{ nL/min} = 3375 \text{ nL} = 3.38 \text{ }\mu\text{L}$$

$$0.2 \text{ mg/mL LHRH} = 0.2 \text{ }\mu\text{g}/\mu\text{L} \rightarrow 0.2 \text{ }\mu\text{g}/\mu\text{L} \times 3.38 \text{ }\mu\text{L} = 0.68 \text{ }\mu\text{g}$$

## 6.11 Structures of amino acid side chains

<b>Aspartic Acid, Asp, D</b> <chem>NC(CC(=O)O)C(=O)O</chem>	<b>Glutamic Acid, Glu, E</b> <chem>NC(CCC(=O)O)C(=O)O</chem>	<b>Arginine, Arg, R</b> <chem>NC(CCCNC(=[NH2+])N)C(=O)O</chem>	<b>Lysine, Lys, K</b> <chem>NC(CCCC[NH2+])C(=O)O</chem>	<b>Histidine, His, H</b> <chem>NC(CC1=CN=CN1)C(=O)O</chem>
<b>Alanine, Ala, A</b> <chem>NC(C)C(=O)O</chem>	<b>Glycine, Gly, G</b> <chem>NC(C=O)C(=O)O</chem>	<b>Proline, Pro, P</b> <chem>C1CCNC1C(=O)O</chem>	<b>Valine, Val, V</b> <chem>NC(C(C)C)C(=O)O</chem>	<b>Tryptophan, Trp, W</b> <chem>NC(CC1=C2C=CC=CC2=CN1)C(=O)O</chem>
<b>Leucine, Leu, L</b> <chem>NC(CC(C)C)C(=O)O</chem>	<b>Phenylalanine, Phe, F</b> <chem>NC(CC1=CC=CC=C1)C(=O)O</chem>	<b>Methionine, Met, M</b> <chem>NC(CSC)C(=O)O</chem>	<b>Isoleucine, Ile, I</b> <chem>NC(C(C)C)C(C)C(=O)O</chem>	<b>Asparagine, Asp, N</b> <chem>NC(CC(=O)N)C(=O)O</chem>
<b>Cysteine, Cys, C</b> <chem>NC(CS)C(=O)O</chem>	<b>Glutamine, Gln, Q</b> <chem>NC(CCC(=O)N)C(=O)O</chem>	<b>Serine, Ser, S</b> <chem>NC(CO)C(=O)O</chem>	<b>Threonine, Thr, T</b> <chem>NC(C(O)C)C(=O)O</chem>	<b>Tyrosine, Tyr, Y</b> <chem>NC(CC1=CC=C(O)C=C1)C(=O)O</chem>